CENTRIFUGAL SUPERCHARGER DESIGN METHODS N73-74400
(NASA) 121 p
Unclas
00/99 19521

12p

NATIONAL ADVISORY COMMITTEE FOR AERONAUTICS

Code 5

CLASSIFICATION CHANGE
TO - UNCLASSIFIED ~~CONFIDENTIAL~~
By authority of E.O. No 11652
Changed by AM Hubbard Date 8/23/73

CONFIDENTIAL

The information contained herein must not be published either in whole or in part without express written permission of the National Advisory Committee for Aeronautics.

MEMORANDUM REPORT

9/26/41

CENTRIFUGAL SUPERCHARGER DESIGN METHODS (II)

CONTINENTAL
★★★
LIBRARY
★★★
12801 E. JEFFERSON
DETROIT 14 MICHIGAN

~~CLASSIFIED DOCUMENT~~
This document contains classified information affecting the National Defense of the United States within the meaning of the Espionage Act, USC 50:31 and 32. Its transmission or the revelation of its contents in any manner to an unauthorized person is prohibited by law. Information classified may be imparted only to persons in the military and naval Services of the United States, appropriate civilian officers and employees of the Federal Government who have a legitimate interest therein, and to United States citizens of known loyalty and discretion who of necessity must be informed thereof.

This document will not be indexed or announced in Scientific and Technical Aerospace Reports. The document has received partial Descriptive cataloging only.

September 26, 1941

FILE COPY
To be returned to
the files of the National
Advisory Committee
for Aeronautics
Washington, D. C.

1126

MEMORANDUM REPORT

CENTRIFUGAL SUPERCHARGER DESIGN METHODS (4)

INTRODUCTION

The Special Subcommittee on Supercharger Compressors has agreed to prepare this summary of centrifugal supercharger design methods for the guidance of engine manufacturers. This subcommittee was organized June 7, 1940 and comprises the following membership:

Mr. Val Cronstedt, Pratt & Whitney Aircraft

Mr. Rudolph Birmann, Turbo Engineering Corp.

Mr. R. S. Buck, Pratt & Whitney

Mr. Kenneth Campbell, Wright Aeronautical Corporation

Mr. Opie Chenoweth, Materiel Division, Army Air Corps

Mr. S. Paul Johnston, NACA

Mr. A. J. Larrecq, Allison Engineering Division

Dr. George W. Lewis, NACA

Mr. Oscar W. Schey, NACA

Dr. Chester Smith, General Electric Company

Lieutenant Commander S. B. Spangler, U. S. N.

This subcommittee was appointed in recognition of the need for improving altitude performance of supercharged aircraft engines.

No attempt has been made to treat the subject of supercharger design methods exhaustively, or to mention all the various theories which have been used or proposed. The primary objective has been to separate from pure theory and the mass of test data those derived results which can be concisely expressed in the form of design rules and applied immediately to practical problems.

The information furnished by four manufacturers to members has been reproduced without editing or comments. Naturally there are some inconsistencies and contradictions, reflecting differences of opinion. However, it is to be noted that the information here given represents general practice, and the design rules should not be construed as recommendations for all cases. Usually each engine has its own particular problems and imposes its own set of limitations on supercharger design, so that from the combined standpoint of efficiency, trouble-free mechanical operation, size, and weight, a better overall result may frequently be obtained by modification of the requirements as here given. It does not necessarily follow that a design which is best for one engine will also be best for another engine.

The general index given on the next page was designed to facilitate comparisons and to provide easy reference to a particular topic in each of the four reports. There are, in general, four sets of page references for each topic; each set refers to a particular report. The reports are denoted by the letters A, B, C, and D. For example, information about the impeller entrance air velocity may be found on page 11 of report A, page 6 of report B, page 26 of report C, and not at all in report D, except perhaps by inference.

Report C is composed of excerpts from a more complete report written in 1937, and for that reason, references are given to figures and parts of the original report that are not contained in report C. Report C, however, includes what is considered the most important parts of the complete report.

GENERAL INDEX

	Page A	B	C	D
Design specifications	3		6	
Design assumptions	5			
Attitude pressure and temperature	5			
Pressure drop through carburetor	6			
Pressure drop through cooler	6			
Temperature drop through fuel vaporization	6			
Efficiencies	6			
Calculation of operating conditions				
Impeller tip velocity	7		6	
Temperature use	7			
Power required	7			
Load coefficient	3,4,5		6	2
Inlet passage				
Inlet elbow and guide vanes	25	5		1
Passage velocity		5	26	
Area	25	5	25	
Surface finish		5		
Other factors		5		1

	Page			
	A	B	C	D
Impeller design				
Velocity at impeller entrance	11	6	26	
Outer diameter	7			
Blade exit width	8			
Number of blades	9		27	1
Hub diameter	10			
Eye diameter	10			
Area ratio		6	7,24,25	
Bucket or inducer	11	6	7,26	1
Impeller passage shape	12			
Blade thickness	13			1
Scallops	13	6		1
Impeller recess	14			2
Impeller-casing clearance	14		27	
Pressure-equalizing holes	15	6	28	1
Vanes on rear side	15			
Air condition, velocity at impeller exit	21	6,12,20		
Shape of blade tip		6,12,13		
Fillets		6		
Fuel spinner		6		
Impeller performance		10,11,20		

	Page			
	A	B	C	D
Diffuser design				
Inner diameter	16	8,14	9,36	1
Outer diameter	16			
Number of vanes	17			1
Computing air condition at diffuser throat from impeller exit condition		14,15	8	
Diffuser width	17,21	7,8		
Inlet passage height	18	16		
Rate of expansion	19	7,8,17	9,33	1
Ratio of expansion	20	7	9,33,34	
Vane tip	21	15	9,35, 36	1
Vane thickness	20	18		
Discharge velocity		7,18		
Vane shape		7,18,23	9,11,32	
Axial position and direction of channel		7		
Surface finish	21	7,23		
Diffuser rim scalloping				1
Diffuser losses		22,23		
Impeller-diffuser performance		12		
Collector and scroll design				
Location	22	8		2
Shape	22	8		
Type of outlet	22	8		

	Page			
	A	B	C	D
Collector and scroll design (continued)				
Scroll area	23			2
Collector passage area	24	8		
Velocity in collector passage				2
Guide vanes	25			
Surface finish		8		
Miscellaneous				
Heat transfer from engine		8,24		
The T-S diagram		19		
Examples of design		25	9,11	
Dimensional theory, equation of performance, and rating parameters			13-16	
Thermodynamic correlations		9-16, 19-13	16-20	

REPORT A

CONTENTS

		Page
	Introduction	1
I.	Notation	1
II.	Design Specifications	3
III.	Design Assumptions	5
IV.	Calculation of Impeller Tip Velocity, Temperature Rise, and Power Required	7
V.	Impeller Dimensions	7
	1. Outer Diameter	7
	2. Blade Exit Width	8
	3. Number of Blades	9
	4. Hub Diameter	10
	5. Annulus ("Eye) Diameter	10
	6. Inlet Buckets	11
	7. Impeller Passage Shape	12
	8. Blade Thickness	13
	9. Scallops	13
	10. Impeller Recess	14
	11. Impeller Clearance	14
	12. Pressure-equalizing Holes	15
	13. Vanes on Rear Side of Impeller	15
	14. Shrouded Impeller	16
VI.	Diffuser Dimensions	16
	1. Inner Diameter	16
	2. Outer Diameter	16
	3. Number of Vanes	17
	4. Diffuser Width	18
	5. Inlet Passage Height	18
	6. Rate of Expansion	20
	7. Expansion Ratio	20
	8. Vane Thickness	21
	9. Diffuser Surface	21
	10. Inlet Tips of Vanes	21
	11. Spacing of Vanes	21
	12. Vaneless Diffuser	22
VII.	Scroll and Collector Ring	23
	1. Location	23
	2. Shape	23
	3. Type of Outlet	24
	4. Scroll Area	25
	5. Collector Passage Area	25
	6. Guide Vanes	26
VIII.	Inlet Passage	27
	1. General	27

Tables, Curves, and Illustrations

Fig. 1 Curve of Impeller Compression Factor
Fig. 2 Velocity Diagrams
Fig. 3 Diffuser Vane Inlet Passage Height
Fig. 4 Recommended Shape of Intake Elbow
Tables of Annulus Diameter - Part I
Tables of Annulus Diameter - Part II
Tables of Root Mean Square Diameter - Part I
Tables of Root Mean Square Diameter - Part II
Tables of "Y" for Normal Air and Perfect Diatomic Gases

DIGEST OF GEARED SUPERCHARGER DESIGN METHOD

INTRODUCTION: This digest outlines a working method for the aerodynamic design of geared superchargers. For the sake of brevity, no attempt is made to give either the fundamental theory or the test data on which the design constants are based, but only to present as concisely as possible the derived results in the form of practical working rules useful to the designer. Since nearly all geared superchargers use radial blade impellers, the discussion is limited to impellers of this type.

I. NOTATION

The following notation is used. The meaning of each symbol is briefly indicated, but in some cases a more complete definition and formula for calculation are given later.

Symbol	Meaning	Units
A_1	Impeller inlet area	sq. in.
A_2	Impeller exit area - actual	"
A'_2	Impeller exit area - "effective"	"
A_3	Diffuser vane inlet area	"
A_4	Diffuser vane exit area	"
A_5	Scroll or collector ring area	"
D	Engine displacement	c.f.m.
d_o	Impeller hub diameter	in.
d_a	Impeller annulus ("eye") diameter	"

Symbol	Meaning	Units
d_m	Root mean square diameter of impeller inlet buckets	in.
d_2	Impeller outer diameter	"
d_3	Diffuser inner diameter	"
d_4	Diffuser outer diameter	"
e_2	Impeller tip width	"
e_3	Diffuser width (axial)	"
e_s	Shaft efficiency	Non-dimensional
e_t	Temperature-rise ratio	"
f	Impeller compression factor	"
h_1	Impeller entrance bucket passage height-actual	in.
h_1'	Impeller entrance bucket passage height-theoretical	"
h_3	Diffuser vane inlet passage height	"
n_b	Number of impeller blades	Non-dimensional
n_v	Number of diffuser vanes	"
N	Impeller speed	RPM
p_o	Atmospheric pressure at specified altitude	"Hg abs.
p_e	Engine exhaust manifold pressure	"
p_1	Pressure at impeller inlet	"
p_6	Pressure at compressor discharge	"
p_E	Engine intake manifold pressure	"
P	Power required to drive compressor	HP
q_1	Volume flow at impeller inlet conditions	c.f.m.
q_2	Volume flow at impeller exit conditions	"
q_E	Volume flow at intake manifold conditions	"

Symbol	Meaning	Units
q_c	Engine clearance volume flow	c.f.m.
r	Compressor pressure ratio	Non-dimensional
R_2	Velocity of air relative to blade at impeller exit	ft/sec.
T_o	Atmospheric temperature at specified altitude	^oF abs.
T_1	Temperature at impeller inlet	"
T_6	Temperature at compressor discharge	"
T_E	Temperature in intake manifold	"
V_1	Absolute velocity of air at impeller inlet	ft/sec.
V_2	Impeller tip velocity	"
V_m	Linear velocity of point on impeller at diameter d_m	"
w	Weight flow	lbs/min.
Y	Isentropic factor $= \left(\frac{p_6}{p_1}\right)^{.283} - 1$	Non-dimensional
α	Tangential angle of relative air velocity at impeller inlet	degrees
β_2	Tangential angle of absolute air velocity at impeller exit	"
β_3	Vortex angle of air in vaneless diffuser	"
η	Pressure coefficient	Non-dimensional

II. DESIGN SPECIFICATIONS

1. If weight flow and pressure ratio, or the equivalent, are specified, use these values directly, converting weight flow into volume flow by use of the proper specific weights, which usually cannot be determined until the pressures and temperatures throughout the

system have been calculated in accordance with the procedure explained later.

2. If engine data and pressure ratio, or the equivalent, are specified, calculate flow from engine bore, stroke, number of cylinders, and speed, using a reasonable volumetric efficiency based upon whatever knowledge of the engine is available. In the absence of more definite information, a volumetric efficiency of 90%, based on intake manifold pressure and temperature, can ordinarily be assumed, but for very high engine speeds this may be reduced to 85%.

If the intake manifold pressure exceeds the exhaust manifold pressure by an appreciable amount, allowance should be made for the compression of the residual gas in the clearance space by the incoming charge by adding to the displacement volume flow the additional flow in the clearance space, which is equal to

$$\frac{p_E - p_e}{p_E} \, q_c$$

Usually it can be assumed that

$$p_E \approx p_6$$

and

$$p_e \approx p_o$$

3. If the specific air consumption and engine output are given, determine the volume flow from these data and the proper specific weights. In any case where method (2) is used, the calculated flow should be checked by assuming a reasonable specific air consumption for the type of

engine under consideration. For most modern high power radial engines, the specific air consumption can be taken as 0.120 lbs/min/BHP, although this figure may vary somewhat with engine speed. For in-line liquid-cooled engines, the air consumption will usually be lower, and may be taken as 0.110 lbs/min/BHP in the absence of more definite information.

The flow finally used should be consistent with reasonable assumptions and customary values as determined by both methods (2) and (3).

4. Sometimes the specifications require a given engine power to be maintained to a given altitude. This requires a calculation of the intake manifold pressure required for the necessary weight flow, taking due account of the temperature rise corresponding to the pressure.

5. In some cases a definite load coefficient (q_1/N) is specified. The inlet volume flow is found from this value after the speed N necessary to obtain the specified pressure is determined.

III. DESIGN ASSUMPTIONS

The following assumptions may ordinarily be made in the absence of more definite information. With reference to efficiencies, it will be necessary to make an estimate based on the general design, effect of space limitations, impeller tip speed, type of inlet, etc.

1. Altitude pressure and temperature--from N.A.C.A. Report No. 218.

2. Pressure drop through carburetor - 1" Hg. (This may be increased to 1.25" Hg or 1.5" Hg for large flows and relatively small carburetor throat areas, and decreased to 0.75" Hg for relatively small flows). Ordinarily, therefore, if a carburetor precedes the supercharger,

$$p_1 = p_o - 1.0$$

3. Pressure drop through cooler, if used - 0.75" Hg.

4. Total temperature drop due to fuel vaporization if carburetor precedes supercharger - 40° F. It is assumed that 20° F drop occurs between carburetor and the impeller inlet, and the remaining 20° F during compression in the supercharger. Therefore, when a carburetor precedes the supercharger,

$$T_1 = T_o - 20$$

5. Efficiencies

	Good	Moderate
Pressure Coefficient	.68	.63
Temperature-Rise Ratio	.70	.64
Adiabatic Shaft Efficiency	.66	.60

The shaft efficiency includes the losses in gears and bearings, but in some cases, especially for very high speeds, it may be better to treat these separately. It is quite possible to obtain efficiencies better than those listed above under "good", but for design purposes it is best to use values on the conservative side.

IV. CALCULATION OF IMPELLER TIP VELOCITY, TEMPERATURE RISE, AND POWER REQUIRED

1. Impeller tip velocity.

$$V_2 = \sqrt{\frac{6083\ YT_1}{\eta}}$$

2. Temperature rise.

When there is no carburetor preceding the supercharger (fuel injection), the temperature rise through the supercharger is

$$T_6 - T_1 = \frac{YT_1}{e_t}$$

When a carburetor precedes,

$$T_6 - T_1 = \frac{YT_1}{e_t} - 20$$

3. Power required,

$$P = \frac{.007574\ Yp_1 q_1}{e_s}$$

or

$$P = \frac{.00573\ wYT_1}{e_s}$$

V. IMPELLER DIMENSIONS

1. Outer Diameter. In theory, this should be determined by (a) making the entire compressor geometrically similar to an existing compressor which is known to have high efficiency, and (b) making the parameter q_1/Nd_2^3 (known as "quantity constant") the same for both compressors.

In practice, there is considerable limitation on the extent to which this can be done, and the impeller diameter is more often determined by space limitations, stress considerations, allowable bearing speeds or loads, available gear ratios,

permissible acceleration forces, etc. It is always advisable, however, after a design has been made, to check its general suitability by calculating the value of the quantity constant. For this purpose the expression may be recast into the form

$$\frac{q_1 \left(\frac{N}{1000}\right)^2}{(50.9\ Y\ T_1/520)^{3/2}}$$

which has been used considerably in the past, and the values of which have been well correlated with efficiency from a large number of tests. The value of this number should ordinarily be between 20,000 and 40,000 for best efficiency. The efficiency gradually falls off with increasing values, but the loss is not excessive up to 100,000, where the efficiency may be decreased by an amount of the order of 0.05. The efficiency may be decreased a similar amount for a decrease of this number to 10,000, but any further decrease is likely to result in a very sharp loss, and it is desirable to keep the number well above 10,000 if possible.

2. Blade Exit Width. Knowledge of the volume flow at impeller exit conditions is required to determine the exit width, and this is found from the relation

$$q_2 = f q_1$$

Values of f, the impeller compression factor, which is a function of impeller tip velocity and impeller inlet temperature, are shown on the accompanying curve sheet, Figure 1. The plotted values are based on a reasonable impeller compression efficiency.

The exit width is usually determined by making the angle β_2 (angle between the absolute velocity of the air leaving the impeller and the tangential direction) a value conducive to high efficiency, as determined by previous experience. This angle is usually taken between 5° and 10°, with an average value of about 7.5°, for moderate impeller tip speeds. For high tip speeds, it is desirable to increase the angle to 10°, or even to 12°, but this usually proves rather inconvenient because a large angle necessitates a relatively large outer diffuser diameter for good efficiency.

Having selected angle β_2, the relative velocity at the impeller tip is found from the relation (see Figure 2)

$$R_2 = V_2 \tan \beta_2$$

The corresponding impeller exit area is

$$A_2 = \frac{144}{60} \frac{q_2}{R_2}$$

and the blade width at the tip

$$e_2 = \frac{A_2}{\pi d_2}$$

When scallops are used, this width is taken as the overall width, including the web thickness, since the air can spread out to the full width in the scalloped portion of the web.

3. Number of Blades. This is usually taken as 16 or 22. The efficiency would begin to fall off appreciably if fewer than 16 blades were used, and any gain with more than 22 would ordinarily not be sufficient to compensate for the increased weight.

The choice between 16 and 22 blades is usually dependent upon the general proportions of the impeller. If the outer diameter is relatively small (about 7"—8"), 16 blades will give a reasonable spacing between the tips of adjacent blades. For large diameters (11"—12"), this spacing would be too great, and is reduced by using 22 blades.

On the other hand, if the hub diameter is relatively large, and there are only 16 blades, it may not be possible to use buckets of sufficient axial length, or to bend them over sufficiently, to obtain good entrance passages. It may be necessary in such cases to use 22 blades regardless of the outer diameter.

4. Hub Diameter. This is ordinarily determined by other than aerodynamic considerations. The shaft must be large enough for both torsional strength and stiffness, and usually this must be verified by a calculation of the critical speed. Sometimes the impeller shaft is made hollow to permit another shaft to pass through the center, and this will require a large hub diameter. The diameter must also be large enough so that there will be sufficient space between the blades to permit the necessary radius on the milling cutter for a sturdy fillet at the base of the blades.

5. Annulus ("Eye") Diameter. This diameter is selected to make the square of the relative velocity at the inlet a minimum for given values of q_1/N and hub diameter. The equation is

$$d_a = \sqrt{125.3\ (q_1/N)^{2/3} + d_o^2}$$

Values can be taken directly from the Tables of Annulus Diameter.

6. Inlet Buckets. The inlet bucket blades are made in the shape of helical surfaces, the generators of which are inclined in order to avoid excessive overhang of the buckets. The design is based on a velocity diagram (see Figure 2) taken at the root mean square diameter d_m, this being the diameter of the circle dividing the annular area at the inlet into equal inner and outer portions. Values of this diameter may be taken from the Tables of Root Mean Square Diameter. The absolute velocity is taken in the axial direction.

The theoretical passage height between two blades at the root mean square diameter (i.e., the width of the passage perpendicular to the direction of flow at this diameter) is obtained by the following self-explanatory process of calculation.

$$A_1 = \frac{\pi}{4}\left(d_a^2 - d_o^2\right)$$

$$V_1 = \frac{144}{60}\,\frac{q_1}{A_1}$$

$$V_m = \frac{\pi d_m N}{720}$$

$$\tan\alpha = \frac{V_1}{V_m}$$

$$h_1' = \frac{\pi d_m \sin\alpha}{n_b}$$

It has been found that this theoretical value should be increased by about 30% for best results, so that

$$h_1 = 1.3\ h_1'$$

The passage height is the actual width of the air passage, and does not include any thickness of blade. It is to be noted that this method is concerned more with providing sufficient area than with maintaining a certain theoretical angle. It has been found that the actual angle may vary over wide limits without appreciably affecting the efficiency, provided that the passage area is sufficiently large. In many cases a factor considerably greater than 1.3 may be used, especially when the blade would otherwise have to be bent over more than 45° at the annulus diameter. It has been found that a bend of more than 45° introduces serious danger of fracture or of incipient cracks, with little or no further gain in efficiency, so that this is ordinarily taken as the limiting angle of bend, regardless of the fact that the resulting passage height may be considerably greater than the calculated value.

Starting with the value of the passage height at the root mean square diameter, the inclined helical surface is then laid out by descriptive geometry methods.

7. Impeller Passage Shape. The variation of the impeller passage area from inlet to exit has not been found very critical, and, in fact, the actual effective area is very difficult to determine. However, impellers are laid out to give a constant increase, though not necessarily a constant rate of increase, of area from inlet to exit, the area being measured as nearly as possible normal to the direction of flow. The selection of the milling cutter radius is dictated partly by the necessity

of leaving enough metal in the web for necessary strength and thickness. The angle on the open side of the blades is usually between 10° and 15°.

8. Blade Thickness. The thickness of the blades does not effect the efficiency to a great extent, but there is a small gain in keeping them as thin as possible. A slight gain may also be obtained by sharpening the entrance edges of the inlet buckets. The blades are usually designed with a taper of from 4° to 6° included angle, the larger angles being used, in general, with the wider blades in order to increase the stiffness sufficiently to raise the natural frequencies above resonant values. Since this makes the blades rather thick near the base, it is customary to thin them, particularly if the blades are rather wide, for a distance of about 1" to 1 1/2" back from the outer tip, the metal being removed on the trailing side. Although it has not been found that this has a very appreciable effect on the efficiency (there are indications of a slight gain), this thinning helps to increase the natural frequency of the blade slightly and also to decrease the weight of the impeller.

9. Scallops. It is customary to have scallops in the outer portion of the web for four reasons: (a) to lighten the impeller by removing metal at a place where it does least good, (b) to decrease the stresses near the center of the impeller, (c) to decrease the impeller thrust by decreasing the effective area on which the pressure difference acts, and (d) to furnish a convenient place for balancing the impeller. The effect on the efficiency is small, but there is apparently a slight gain

when the scallops are used. The efficiency is not appreciably affected by beveling or rounding the edges of the scallops, at least not for customary web thicknesses.

10. Impeller Recess. Sometimes the impeller may be set in a recess in the casing, so that the web at the periphery lies entirely below the diffuser surface, and the web surface adjacent to the impeller air passage blends smoothly into the diffuser surface. Such a design, however, appears to be on the whole a little less efficient than the conventional arrangement in which the diffuser inner surface is extended in a straight line behind the impeller, making a definite outward "step" in the flow path from the impeller to the diffuser.

11. Impeller Clearance. The clearance between the impeller and casing may vary over a considerable range without effecting the efficiency very much, particularly for the wider impellers. However, it is desirable to limit the clearance to about 0.040"—0.045" on the front side, and to 0.030"—0.035" on the rear side, a somewhat greater clearance being customary on the front side because the direction of thrust is from rear to front in service operation. A little more clearance is allowable around the annulus than near the outer tips of the blades; if necessary, the clearance here may be about 0.045"--0.055".

Although the clearances just given are not large enough to cause appreciable loss, and are usually the minimum necessary to insure proper mechanical operation, it may be possible in some cases (small diameter and low speed) to decrease them,

and some small gain would be expected from doing so. Usually the most gain will be found to occur at large values of load coefficient where the compressor would normally not operate; the increase of efficiency in the usual operating range will ordinarily not be more than 0.01.

12. Pressure-equalizing Holes. These are used to reduce the impeller thrust, and are not necessary if the thrust bearings are adequate. Although they theoretically cause a loss, in tests made up to the present time no evidence has been found that they affect the efficiency appreciably. However, their effect would be expected to vary with the pressure ratio, impeller diameter, impeller clearance, and number, size, and location of holes, so that in certain cases it is possible that a detectable loss may result.

Ordinarily the total area of the holes is made about 75% of the impeller clearance leakage area measured at the outer diameter of the impeller--that is, the impeller circumference multiplied by the clearance on the rear side. The number of holes is made equal to, or half, the number of blades, depending upon stress considerations. The holes are located on a pitch circle with a diameter somewhat less than the annulus diameter, in order that sufficient flow may occur to permit reasonable equalization of the pressures (they cannot be completely equalized), but not close enough to the bore to unduly increase the stresses in this region.

13. Vanes on Rear Side of Impeller. It has been found in the case of one impeller that the addition of a narrow vane (5/32" wide) on the rear side of the impeller opposite each blade, although intended primarily to reduce the impeller thrust, actually increased the capacity and the efficiency at the higher

load coefficients. The vanes did not fit into a recess in the casing. They extended from the outer diameter to a point somewhat inside the annulus diameter. Since this gain has not yet been verified by test of similar vanes on another impeller, the question as to their general value is still held in abeyance.

14. Shrouded Impeller. With the impeller clearances previously specified, the addition of a shroud on the front side of the blades will result in only a small increase of efficiency, mostly at the higher load coefficients beyond the normal operating range. The gain in the usual operating region will not be more than 0.01 or 0.02, and hardly worth the manufacturing and mechanical difficulties involved.

VI. DIFFUSER DIMENSIONS

1. Inner Diameter. Ordinarily the diametral clearance between the impeller tip and the inside diameter of the vanes should be at least 15% of the impeller diameter, or

$$d_3 = 1.15\ d_2$$

If the outer diameter of the diffuser is so limited that this will not allow sufficient radial depth for good diffuser passages, the inner diameter may be brought closer to the impeller. Except possibly for very high tip speeds, this can be done without appreciable loss of efficiency, but it is undesirable if it can be avoided because of the increased magnitude of the impulses tending to cause synchronous vibration in the impeller.

2. Outer Diameter. Ordinarily, if space permits,

$$d_4 = 1.8\ d_2$$

for a vane diffuser, and

$$d_4 = 2.2\ d_2$$

for a vaneless diffuser. In airplane superchargers it is often impracticable to use such large diameters, and a ratio as low as 1.4 has been used for a vane diffuser without excessive loss of efficiency. The smaller the radial depth of diffuser, however, the greater the number of vanes required for good diffusing passages, and there may be objections to a large number of vanes.

3. Number of Vanes. The number of vanes may vary over a considerable range without affecting the efficiency very much, provided that the same total inlet area is maintained. Usually the number should be kept as small as possible in order to reduce to a minimum the frequency of the exciting impulses which tend to cause synchronous vibration in the impeller blades. This frequency, expressed in cycles per second, is

$$\frac{Nn}{60}v$$

and it should, if practicable, be made lower than the lowest natural frequency of the impeller. The latter is ordinarily made as high as possible.

It is usually necessary to use at least six diffuser vanes in order to obtain good passages. In the case of radial engines, the number of vanes is often made the same as the number of outlets in order to provide additional insurance of equal distribution to the cylinders. A vane passage can be considered to have good proportions when the inlet passage height is approximately equal to the width, and the length of the passage is approximately

four times the inlet passage height.

4. Diffuser Width. For a diffuser with parallel side walls, the axial width is ordinarily taken as the total tip width of an impeller blade plus the clearance on the rear side of the impeller. However, the width may be appreciably greater with good results, especially if the extra amount is added on the rear side, leaving the front approximately in line with the corners of the impeller blades. The terms "front" and "rear" refer to the open and shrouded sides of the impeller, respectively.

Sometimes the diffuser may be made with flaring walls, so that the diffusion process is carried out in both the axial and the radial directions. Although this may reduce the outer diameter for a given expansion, this type of diffuser is not quite so efficient as the radial type, particularly if the axial angle of divergence is large, so that high axial acceleration is required.

5. Inlet Passage Height. The inlet passage height is the dimension of a vane passage measured in a direction normal to the direction of flow at the passage entrance, as indicated in Figure 3.

To determine this height, the "effective" impeller exit area is first calculated from the formula

$$A_2' = A_2 \sin \beta_2$$

The inlet area of a single vane passage is the product of the passage height and the axial width. A_3, the total area for all passages, is usually made from 1.9 to 2.1 times as great as A_2'. On the average, for moderate impeller tip velocities,

$$\frac{A_3}{A_2'} = 2$$

The value of this ratio controls to a large extent the location of the characteristic curves with respect to load coefficient. By increasing the ratio, the curves are shifted to the right (to cover a range of higher load coefficients); by decreasing the ratio, the curves are shifted to the left (to cover a range of lower load coefficients). If the ratio is increased to as much as 2.3, the operating point on which the calculation is based will be quite close to the point at which unstable flow begins, even for moderate impeller tip velocities. If it is as low as 1.8, the pressure coefficient at the operating point will be appreciably lower than the maximum, but the temperature-rise ratio will not ordinarily be far from its peak value. If the ratio is as low as 1.65, both pressure coefficient and temperature-rise ratio may be definitely below their peak values. However, for very high impeller tip velocities, it may be necessary to make the ratio as low as 1.55 or 1.6 to insure stability of flow.

Having determined A_3, the inlet passage height, for equally spaced vanes, is given by

$$h_3 = \frac{A_3}{n_v e_3}$$

For unequally spaced vanes, the total of the passage heights for all the vane passages would be maintained the same, but the individual passage heights would be made proportional to the angles subtended by the corresponding vane inlet tips. This is discussed further under Spacing of Vanes.

It is to be noted that this method is concerned more with maintenance of a proper diffuser inlet area than with a theoretical angle, just as in the case of the impeller entrance buckets. While there is, of course, some connection between the angle and the area, it has been found that the angle at the tip may be varied over a considerable range without affecting the performance much so long as the inlet area is maintained substantially the same.

6. Rate of Expansion. Ordinarily the rate of expansion should be such that the passage height (measured normal to the direction of flow) increases at the rate of 1" for every 10" of passage length for diffusers of conventional type. This rate may vary from 1" in 7" to 1" in 14" if necessary without excessive loss, but the extremes are ordinarily not to be recommended. When there is diffusion in the axial direction also, the rate of expansion must be based on a corresponding change in the cross-sectional areas.

7. Expansion Ratio. The expansion ratio, or ratio of diffuser vane exit area to inlet area (both measured normal to the direction of flow), should ordinarily be at least 1.5, and preferably 1.6. Values as low as 1.4 have been used, but this is not recommended, as a loss would be expected with even moderate impeller tip velocities. Ratios as high as 2 have been employed at times without much detrimental effect on the efficiency. The exit area should be selected with some regard to the area of the scroll or collector passage into which the diffuser discharges, since sudden changes of velocity or pressure should be avoided.

8. Vane Thickness. Ordinarily a thin vane is desirable from efficiency considerations, and the thickness should not exceed 1/8", or, at most, 3/16", unless necessary for strength or for other good reasons. A slight taper is required for casting purposes, and there should be a fillet of 1/8" or 3/16" at the base of the vanes. If it is necessary for shafts, pipes, etc., to pass through the diffuser, vanes should be faired around them to provide smooth, continuous passages, and if it is necessary to thicken one or more vanes for this purpose, it may be found desirable to make all the vanes the same shape in order to promote symmetry and equal distribution.

9. Diffuser Surface: At moderate impeller tip velocities a small gain in efficiency (of the order of 0.01 to 0.02) may be realized by polishing the diffuser surface, but hitherto, at least, this gain has not been considered sufficient to compensate for the increased cost. It is possible that the gain will be greater with very high velocities, but no data are available at present to confirm this.

10. Inlet Tips of Vanes. Usually a small gain is obtained by sharpening the inlet tips, but the effect is often difficult to detect. Rounding the tips with a large radius usually results in a loss.

11. Spacing of Vanes. Usually the vanes will be equally spaced. In some cases, however, either because shafts or other obstructions pass through the diffuser, or in order to minimize the danger of synchronous vibration, the vanes may be unequally

spaced. In such cases both the inlet and exit passage heights should be approximately proportional to their corresponding arcs; i.e., to the subtended angles, with the total inlet area the same as if the vanes were equally spaced. Usually it will not be possible to keep the expansion ratio and rate of expansion exactly the same in all the passages, and a compromise must be worked out which will retain so far as practicable the proportionality of passage heights and arcs, while at the same time keeping reasonable expansion rates and ratios. The diffuser inlet area should not be compromised, however, and the proportionality of inlet passage heights and arcs should be distinctly favored.

12. Vaneless Diffuser: A supercharger with a vane diffuser will normally have a higher peak efficiency and a smaller outer diameter than a corresponding supercharger with a vaneless diffuser. However, the vaneless diffuser is occasionally preferred because the characteristic curves are not so peaked, and because the cost is less.

It has been found desirable in the case of a vaneless diffuser to increase the impeller exit angle β_2 to at least 12°, and sometimes to 15°. An average value would be 14°. The diffuser converges from the impeller tip to a section with parallel side walls, of axial width considerably less than that of the impeller, and then diverges again at the periphery to make a gradual transition into the scroll or collector passage. The axial width of the parallel portion is made such that the

vortex angle $_3$ will be about 35°. The width is calculated from the relation

$$e_3 = e_2 \frac{\tan \beta_2}{\tan \beta_3}$$

The included angle of both the converging and diverging portions should be about 30°, but this may be increased to as much as 45° if the radial space available is limited. Preferably this angle should be divided equally on both sides of the radial plane, but if necessary may be taken entirely on one side. The radial lengths of the converging and diverging sections should be approximately equal.

VII. SCROLL AND COLLECTOR RING

1. Location. Best results are obtained if the passage can be located entirely outside the diffuser, but this is often not practicable. If the passage is brought in toward the center, about half the area should be located on each side of the diffuser, since this will permit closest approach to the ideal position. It is not desirable to have a long, narrow section of area along one side of the diffuser and most of the area on the other side; in such cases it would be better to have all the area on one side. It is never desirable to bring the scroll or collector passage in toward the center so much that any portion lies within the inner diameter of the diffuser, but occasionally this may be unavoidable.

2. Shape. There is apparently little difference in efficiency between the circular and the nearly square sections. The latter, however, is usually more economical of space, and

since it is at least as efficient, is usually used rather than the circular shape. Long, elongated sections are usually to be avoided, but it may be necessary at times to use shapes which are not ideal in order to obtain the necessary area.

3. Type of Outlet. A tangential outlet is preferable for a scroll passage. With such an outlet the efficiency may be increased about 0.02 to 0.04 at the higher load coefficients as compared with a radial outlet for the same supercharger. It is sometimes possible to use a semi-tangential outlet which retains some of the advantages of the tangential design and at the same time discharges the air in an approximately radial direction at the desired place.

If it is necessary to use a radial outlet, the scroll should be calculated as though a tangential outlet were to be used, the fictitious outlet being assumed in a plane passing through the center line of the radial outlet. The actual area of the radial outlet is made about 10% greater than the calculated area of the fictitious tangential outlet, and the passage is gradually blended into the calculated scroll at a section about 45° from the center line of the outlet.

In the case of radial engine superchargers with a number of outlets equally spaced around the collector passage, it is probable that the efficiency during engine operation will not differ much whether the outlets are tangential or radial. While it is likely that the flow in the collector passage is mostly in one direction, it is entirely possible that at its maximum

induction rate a cylinder will draw air from both directions. For this reason it is probable that the radial outlet is at least as good as the tangential, and possibly a little better. Generous radii should be used at the junctions of the outlets and collector passage.

4. Scroll Area. If a mixture of fuel and air passes through the supercharger, the scroll exit area is usually such that the exit velocity is about 150 ft/sec. at rated flow. Larger areas would be likely to result in fuel deposition, particularly at engine idling speeds. If air alone passes through the supercharger, it is desirable to decrease this velocity to 100 ft/sec., although somewhat higher velocities could be used without excessive losses.

Theoretically, the area at the small end of the scroll should be zero, but it has been found better to make the small end area from one-quarter to one-third of the maximum area, and to increase uniformly, as nearly as is practicable, to the maximum area. There is usually an opening at the junction of the large and small ends, permitting some recirculation and equalization of pressures. Tests indicate that this is somewhat better, on the whole, than having no communication at all between the sections, although the effect on the efficiency in most cases is very small.

5. Collector Passage Area. The flow in the constant area collector passage of a supercharger for a radial engine is so intermittent and irregular that it is very difficult to calculate

the cross-sectional area from rational formulas. The following formulas, however, which have some rational basis, have been found to give good results.

For 7- and 9-cylinder engines

$$A_5 = 2600 \frac{D}{Nd_2}$$

For 14-cylinder engines

$$A_5 = 1300 \frac{D}{Nd_2}$$

The difference in constants is due to the different character of the flow arising from the difference in firing orders.

It has also been found that a reasonable area may be calculated by assuming a fictitious equivalent velocity of about 275 ft/sec., and applying this to the volume flow at intake manifold conditions, That is,

$$A_5 = \frac{144}{60} \frac{q_E}{275}$$

6. Guide Vanes. It is customary to insert vanes in scroll passages of large area, especially near the large end. These vanes serve mostly for mechanical support, but can be shaped so as to guide the air flow, particularly at the bend of a radial outlet. However, round sections of the smallest practicable diameter are usually at least equal to, and often better than, airfoil shapes, and should ordinarily be used unless mechanical considerations dictate otherwise.

VIII. INLET PASSAGE

1. General. The ideal inlet, from the supercharger viewpoint, would be one in which the impeller takes in air directly from atmosphere, or through a short length of axial passage. Usually, however, an intake duct with an elbow is necessary. Because of the wide variety of conditions and limitations met in actual installations, no generally applicable design can be specified. However, there should always be as much axial length as possible in front of the impeller, and if sufficient length cannot be obtained, suitable guide vanes should be inserted to make the flow into the impeller uniform. Some experimentation is usually necessary to determine the best number and location of these vanes, but a central vane with plane perpendicular to the plane of the impeller is nearly always desirable to prevent "whirl" at the impeller entrance. Ordinarily the vanes should be kept about 1" away from the impeller entrance buckets to minimize the possibility of synchronous vibration.

The area of the intake passage should be between 10% and 15% more than the circular area corresponding to the annulus diameter of the impeller. The "doughnut" shape is not to be recommended, and there should not be much excess area on the side opposite the intake passage. The general shape recommended, particularly with an overhung impeller, is shown in Figure 4, but of course it is possible to have many variations of this design. If there is some restriction in front of the impeller, caused by a bearing support, gear, or similar obstruction, it may be necessary to depart considerably from this shape for best results. No particular advantage has been found from use of the scroll type inlet passage, and in many cases it is definitely disadvantageous.

TABLES OF ANNULUS DIAMETER - PART I - $d_a = \sqrt{1253\left(\frac{q_1}{N}\right)^{2/3} + d_o^2}$

q_1/N \ d_o =	.5	.75	1.0	1.25	1.5	1.75	2.0	2.25	2.5	2.75
0	.50	.75	1.00	1.25	1.50	1.75	2.00	2.25	2.50	2.75
.01	2.36	2.43	2.52	2.63	2.76	2.90	3.06	3.22	3.40	3.59
.02	3.08	3.13	3.19	3.28	3.39	3.50	3.64	3.78	3.93	4.10
.03	3.51	3.56	3.62	3.70	3.79	3.89	4.01	4.14	4.28	4.43
.04	3.86	3.90	3.96	4.03	4.11	4.22	4.32	4.45	4.57	4.71
.05	4.16	4.20	4.26	4.31	4.39	4.48	4.59	4.70	4.83	4.96
.06	4.41	4.44	4.49	4.55	4.62	4.72	4.82	4.92	5.04	5.17
.07	4.63	4.66	4.71	4.77	4.84	4.93	5.02	5.12	5.24	5.36
.08	4.85	4.88	4.93	4.98	5.06	5.13	5.23	5.32	5.44	5.56
.09	5.05	5.07	5.12	5.17	5.24	5.31	5.40	5.50	5.61	5.72
.10	5.22	5.24	5.29	5.34	5.40	5.48	5.56	5.66	5.76	5.87
.11	5.39	5.42	5.46	5.51	5.58	5.65	5.73	5.82	5.92	6.03
.12	5.54	5.57	5.61	5.66	5.72	5.79	5.87	5.96	6.06	6.17
.13	5.68	5.71	5.75	5.79	5.85	5.92	6.00	6.09	6.19	6.29
.14	5.84	5.86	5.89	5.95	6.00	6.07	6.15	6.23	6.33	6.43
.15	5.96	5.99	6.03	6.08	6.13	6.20	6.27	6.35	6.46	6.56
.16	6.10	6.13	6.16	6.21	6.26	6.33	6.40	6.49	6.58	6.68
.17	6.23	6.25	6.29	6.33	6.39	6.45	6.52	6.60	6.69	6.79
.18	6.34	6.36	6.40	6.44	6.49	6.55	6.63	6.71	6.79	6.89
.19	6.45	6.47	6.51	6.55	6.60	6.66	6.73	6.81	6.90	6.99
.20	6.57	6.59	6.63	6.67	6.72	6.78	6.85	6.93	7.01	7.10
.21	6.67	6.69	6.73	6.77	6.82	6.88	6.95	7.02	7.11	7.20
.22	6.77	6.80	6.83	6.87	6.92	6.98	7.05	7.12	7.20	7.29
.23	6.88	6.90	6.93	6.97	7.02	7.08	7.14	7.22	7.30	7.39
.24	6.97	7.00	7.03	7.07	7.12	7.17	7.24	7.31	7.39	7.48
.25	7.04	7.07	7.10	7.14	7.18	7.24	7.30	7.38	7.46	7.54
.26	7.16	7.18	7.21	7.25	7.30	7.36	7.42	7.49	7.57	7.66
.27	7.25	7.27	7.30	7.34	7.39	7.44	7.50	7.57	7.65	7.74
.28	7.34	7.36	7.39	7.43	7.48	7.53	7.59	7.66	7.74	7.82
.29	7.43	7.45	7.48	7.51	7.56	7.61	7.67	7.74	7.82	7.90
.30	7.51	7.53	7.56	7.60	7.64	7.69	7.76	7.82	7.90	7.98
.31	7.59	7.61	7.64	7.68	7.72	7.77	7.83	7.90	7.98	8.06
.32	7.67	7.69	7.72	7.76	7.80	7.85	7.91	7.98	8.05	8.14
.33	7.75	7.77	7.80	7.84	7.88	7.93	7.99	8.06	8.13	8.21
.34	7.83	7.85	7.88	7.92	7.96	8.01	8.06	8.13	8.20	8.28
.35	7.90	7.92	7.95	7.99	8.03	8.08	8.14	8.20	8.27	8.35
.36	7.98	8.00	8.03	8.06	8.10	8.15	8.21	8.27	8.34	8.42
.37	8.05	8.07	8.10	8.13	8.17	8.22	8.28	8.35	8.42	8.49
.38	8.12	8.14	8.17	8.20	8.24	8.29	8.35	8.41	8.48	8.56
.39	8.19	8.21	8.24	8.27	8.31	8.36	8.42	8.48	8.55	8.63
.40	8.26	8.28	8.31	8.34	8.38	8.43	8.49	8.55	8.62	8.69
.41	8.33	8.35	8.38	8.41	8.45	8.50	8.55	8.61	8.68	8.76
.42	8.40	8.42	8.44	8.48	8.52	8.57	8.62	8.68	8.75	8.82
.43	8.47	8.48	8.51	8.54	8.58	8.63	8.68	8.74	8.81	8.89
.44	8.52	8.54	8.57	8.60	8.64	8.69	8.74	8.80	8.87	8.94
.45	8.59	8.61	8.63	8.67	8.71	8.75	8.81	8.87	8.93	9.01
.46	8.66	8.67	8.70	8.73	8.77	8.82	8.87	8.93	9.00	9.07
.47	8.72	8.74	8.76	8.79	8.83	8.88	8.93	8.99	9.05	9.13
.48	8.78	8.80	8.82	8.85	8.89	8.94	8.99	9.05	9.11	9.18
.49	8.84	8.86	8.88	8.91	8.95	9.00	9.05	9.11	9.17	9.24
.50	8.90	8.92	8.94	8.97	9.01	9.06	9.11	9.17	9.23	9.30

TABLES OF ANNULUS DIAMETER - PART II - $d_a = \sqrt{125.3\left(\frac{q_1}{N}\right)^{2/3} + d_o^2}$

$\frac{q_1}{N}$ \ d_o =	3.0	3.25	3.50	3.75	4.0	4.25	4.5	4.75	5.0
0	3.00	3.25	3.50	3.75	4.00	4.25	4.50	4.75	5.00
.01	3.79	3.99	4.19	4.41	4.62	4.84	5.06	5.28	5.51
.02	4.27	4.45	4.63	4.82	5.02	5.22	5.43	5.64	5.85
.03	4.59	4.76	4.94	5.11	5.30	5.49	5.69	5.89	6.09
.04	4.87	5.02	5.19	5.37	5.54	5.73	5.91	6.10	6.30
.05	5.10	5.25	5.41	5.58	5.75	5.93	6.11	6.29	6.49
.06	5.31	5.45	5.61	5.77	5.93	6.10	6.28	6.44	6.55
.07	5.50	5.64	5.78	5.94	6.10	6.27	6.44	6.62	6.80
.08	5.68	5.82	5.96	6.11	6.27	6.43	6.60	6.77	6.95
.09	5.85	5.98	6.12	6.26	6.42	6.58	6.74	6.91	7.08
.10	6.00	6.12	6.26	6.40	6.55	6.71	6.87	7.04	7.21
.11	6.15	6.28	6.41	6.51	6.70	6.81	7.01	7.17	7.34
.12	6.28	6.40	6.54	6.67	6.82	6.96	7.12	7.28	7.45
.13	6.40	6.52	6.65	6.79	6.93	7.08	7.23	7.39	7.55
.14	6.54	6.66	6.79	6.92	7.06	7.20	7.35	7.51	7.67
.15	6.66	6.78	6.90	7.03	7.16	7.31	7.45	7.61	7.77
.16	6.78	6.90	7.02	7.15	7.28	7.42	7.57	7.72	7.87
.17	6.89	7.00	7.13	7.25	7.38	7.52	7.67	7.81	7.97
.18	6.99	7.10	7.29	7.35	7.48	7.61	7.82	7.90	8.06
.19	7.10	7.20	7.32	7.44	7.57	7.71	7.85	7.99	8.15
.20	7.20	7.31	7.43	7.55	7.68	7.81	7.95	8.09	8.28
.21	7.30	7.40	7.52	7.64	7.76	7.89	8.03	8.17	8.32
.22	7.39	7.50	7.61	7.73	7.85	7.98	8.12	8.26	8.41
.23	7.49	7.59	7.70	7.82	7.94	8.07	8.20	8.34	8.49
.24	7.58	7.68	7.79	7.90	8.02	8.15	8.28	8.42	8.57
.25	7.64	7.74	7.85	7.96	8.08	8.21	8.34	8.48	8.62
.26	7.75	7.85	7.96	8.07	8.19	8.31	8.44	8.58	8.72
.27	7.83	7.93	8.04	8.15	8.27	8.39	8.52	8.65	8.79
.28	7.91	8.01	8.12	8.23	8.34	8.46	8.59	8.73	8.87
.29	7.99	8.09	8.19	8.30	8.42	8.54	8.67	8.80	8.94
.30	8.07	8.17	8.27	8.38	8.49	8.61	8.74	8.87	9.01
.31	8.15	8.24	8.34	8.45	8.57	8.69	8.81	8.94	9.08
.32	8.22	8.32	8.42	8.53	8.64	8.76	8.88	9.01	9.14
.33	8.30	8.39	8.49	8.60	8.71	8.83	8.95	9.08	9.21
.34	8.37	8.46	8.56	8.67	8.78	8.89	9.02	9.14	9.28
.35	8.44	8.53	8.63	8.73	8.84	8.96	9.08	9.21	9.34
.36	8.51	8.60	8.70	8.80	8.91	9.03	9.15	9.27	9.40
.37	8.58	8.67	8.77	8.87	8.98	9.09	9.21	9.33	9.46
.38	8.64	8.73	8.83	8.93	9.04	9.15	9.27	9.39	9.53
.39	8.71	8.80	8.90	9.00	9.10	9.21	9.33	9.46	9.59
.40	8.78	8.87	8.96	9.06	9.17	9.28	9.40	9.52	9.64
.41	8.84	8.93	9.02	9.12	9.23	9.34	9.46	9.58	9.70
.42	8.90	8.99	9.08	9.18	9.29	9.40	9.52	9.64	9.76
.43	8.97	9.05	9.15	9.25	9.35	9.46	9.57	9.69	9.82
.44	9.02	9.11	9.20	9.30	9.40	9.51	9.63	9.75	9.87
.45	9.08	9.17	9.26	9.36	9.46	9.57	9.68	9.80	9.93
.46	9.15	9.23	9.32	9.42	9.52	9.63	9.74	9.86	9.98
.47	9.21	9.29	9.38	9.48	9.58	9.69	9.80	9.92	10.03
.48	9.26	9.35	9.44	9.53	9.63	9.74	9.85	9.97	10.09
.49	9.32	9.40	9.49	9.59	9.69	9.79	9.91	10.02	10.14
.50	9.38	9.46	9.55	9.64	9.74	9.85	9.96	10.07	10.19

TABLES OF ROOT MEAN SQUARE DIAMETER - PART I - $d_m = \sqrt{\frac{d_a^2 + d_o^2}{2}}$

d_a \ d_o =	.5	.75	1.0	1.25	1.5	1.75	2.0	2.25	2.5	2.75
2.0	1.46	1.51	1.58	1.67	1.77	1.88	2.00	2.13	2.26	2.40
2.2	1.59	1.64	1.71	1.79	1.88	1.99	2.10	2.22	2.35	2.49
2.4	1.73	1.78	1.84	1.91	2.00	2.10	2.21	2.33	2.45	2.58
2.6	1.87	1.91	1.97	2.04	2.12	2.22	2.32	2.43	2.55	2.68
2.8	2.01	2.05	2.10	2.17	2.25	2.33	2.43	2.54	2.65	2.77
3.0	2.15	2.19	2.24	2.30	2.37	2.45	2.55	2.65	2.76	2.88
3.2	2.29	2.32	2.37	2.43	2.50	2.58	2.67	2.77	2.87	2.98
3.4	2.43	2.46	2.51	2.56	2.63	2.70	2.79	2.88	2.98	3.09
3.6	2.57	2.60	2.64	2.69	2.76	2.83	2.91	3.00	3.10	3.20
3.8	2.71	2.74	2.78	2.83	2.89	2.96	3.04	3.12	3.22	3.32
4.0	2.85	2.88	2.92	2.96	3.02	3.09	3.16	3.25	3.34	3.43
4.2	2.99	3.02	3.05	3.10	3.15	3.22	3.29	3.37	3.46	3.55
4.4	3.13	3.16	3.19	3.23	3.29	3.35	3.42	3.49	3.58	3.67
4.6	3.27	3.30	3.33	3.37	3.42	3.48	3.55	3.62	3.70	3.79
4.8	3.41	3.44	3.47	3.51	3.56	3.61	3.68	3.75	3.83	3.91
5.0	3.55	3.58	3.61	3.64	3.69	3.75	3.81	3.88	3.95	4.03
5.2	3.69	3.71	3.74	3.78	3.83	3.88	3.94	4.01	4.08	4.16
5.4	3.83	3.85	3.88	3.92	3.96	4.01	4.07	4.14	4.21	4.29
5.6	3.98	4.00	4.02	4.06	4.10	4.15	4.21	4.27	4.34	4.41
5.8	4.12	4.14	4.16	4.20	4.24	4.28	4.34	4.40	4.47	4.54
6.0	4.26	4.28	4.30	4.33	4.37	4.42	4.47	4.53	4.60	4.67
6.2	4.40	4.42	4.44	4.47	4.51	4.56	4.61	4.66	4.73	4.80
6.4	4.54	4.56	4.58	4.61	4.65	4.69	4.74	4.80	4.86	4.93
6.6	4.68	4.70	4.72	4.75	4.79	4.83	4.88	4.93	4.99	5.06
6.8	4.82	4.84	4.86	4.89	4.92	4.96	5.01	5.06	5.12	5.19
7.0	4.96	4.98	5.00	5.03	5.06	5.10	5.15	5.20	5.26	5.32
7.2	5.10	5.12	5.14	5.17	5.20	5.24	5.28	5.33	5.39	5.45
7.4	5.24	5.26	5.28	5.31	5.34	5.38	5.42	5.47	5.52	5.58
7.6	5.39	5.40	5.42	5.45	5.48	5.51	5.56	5.60	5.66	5.72
7.8	5.53	5.54	5.56	5.59	5.62	5.65	5.69	5.74	5.79	5.85
8.0	5.67	5.68	5.70	5.73	5.76	5.79	5.83	5.88	5.93	5.98
8.2	5.81	5.82	5.84	5.86	5.89	5.93	5.97	6.01	6.06	6.12
8.4	5.95	5.96	5.98	6.00	6.03	6.07	6.11	6.15	6.20	6.25
8.6	6.09	6.10	6.12	6.14	6.17	6.20	6.24	6.28	6.33	6.38
8.8	6.23	6.24	6.26	6.28	6.31	6.34	6.38	6.42	6.47	6.52
9.0	6.37	6.38	6.40	6.42	6.45	6.48	6.52	6.56	6.60	6.65
9.2	6.52	6.53	6.54	6.56	6.59	6.62	6.66	6.70	6.74	6.79
9.4	6.66	6.67	6.68	6.70	6.73	6.76	6.79	6.83	6.88	6.93
9.6	6.80	6.81	6.83	6.85	6.87	6.90	6.93	6.97	7.01	7.06
9.8	6.94	6.95	6.97	6.99	7.01	7.04	7.07	7.11	7.15	7.20
10.0	7.08	7.09	7.11	7.13	7.15	7.18	7.21	7.25	7.29	7.33
10.2	7.22	7.23	7.25	7.27	7.29	7.32	7.35	7.39	7.43	7.47
10.4	7.36	7.37	7.39	7.41	7.43	7.46	7.49	7.52	7.56	7.61
10.6	7.50	7.51	7.53	7.55	7.57	7.60	7.63	7.66	7.70	7.74
10.8	7.65	7.66	7.67	7.69	7.71	7.74	7.77	7.80	7.84	7.88
11.0	7.79	7.80	7.81	7.83	7.85	7.88	7.91	7.94	7.98	8.02
11.2	7.93	7.94	7.95	7.97	7.99	8.02	8.05	8.08	8.11	8.15
11.4	8.07	8.08	8.09	8.11	8.13	8.15	8.18	8.21	8.25	8.29
11.6	8.21	8.22	8.23	8.25	8.27	8.29	8.32	8.35	8.39	8.43
11.8	8.35	8.36	8.37	8.39	8.41	8.43	8.46	8.49	8.53	8.57
12.0	8.49	8.50	8.51	8.53	8.55	8.57	8.60	8.63	8.67	8.71

TABLES OF ROOT MEAN SQUARE DIAMETER - PART II - $d_m = \sqrt{\frac{d_a^2 + d_o^2}{2}}$

d_a \ d_o =	3.0	3.25	3.50	3.75	4.0	4.25	4.5	4.75	5.0
2.0	2.55	2.70	2.85	3.00	3.16	3.32	3.48	3.64	3.81
2.2	2.63	2.77	2.92	3.07	3.23	3.38	3.54	3.70	3.86
2.4	2.72	2.86	3.00	3.15	3.30	3.45	3.61	3.76	3.92
2.6	2.81	2.94	3.08	3.23	3.37	3.52	3.67	3.83	3.99
2.8	2.90	3.03	3.17	3.31	3.45	3.60	3.75	3.90	4.05
3.0	3.00	3.13	3.26	3.40	3.54	3.68	3.82	3.97	4.12
3.2	3.10	3.22	3.35	3.48	3.62	3.76	3.90	4.05	4.20
3.4	3.21	3.33	3.45	3.58	3.71	3.85	3.99	4.13	4.28
3.6	3.31	3.43	3.55	3.68	3.81	3.94	4.07	4.21	4.36
3.8	3.42	3.53	3.65	3.77	3.90	4.03	4.16	4.30	4.44
4.0	3.53	3.64	3.76	3.88	4.00	4.13	4.26	4.39	4.53
4.2	3.65	3.76	3.87	3.98	4.10	4.22	4.35	4.48	4.62
4.4	3.77	3.87	3.98	4.09	4.21	4.33	4.45	4.58	4.71
4.6	3.88	3.98	4.09	4.20	4.31	4.43	4.55	4.67	4.80
4.8	4.00	4.10	4.20	4.31	4.42	4.53	4.65	4.77	4.90
5.0	4.12	4.22	4.32	4.42	4.53	4.64	4.76	4.88	5.00
5.2	4.25	4.34	4.43	4.53	4.64	4.75	4.86	4.98	5.10
5.4	4.37	4.46	4.55	4.65	4.75	4.86	4.97	5.08	5.20
5.6	4.49	4.58	4.67	4.77	4.87	4.97	5.08	5.19	5.31
5.8	4.62	4.70	4.79	4.88	4.98	5.08	5.19	5.30	5.41
6.0	4.74	4.82	4.91	5.00	5.10	5.20	5.30	5.41	5.52
6.2	4.87	4.95	5.03	5.12	5.22	5.32	5.42	5.52	5.63
6.4	5.00	5.08	5.16	5.25	5.34	5.43	5.53	5.63	5.74
6.6	5.13	5.20	5.28	5.37	5.46	5.55	5.65	5.75	5.85
6.8	5.26	5.33	5.41	5.49	5.58	5.67	5.77	5.87	5.97
7.0	5.39	5.46	5.53	5.61	5.70	5.79	5.88	5.98	6.08
7.2	5.52	5.59	5.66	5.74	5.82	5.91	6.00	6.10	6.20
7.4	5.65	5.72	5.79	5.87	5.95	6.03	6.12	6.22	6.32
7.6	5.78	5.85	5.92	5.99	6.07	6.16	6.25	6.34	6.43
7.8	5.91	5.98	6.05	6.12	6.20	6.28	6.37	6.46	6.55
8.0	6.04	6.11	6.17	6.25	6.32	6.40	6.49	6.58	6.67
8.2	6.17	6.24	6.30	6.38	6.45	6.53	6.61	6.70	6.79
8.4	6.31	6.37	6.43	6.50	6.58	6.66	6.74	6.82	6.91
8.6	6.44	6.50	6.57	6.63	6.71	6.78	6.86	6.95	7.03
8.8	6.57	6.63	6.70	6.76	6.83	6.91	6.99	7.07	7.16
9.0	6.71	6.77	6.83	6.89	6.96	7.04	7.12	7.20	7.28
9.2	6.84	6.90	6.96	7.02	7.09	7.17	7.24	7.32	7.40
9.4	6.98	7.03	7.09	7.16	7.22	7.29	7.37	7.45	7.53
9.6	7.11	7.17	7.23	7.29	7.35	7.42	7.50	7.57	7.65
9.8	7.25	7.30	7.36	7.42	7.48	7.55	7.62	7.70	7.78
10.0	7.38	7.43	7.49	7.55	7.62	7.68	7.75	7.83	7.91
10.2	7.52	7.57	7.62	7.68	7.75	7.81	7.88	7.96	8.03
10.4	7.65	7.70	7.76	7.82	7.88	7.94	8.01	8.08	8.16
10.6	7.79	7.84	7.89	7.95	8.01	8.07	8.14	8.21	8.29
10.8	7.93	7.98	8.03	8.08	8.14	8.21	8.27	8.34	8.41
11.0	8.06	8.11	8.16	8.22	8.28	8.34	8.40	8.47	8.54
11.2	8.20	8.25	8.30	8.35	8.41	8.47	8.53	8.60	8.67
11.4	8.34	8.38	8.43	8.49	8.54	8.60	8.67	8.73	8.80
11.6	8.47	8.52	8.57	8.62	8.68	8.74	8.80	8.86	8.93
11.8	8.61	8.65	8.70	8.75	8.81	8.87	8.93	8.99	9.06
12.0	8.75	8.79	8.84	8.89	8.94	9.00	9.06	9.13	9.19

Values of "Y" for Normal Air and Perfect Diatomic Gases

$$(Y = (r^{0.283} - 1)$$

r	0°	1	2	3	4	.5	6	7	8	9
1.00	0.00	000	028	057	085	113	141	169	198	226	254
1.01		282	310	338	366	394	422	450	478	506	534
1.02		562	590	618	646	673	701	729	757	785	812
1.03		840	868	895	923	951	978	006	034	061	089
1.04	0.01	116	144	171	199	226	253	281	308	336	363
1.05		390	418	445	472	500	527	554	581	608	636
1.06		663	690	717	744	771	798	825	852	879	906
1.07		933	960	987	014	041	068	095	122	148	175
1.08	0.02	202	229	255	282	309	336	362	389	416	442
1.09		469	495	522	549	576	602	628	655	681	708
1.10		734	760	787	813	840	866	892	919	945	971
1.11		997	024	050	076	102	129	155	181	207	233
1.12	0.03	259	285	311	337	363	389	415	441	467	493
1.13		519	545	571	597	623	649	675	700	726	752
1.14		778	804	829	855	881	906	932	958	983	009
1.15	0.04	035	060	086	111	137	162	188	213	239	264
1.16		290	315	341	366	391	417	442	467	493	518
1.17		543	569	594	619	644	670	695	720	746	770
1.18		796	821	846	871	896	921	946	971	996	021
1.19	0.05	046	071	096	121	146	171	196	221	245	270
1.20		295	320	345	370	394	419	444	469	493	518
1.21		543	567	592	617	641	666	691	715	740	764
1.22		789	813	838	862	887	911	936	960	985	009
1.23	0.06	034	058	082	107	131	155	180	204	228	253
1.24		277	301	325	350	374	398	422	446	470	495
1.25		519	543	567	591	615	639	663	687	711	735
1.26		759	783	807	831	855	879	903	927	951	974
1.27		998	022	046	070	094	117	141	165	189	212
1.28	0.07	236	260	283	307	331	354	378	402	425	449
1.29		472	496	520	543	567	590	614	637	661	684
1.30		708	731	754	778	801	825	848	871	895	918
1.31		941	965	988	011	035	058	081	104	128	151
1.32	0.08	174	197	220	243	267	290	313	336	359	382
1.33		405	428	451	474	497	520	543	566	589	612
1.34		635	658	681	704	727	750	773	795	818	841
1.35		864	887	910	932	955	978	001	023	046	069
1.36	0.09	092	114	137	160	182	205	228	250	273	295
1.37		318	341	363	386	408	431	453	476	498	521
1.38		543	566	588	611	633	655	678	700	723	745
1.39		767	790	812	834	857	879	901	923	948	968
1.40		990	012	035	057	079	101	123	145	168	190
1.41	0.10	212	234	256	278	300	322	344	366	389	411
1.42		433	455	477	499	521	542	564	586	608	630
1.43		652	674	696	718	740	761	783	805	827	849
1.44		871	892	914	936	958	979	001	023	045	066
1.45	0.11	088	110	131	153	175	196	218	239	261	283
1.46		304	326	347	369	390	412	433	455	476	498
1.47		520	541	562	584	605	627	648	669	691	712
1.48		734	755	776	798	819	840	862	883	904	925
1.49		947	968	989	010	032	053	074	095	116	138
1.50	0.12	159	180	201	222	243	264	286	307	328	349
1.51		370	391	412	433	454	475	496	517	538	559
1.52		580	601	622	643	664	685	706	726	747	768
1.53		789	810	831	852	872	893	914	935	956	977
1.54		997	018	039	060	080	101	122	142	163	184
1.55	0.13	205	225	246	266	287	308	328	349	370	390
1.56		411	431	452	472	493	513	534	554	575	595
1.57		616	636	657	677	698	718	739	759	780	800
1.58		820	841	861	881	902	922	942	963	983	003
1.59	0.14	024	044	064	085	105	125	145	165	186	206
1.60		226	246	267	287	307	327	347	367	387	408
1.61		428	448	468	488	508	528	548	568	588	608
1.62		628	648	668	688	708	728	748	768	788	808
1.63		828	848	868	888	908	928	948	968	988	007
1.64	0.15	027	047	067	087	107	126	146	166	186	206
1.65		225	245	265	284	304	324	344	363	383	403
1.66		423	442	462	481	501	521	540	560	580	599
1.67		619	638	658	678	697	717	736	756	775	795
1.68		814	834	853	873	892	912	931	951	970	990
1.69	0.16	009	028	048	067	087	106	125	145	164	184
1.70		203	222	242	261	280	299	319	338	357	377
1.71		396	415	434	454	473	492	511	531	550	569
1.72		588	607	626	646	665	684	703	722	741	760
1.73		780	799	818	837	856	875	894	913	932	951
1.74		970	989	008	027	046	065	084	103	122	141
1.75	0.17	160	179	198	217	236	255	274	292	311	330
1.76		349	368	387	406	425	443	462	481	500	519
1.77		538	556	575	594	613	631	650	669	688	706
1.78		725	744	762	781	800	818	837	856	874	893
1.79		912	930	949	968	986	005	023	042	061	079
1.80	0.18	098	116	135	153	172	191	209	228	246	265
1.81		283	302	320	339	357	376	394	412	431	449
1.82		468	486	505	523	541	560	578	596	615	633
1.83		652	670	688	707	725	743	762	780	798	816
1.84		835	853	871	890	908	926	944	962	981	999
1.85	0.19	017	035	054	072	090	108	126	144	163	181
1.86		199	217	235	253	271	289	308	326	344	362
1.87		380	398	416	434	452	470	488	506	524	542
1.88		560	578	596	614	632	650	668	686	704	722
1.89		740	758	776	794	811	829	847	865	883	901
1.90		919	937	954	972	990	008	026	044	061	079
1.91	0.20	097	115	133	150	168	186	204	221	239	257
1.92		275	292	310	328	345	363	381	399	416	434
1.93		452	469	487	504	522	540	557	575	593	610
1.94		628	645	663	681	698	716	733	751	768	786
1.95		804	821	839	856	874	891	909	926	944	961
1.96		979	996	013	031	048	066	083	101	118	135
1.97	0.21	153	170	188	205	222	240	257	275	292	309
1.98		327	344	361	379	396	413	431	448	465	482

Proportional Parts

29		28	
1	2.9	1	2.8
2	5.8	2	5.6
3	8.7	3	8.4
4	11.6	4	11.2
5	14.5	5	14.0
6	17.4	6	16.8
7	20.3	7	19.6
8	23.2	8	22.4
9	26.1	9	25.2

27		26	
1	2.7	1	2.6
2	5.4	2	5.2
3	8.1	3	7.8
4	10.8	4	10.4
5	13.5	5	13.0
6	16.2	6	15.6
7	18.9	7	18.2
8	21.6	8	20.8
9	24.3	9	23.4

25		24	
1	2.5	1	2.4
2	5.0	2	4.8
3	7.5	3	7.2
4	10.0	4	9.6
5	12.5	5	12.0
6	15.0	6	14.4
7	17.5	7	16.8
8	20.0	8	19.2
9	22.5	9	21.6

23		22	
1	2.3	1	2.2
2	4.6	2	4.4
3	6.9	3	6.6
4	9.2	4	8.8
5	11.5	5	11.0
6	13.8	6	13.2
7	16.1	7	15.4
8	18.4	8	17.6
9	20.7	9	19.8

21		20	
1	2.1	1	2.0
2	4.2	2	4.0
3	6.3	3	6.0
4	8.4	4	8.0
5	10.5	5	10.0
6	12.6	6	12.0
7	14.7	7	14.0
8	16.8	8	16.0
9	18.9	9	18.0

19		18	
1	1.9	1	1.8
2	3.8	2	3.6
3	5.7	3	5.4
4	7.6	4	7.2
5	9.5	5	9.0
6	11.4	6	10.8
7	13.3	7	12.6
8	15.2	8	14.4
9	17.1	9	16.2

17		16	
1	1.7	1	1.6
2	3.4	2	3.2
3	5.1	3	4.8
4	6.8	4	6.4
5	8.5	5	8.0
6	10.2	6	9.6
7	11.9	7	11.2
8	13.6	8	12.8
9	15.3	9	14.4

15		14	
1	1.5	1	1.4
2	3.0	2	2.8
3	4.5	3	4.2
4	6.0	4	5.6
5	7.5	5	7.0
6	9.0	6	8.4
7	10.5	7	9.8
8	12.0	8	11.2
9	13.5	9	12.6

13		12	
1	1.3	1	1.2
2	2.6	2	2.4
3	3.9	3	3.6
4	5.2	4	4.8
5	6.5	5	6.0
6	7.8	6	7.2
7	9.1	7	8.4
8	10.4	8	9.6
9	11.7	9	10.8

r	0	1	2	3	4	5	6	7	8	9
1.99	0.21	500	517	534	552	569	586	603	620	638	655
2.00		672	689	707	724	741	758	775	792	810	827
2.01		844	861	878	895	913	930	947	964	981	998
2.02	0.22	015	032	049	066	084	101	118	135	152	169
2.03		186	203	220	237	254	271	288	305	322	339
2.04		356	373	390	407	424	441	458	474	491	508
2.05		525	542	559	576	593	610	627	644	660	677
2.06		694	711	728	745	762	778	795	812	829	846
2.07		863	879	896	913	930	946	963	980	997	013
2.08	0.23	030	047	064	080	097	114	130	147	164	181
2.09		197	214	231	247	264	281	297	314	331	347
2.10		364	380	397	414	430	447	463	480	497	513
2.11		530	546	563	579	596	613	629	646	662	679
2.12		695	712	728	745	761	778	794	811	827	844
2.13		860	877	893	909	926	942	959	975	992	008
2.14	0.24	024	041	057	074	090	106	123	139	155	172
2.15		188	204	221	237	253	270	286	302	319	335
2.16		351	368	384	400	416	433	449	465	481	498
2.17		514	530	546	563	579	595	611	627	644	660
2.18		676	692	708	724	741	757	773	789	805	821
2.19		838	854	870	886	902	918	934	950	966	983
2.20		999	015	031	047	063	079	095	111	127	143
2.21	0.25	159	176	191	207	223	239	255	271	287	303
2.22		319	335	351	367	383	399	415	431	447	463
2.23		479	495	511	526	542	558	574	590	606	622
2.24		638	654	669	685	701	717	733	749	765	780
2.25		796	812	828	844	859	875	891	907	923	938
2.26		954	970	986	001	017	033	049	064	080	096
2.27	0.26	112	127	143	159	175	190	206	222	237	253
2.28		269	284	300	316	331	347	363	378	394	409
2.29		425	441	456	472	488	503	519	534	550	566
2.30		581	597	612	628	643	659	675	690	706	721
2.31		737	752	768	783	799	814	830	845	861	876
2.32		892	907	923	938	954	969	984	000	015	031
2.33	0.27	046	062	077	092	108	123	139	154	169	185
2.34		200	216	231	246	262	277	292	308	323	338
2.35		354	369	384	400	415	430	446	461	476	492
2.36		507	522	538	553	568	583	599	614	629	644
2.37		660	676	690	705	721	736	751	766	781	797
2.38		812	827	842	857	873	888	903	918	933	948
2.39		964	979	994	009	024	039	054	070	085	100
2.40	0.28	115	130	145	160	175	190	205	220	236	251
2.41		266	281	296	311	326	341	356	371	386	401
2.42		416	431	446	461	476	491	506	521	536	551
2.43		566	581	596	611	626	641	656	671	686	701
2.44		716	730	745	760	775	790	805	820	835	850
2.45		865	879	894	909	924	939	954	969	984	998
2.46	0.29	013	028	043	058	073	087	102	117	132	147
2.47		162	178	191	206	221	236	250	265	280	295
2.48		309	324	339	353	368	383	398	412	427	442
2.49		457	471	486	501	516	530	545	559	574	589
2.50		604	618	633	647	662	677	691	706	721	735
2.51		750	765	779	794	808	823	838	852	867	881
2.52		896	911	925	940	954	969	984	998	013	027
2.53	0.30	042	058	071	085	100	114	129	144	158	173
2.54		187	202	216	231	245	260	274	289	303	318
2.55		332	346	361	376	390	404	419	433	448	462
2.56		476	491	505	520	534	548	563	577	592	606
2.57		620	635	649	663	678	692	707	721	735	750
2.58		764	778	793	807	821	836	850	864	879	893
2.59		907	921	936	950	964	979	993	007	021	036
2.60	0.31	050	064	079	093	107	121	136	150	164	178
2.61		193	207	221	235	249	264	278	292	306	320
2.62		335	349	363	377	391	405	420	434	448	462
2.63		476	490	505	519	533	547	561	575	589	603
2.64		618	632	646	660	674	688	702	716	730	744
2.65		759	773	787	801	815	829	843	857	871	885
2.66		899	913	927	941	955	969	983	997	011	025
2.67	0.32	039	053	067	081	095	109	123	137	151	165
2.68		179	193	207	221	235	249	262	276	290	304
2.69		318	332	346	360	374	388	402	416	429	443
2.70		457	471	485	499	513	527	540	554	568	582
2.71		596	610	624	637	651	665	679	693	707	720
2.72		734	748	762	776	789	803	817	831	845	858
2.73		872	886	900	913	927	941	955	968	982	996
2.74	0.33	010	023	037	051	065	078	092	106	119	133
2.75		147	161	174	188	202	216	229	243	256	270
2.76		284	297	311	325	338	352	366	379	393	407
2.77		420	434	448	461	475	488	502	516	529	543
2.78		556	570	584	597	611	624	638	651	665	679
2.79		692	706	719	733	746	760	773	787	801	814
2.80		828	841	855	868	882	895	909	922	936	949
2.81		963	976	990	003	017	030	044	057	070	084
2.82	0.34	097	111	124	138	151	165	178	191	205	218
2.83		232	245	259	272	285	299	312	326	339	352
2.84		366	379	393	406	419	433	446	459	473	486
2.85		500	513	526	540	553	566	580	593	606	620
2.86		633	646	660	673	686	700	713	726	739	753
2.87		766	779	793	806	819	832	846	859	872	886
2.88		899	912	925	939	952	965	978	991	005	018
2.89	0.35	031	044	058	071	084	097	110	124	137	150
2.90		163	176	190	203	216	229	242	255	269	282
2.91		295	308	321	334	347	361	374	387	400	413
2.92		426	439	452	466	479	492	505	518	531	544
2.93		557	570	584	597	610	623	636	649	662	676
2.94		688	701	714	727	740	753	767	780	793	806
2.95		819	832	845	858	871	884	897	910	923	936
2.96		949	962	975	988	001	014	027	040	053	066
2.97	0.36	079	092	105	118	131	144	157	169	182	195
2.98		208	221	234	247	260	273	286	299	312	324
2.99		337	350	363	376	389	402	416	428	440	453

Values of "Y" for Normal Air and Perfect Diatomic Gases

r	0	1	2	3	4	5	6	7	8	9
3.0	0.3647	0.3659	0.3672	0.3685	0.3698	0.3711	0.3723	0.3736	0.3749	0.3761
3.1	0.3774	0.3786	0.3799	0.3811	0.3824	0.3836	0.3849	0.3861	0.3874	0.3886
3.2	0.3898	0.3911	0.3923	0.3935	0.3947	0.3959	0.3971	0.3984	0.3996	0.4008
3.3	0.4020	0.4032	0.4044	0.4056	0.4068	0.4080	0.4091	0.4103	0.4115	0.4127
3.4	0.4139	0.4150	0.4162	0.4174	0.4186	0.4197	0.4209	0.4220	0.4232	0.4244
3.5	0.4255	0.4267	0.4278	0.4290	0.4301	0.4313	0.4324	0.4335	0.4347	0.4358
3.6	0.4369	0.4380	0.4392	0.4403	0.4414	0.4425	0.4437	0.4448	0.4459	0.4470
3.7	0.4481	0.4492	0.4503	0.4514	0.4525	0.4536	0.4547	0.4558	0.4569	0.4580
3.8	0.4591	0.4602	0.4612	0.4623	0.4634	0.4645	0.4656	0.4666	0.4677	0.4688
3.9	0.4698	0.4709	0.4720	0.4730	0.4741	0.4752	0.4762	0.4773	0.4783	0.4794
4.0	0.4804	0.4815	0.4825	0.4835	0.4846	0.4856	0.4867	0.4877	0.4887	0.4898
4.1	0.4908	0.4918	0.4928	0.4939	0.4949	0.4959	0.4970	0.4980	0.4990	0.5000
4.2	0.5010	0.5020	0.5030	0.5040	0.5050	0.5060	0.5070	0.5080	0.5090	0.5100
4.3	0.5110	0.5120	0.5130	0.5140	0.5150	0.5160	0.5170	0.5179	0.5189	0.5199
4.4	0.5209	0.5219	0.5228	0.5238	0.5248	0.5258	0.5267	0.5277	0.5287	0.5296
4.5	0.5306	0.5316	0.5325	0.5335	0.5344	0.5354	0.5363	0.5373	0.5382	0.5392
4.6	0.5401	0.5411	0.5420	0.5430	0.5439	0.5449	0.5458	0.5467	0.5477	0.5486
4.7	0.5495	0.5505	0.5514	0.5523	0.5533	0.5542	0.5551	0.5560	0.5570	0.5579
4.8	0.5588	0.5597	0.5606	0.5616	0.5625	0.5634	0.5643	0.5652	0.5661	0.5670
4.9	0.5679	0.5688	0.5697	0.5706	0.5715	0.5724	0.5733	0.5742	0.5751	0.5760
5.0	0.5769	0.5778	0.5787	0.5796	0.5805	0.5814	0.5822	0.5831	0.5840	0.5849
5.1	0.5858	0.5867	0.5875	0.5884	0.5893	0.5902	0.5910	0.5919	0.5928	0.5936
5.2	0.5945	0.5954	0.5962	0.5971	0.5980	0.5988	0.5997	0.6006	0.6014	0.6023
5.3	0.6031	0.6040	0.6048	0.6057	0.6065	0.6074	0.6082	0.6091	0.6099	0.6108
5.4	0.6116	0.6125	0.6133	0.6142	0.6150	0.6159	0.6167	0.6175	0.6184	0.6192
5.5	0.6200	0.6209	0.6217	0.6225	0.6234	0.6242	0.6250	0.6258	0.6267	0.6275
5.6	0.6283	0.6291	0.6300	0.6308	0.6316	0.6324	0.6332	0.6340	0.6349	0.6357
5.7	0.6365	0.6373	0.6381	0.6389	0.6397	0.6405	0.6413	0.6421	0.6430	0.6438
5.8	0.6446	0.6454	0.6462	0.6470	0.6478	0.6486	0.6494	0.6502	0.6509	0.6517
5.9	0.6525	0.6533	0.6541	0.6549	0.6557	0.6565	0.6573	0.6581	0.6588	0.6596
6.0	0.6604	0.6612	0.6620	0.6628	0.6635	0.6643	0.6651	0.6659	0.6666	0.6674
6.1	0.6682	0.6690	0.6697	0.6705	0.6713	0.6721	0.6729	0.6736	0.6744	0.6752
6.2	0.6759	0.6767	0.6774	0.6782	0.6789	0.6797	0.6805	0.6812	0.6820	0.6827
6.3	0.6835	0.6843	0.6850	0.6858	0.6865	0.6873	0.6880	0.6888	0.6895	0.6903
6.4	0.6910	0.6918	0.6925	0.6933	0.6940	0.6948	0.6955	0.6963	0.6970	0.6978
6.5	0.6985	0.6992	0.7000	0.7007	0.7014	0.7021	0.7028	0.7036	0.7043	0.7050
6.6	0.7058	0.7065	0.7073	0.7080	0.7087	0.7095	0.7102	0.7110	0.7117	0.7124
6.7	0.7131	0.7138	0.7145	0.7153	0.7160	0.7167	0.7174	0.7181	0.7189	0.7196
6.8	0.7203	0.7210	0.7217	0.7224	0.7232	0.7239	0.7246	0.7253	0.7260	0.7267
6.9	0.7274	0.7281	0.7288	0.7295	0.7302	0.7309	0.7316	0.7323	0.7330	0.7338
7.0	0.7345	0.7352	0.7359	0.7366	0.7373	0.7380	0.7386	0.7393	0.7400	0.7407
7.1	0.7414	0.7421	0.7428	0.7435	0.7442	0.7449	0.7456	0.7463	0.7470	0.7477
7.2	0.7483	0.7490	0.7497	0.7504	0.7511	0.7518	0.7524	0.7531	0.7538	0.7545
7.3	0.7552	0.7559	0.7565	0.7572	0.7579	0.7586	0.7592	0.7599	0.7606	0.7613
7.4	0.7620	0.7626	0.7633	0.7640	0.7646	0.7653	0.7660	0.7666	0.7673	0.7680
7.5	0.7687	0.7693	0.7700	0.7706	0.7713	0.7720	0.7726	0.7733	0.7740	0.7746
7.6	0.7753	0.7760	0.7766	0.7773	0.7779	0.7786	0.7792	0.7799	0.7806	0.7812
7.7	0.7819	0.7825	0.7832	0.7838	0.7845	0.7851	0.7858	0.7864	0.7871	0.7877
7.8	0.7884	0.7890	0.7897	0.7903	0.7910	0.7916	0.7923	0.7929	0.7936	0.7942
7.9	0.7949	0.7955	0.7961	0.7968	0.7974	0.7981	0.7987	0.7993	0.8000	0.8006
8.0	0.8013	0.8019	0.8025	0.8032	0.8038	0.8044	0.8051	0.8057	0.8063	0.8070
8.1	0.8076	0.8082	0.8089	0.8095	0.8101	0.8108	0.8114	0.8120	0.8126	0.8133
8.2	0.8139	0.8145	0.8151	0.8158	0.8164	0.8170	0.8176	0.8183	0.8189	0.8195
8.3	0.8201	0.8207	0.8214	0.8220	0.8226	0.8232	0.8238	0.8245	0.8251	0.8257
8.4	0.8263	0.8269	0.8275	0.8281	0.8288	0.8294	0.8300	0.8306	0.8312	0.8318
8.5	0.8324	0.8330	0.8336	0.8343	0.8349	0.8355	0.8361	0.8367	0.8373	0.8379
8.6	0.8385	0.8391	0.8397	0.8403	0.8409	0.8415	0.8421	0.8427	0.8433	0.8439
8.7	0.8445	0.8451	0.8457	0.8463	0.8469	0.8475	0.8481	0.8487	0.8493	0.8499
8.8	0.8505	0.8511	0.8517	0.8523	0.8529	0.8535	0.8541	0.8547	0.8552	0.8558
8.9	0.8564	0.8570	0.8576	0.8582	0.8588	0.8594	0.8600	0.8605	0.8611	0.8617
9.0	0.8623	0.8629	0.8635	0.8641	0.8646	0.8652	0.8658	0.8664	0.8670	0.8676
9.1	0.8681	0.8687	0.8693	0.8699	0.8705	0.8710	0.8716	0.8722	0.8728	0.8734
9.2	0.8739	0.8745	0.8751	0.8757	0.8762	0.8768	0.8774	0.8779	0.8785	0.8791
9.3	0.8797	0.8802	0.8808	0.8814	0.8819	0.8825	0.8831	0.8837	0.8842	0.8848
9.4	0.8854	0.8859	0.8865	0.8871	0.8876	0.8882	0.8888	0.8893	0.8899	0.8905
9.5	0.8910	0.8916	0.8921	0.8927	0.8933	0.8938	0.8944	0.8949	0.8955	0.8961
9.6	0.8966	0.8972	0.8977	0.8983	0.8989	0.8994	0.9000	0.9005	0.9011	0.9016
9.7	0.9022	0.9028	0.9033	0.9039	0.9044	0.9050	0.9055	0.9061	0.9066	0.9072
9.8	0.9077	0.9083	0.9088	0.9094	0.9099	0.9105	0.9110	0.9116	0.9121	0.9127
9.9	0.9132	0.9138	0.9143	0.9149	0.9154	0.9159	0.9165	0.9170	0.9176	0.9181
10.0	0.9187	0.9192	0.9198	0.9203	0.9208	0.9214	0.9219	0.9225	0.9230	0.9235
10.1	0.9241	0.9246	0.9252	0.9257	0.9262	0.9268	0.9273	0.9278	0.9284	0.9289
10.2	0.9295	0.9300	0.9305	0.9311	0.9316	0.9321	0.9327	0.9332	0.9337	0.9343
10.3	0.9348	0.9353	0.9358	0.9364	0.9369	0.9374	0.9380	0.9385	0.9390	0.9396
10.4	0.9401	0.9406	0.9411	0.9417	0.9422	0.9427	0.9432	0.9438	0.9443	0.9448
10.5	0.9453	0.9459	0.9464	0.9469	0.9474	0.9480	0.9485	0.9490	0.9495	0.9500
10.6	0.9506	0.9511	0.9516	0.9521	0.9526	0.9532	0.9537	0.9542	0.9547	0.9552
10.7	0.9558	0.9563	0.9568	0.9573	0.9578	0.9583	0.9589	0.9594	0.9599	0.9604
10.8	0.9609	0.9614	0.9619	0.9625	0.9630	0.9635	0.9640	0.9645	0.9650	0.9655
10.9	0.9660	0.9665	0.9671	0.9676	0.9681	0.9686	0.9691	0.9696	0.9701	0.9706
11.0	0.9711	0.9716	0.9721	0.9726	0.9732	0.9737	0.9742	0.9747	0.9752	0.9757
11.1	0.9762	0.9767	0.9772	0.9777	0.9782	0.9787	0.9792	0.9797	0.9802	0.9807
11.2	0.9812	0.9817	0.9822	0.9827	0.9832	0.9837	0.9842	0.9847	0.9852	0.9857
11.3	0.9862	0.9867	0.9872	0.9877	0.9882	0.9887	0.9892	0.9897	0.9902	0.9907
11.4	0.9912	0.9916	0.9921	0.9926	0.9931	0.9936	0.9941	0.9946	0.9951	0.9956
11.5	0.9961	0.9966	0.9971	0.9975	0.9980	0.9985	0.9990	0.9995	1.0000	1.0005
11.6	1.0010	1.0015	1.0019	1.0024	1.0029	1.0034	1.0039	1.0044	1.0049	1.0054
11.7	1.0058	1.0063	1.0068	1.0073	1.0078	1.0083	1.0087	1.0092	1.0097	1.0102
11.8	1.0107	1.0112	1.0116	1.0121	1.0126	1.0131	1.0136	1.0140	1.0145	1.0150
11.9	1.0155	1.0160	1.0164	1.0169	1.0174	1.0179	1.0184	1.0188	1.0193	1.0198
12.0	1.0203	1.0207	1.0212	1.0217	1.0222	1.0226	1.0231	1.0236	1.0241	1.0245

From "Engineering Computations for Air and Gases" by Moss and Smith, Transactions A.S.M.E., Vol. 52, 1930, Paper APM-52-8

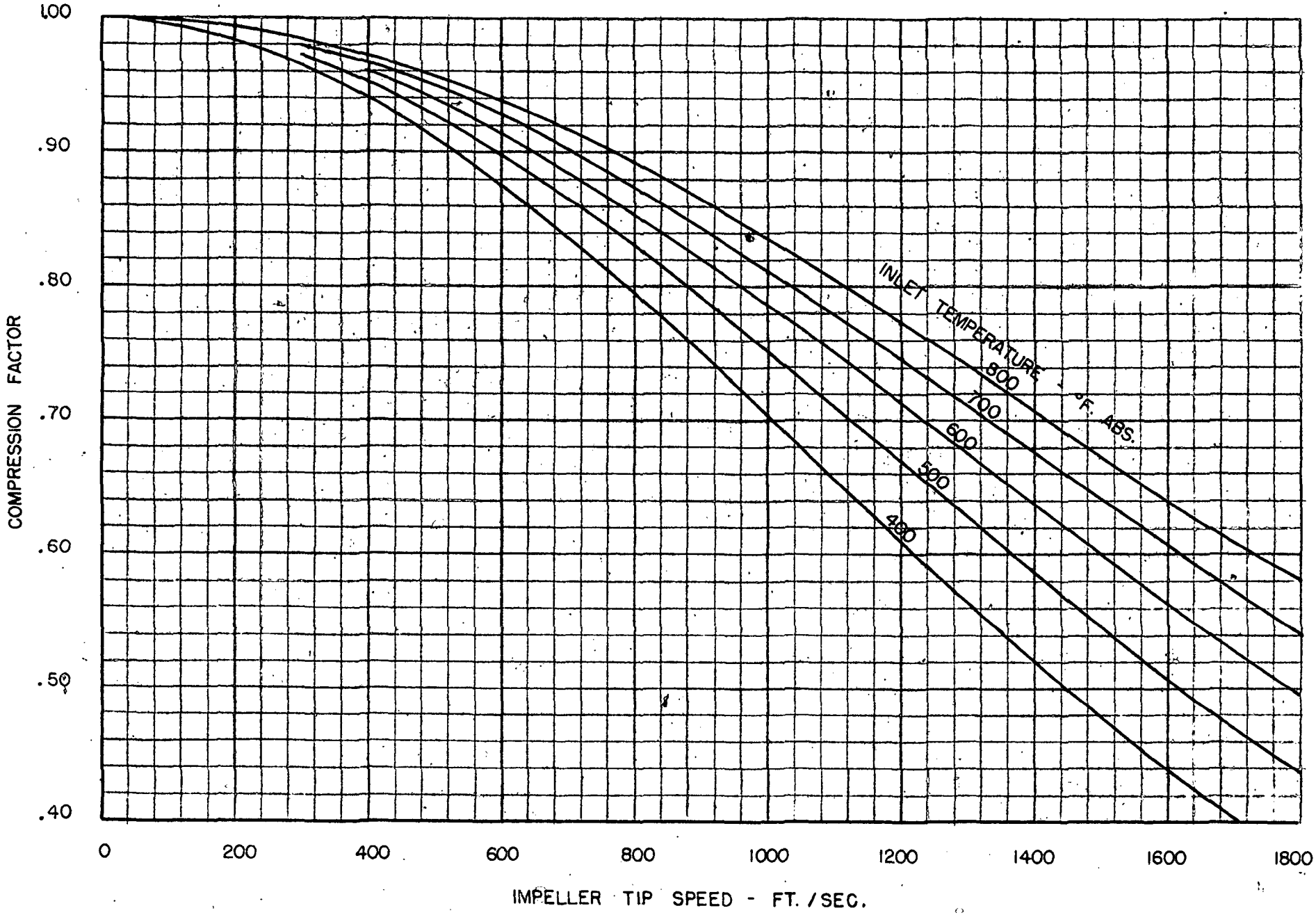

FIG. 1 IMPELLER COMPRESSION FACTOR

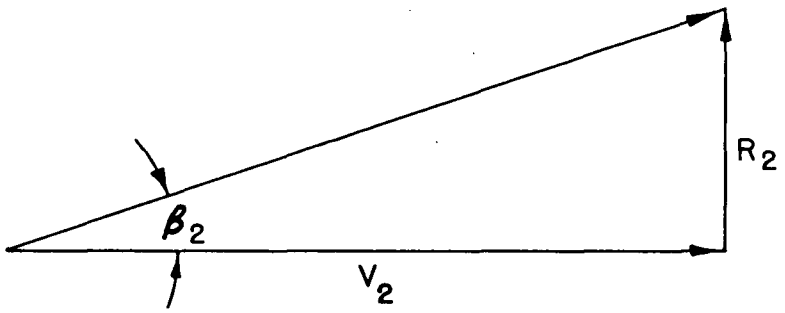

AT IMPELLER EXIT

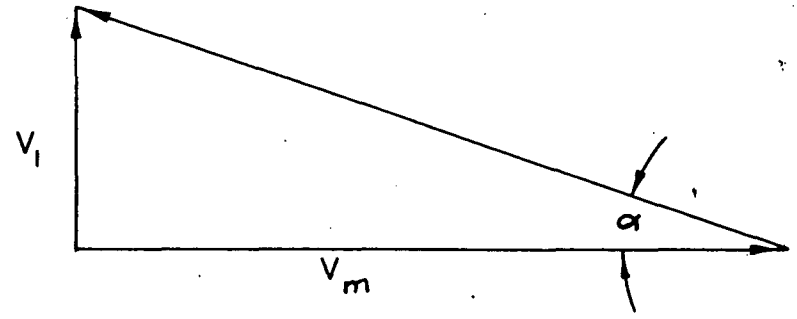

AT IMPELLER INLET

FIGURE 2

VELOCITY DIAGRAMS

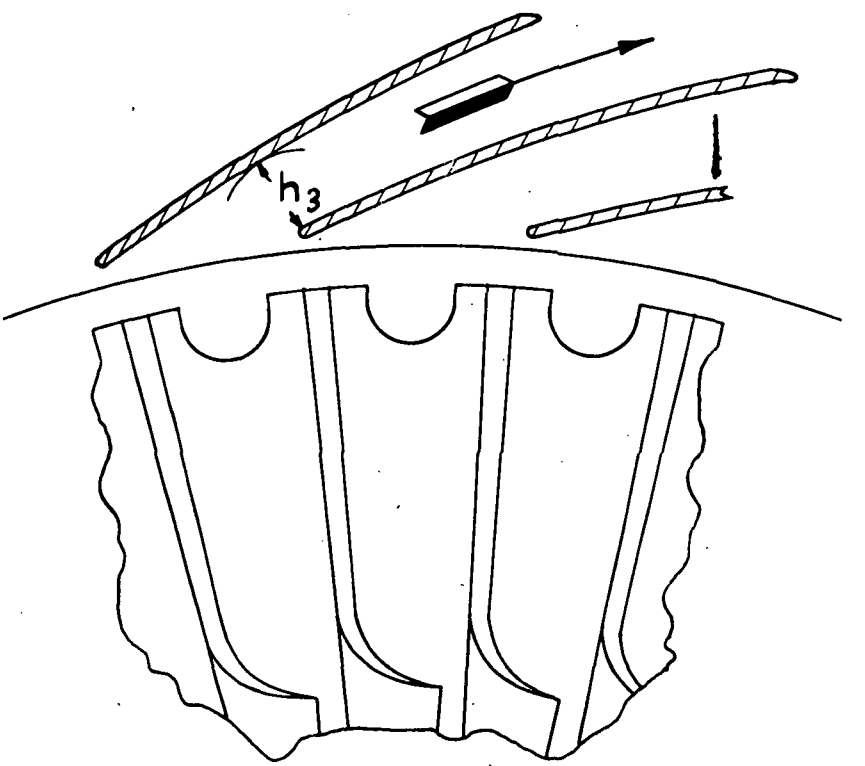

FIGURE 3

INLET PASSAGE HEIGHT
OF DIFFUSER VANE PASSAGE, h_3

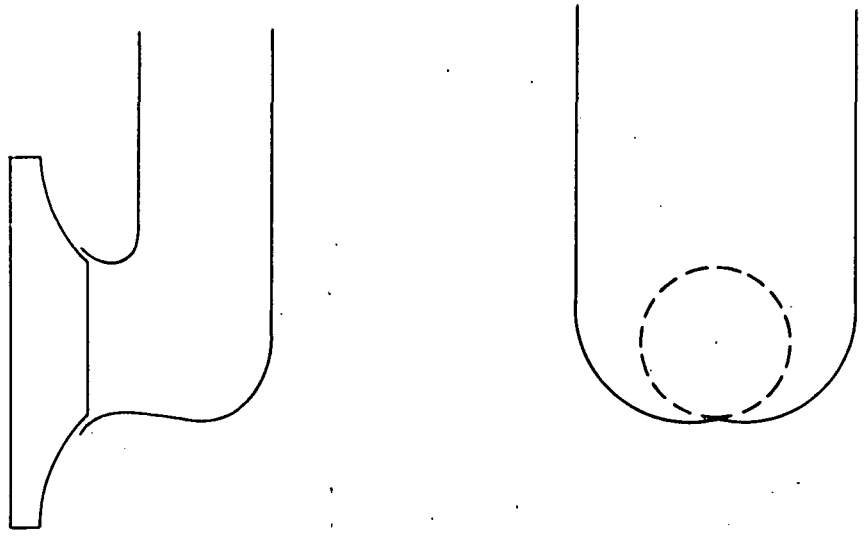

FIGURE 4

RECOMMENDED SHAPE
OF INLET ELBOW

REPORT B

Page intentionally left blank

INDEX

	Page
TITLE	1
INDEX	2
INTRODUCTION	3
OBJECT	4
RESUME	4
CONCLUSIONS AND RECOMMENDATIONS	4
General	4
Inlet	5
Impeller	5
Diffuser	7
Impeller-Diffuser Clearance	8
Collector Case and Manifold	8
METHOD OF ANALYSIS	
PART I (No losses considered)	9
General Relations	9
Impeller Performance	10
Combination Impeller-Diffuser Performance	12
Clearance Space Calculations	14
Vaned Type Diffusers	16
PART II (Losses considered)	19
APPENDIX I (Illustrative example)	25
SYMBOLS	39

"Page missing from available version"

OBJECT

To formulate the methods for designing the flow paths of centrifugal superchargers.

RESUME

In the section entitled, "Conclusions and Recommendations", general design facts are briefly stated for purposes of convenience. The justifications of these facts are given under "METHOD OF ANALYSIS".

The "METHOD OF ANALYSIS", which is divided into two parts is as follows:

PART I describes the method which is used for calculating the flow passages of a centrifugal supercharger on the assumption that there are no losses.

In PART II an attempt is made to allocate and actually evaluate the various losses.

In APPENDIX I an example is worked out in detail to illustrate the design of a supercharger corresponding to a given set of engine requirements by the methods herein described.

A list of symbols is given on the last page of this report.

CONCLUSIONS AND RECOMMENDATIONS

General

The theoretical effects of certain variables, such as slip, impeller discharge velocity, and diffuser discharge velocity, are shown in Figure 3 on Page #36. They are as follows:

1. Impeller design should be such that the energy imparted by it to the air is in a form which is most conductive to high efficiency. The highest efficiency will be expected when the temperature ratio through it is a maxium. This will occur when the slip-factor is in the neighborhood of $F_s = 1$; and the radial component of the discharge velocity is a minimum; that is, when $N = 0.25$, approximately. (See Figure 3). Under no conditions should an impeller be operated with the temperature ratio T_2/T_1 equal to 1.

2. In the case of the diffuser, the temperature ratio should likewise be a maximum for best efficiency. This condition will occur when the discharge velocity from the diffuser is a minimum, consistent with design limitations; that is $N^1 = 0.25$ approximately.

3. The design of impeller-diffuser combination should be based upon the region above $T/T_1 = 1$ and in the neighborhood of $F_s = 1$ shown in Figure 3.

4. The number of energy transformations in which the working fluid is accelerated and decelerated should be kept to a minimum.

Inlet

The performance of a supercharger depends upon the inlet conditions; because if the inlet conditions are poor, any loss there will be multiplied approximately by the compression ratio of the overall supercharger when referred to the supercharger discharge pressure.

1. An axial inlet approaching bench-test conditions would be ideal. This would give the least pressure loss and the best distribution.

2. Where an inlet elbow is required, it must be designed so that the air enters the impeller axially and with uniform velocity traverse with respect to the inlet casing. This can be accomplished by turning vanes and a suitable enlargement of the inlet passage ahead of the impeller entrance. If turning vanes are used they should be brought to within less than 3/16" from the impeller inlet blades.

3. The inlet passage velocity should be kept below 300 feet per second at the design conditions (full throttle and rated altitude).

4. The impeller shaft bearing boss, in the inlet casing, should be flush with the root diameter of the impeller blades, so that there is a well-matched and continuous flow passage.

5. Changes in area or rapid expansions in the passage between the carburetor and the rear section inlet should be avoided.

6. All inlet surfaces should be smooth. If rough sand castings are used, they may require hand finishing. The possibilities of die and permanent mold castings should be considered.

7. There should be no bosses or other unnecessary obstructions to interrupt a smooth flow surface.

8. To keep heat transfer to a minimum, the inlet surface should not be in contact with the hot engine oil. (De-icing problems not considered).

Impeller

1. High impeller throat velocities produce flow separation and impact losses in the impeller passages and corresponding reductions in the final air density. The mean air velocity relative to the casing at the impeller entrance should be between 200 and 300 feet per second at the design conditions.

2. To reduce flow separation at the impeller entrance, the impeller inlet blades should be bent to as large a radius as practicable. Further, the axial-to-radial turn (throat radius of curvature) in the impeller passage should be gradual. One way of accomplishing this is to extend the inlet by the addition of an inducer. This inducer should be designed on the basis of an axial flow fan using airfoil sections, rather than bending the impeller blades as is now common practice. For an inducer, the camber radius should be on the order of 1.5" to 4".

   When an inducer is used in a test-rig the number of splines and the number of impeller blades should be prime with respect to each other. Thus, the inducer can be indexed relative to the impeller in small angular increments so that the position of optimum boundary layer control can be fixed.

3. To insure full impeller channels downstream of the entrance, the net ratio of exit area to inlet area of the impeller should be approximately 0.6 for vaneless diffusers and 0.8 for vaned diffusers, respectively. The area change should be uniform and follow the basic limitations of an equivalent cone.

4. Scallops of the type which have been used in past construction are undesirable from the standpoint of fluid flow; and, from this point of view, should be eliminated. However, with the present trend towards higher tip-speeds, the use of scallops can become essential if reasonable impeller weights are to be obtained. The "faired-in" type of scallop has its merits, and should not be overlooked.

5. The blade tip of the impeller should be reduced in thickness by machining on the driving face rather than on the back face to prevent flow separation, and reduce leaving losses.

6. The thrust balancing holes through the impeller disc should be eliminated. These holes do not accomplish their purpose as thrust balance holes, but do introduce excessive recirculation and turbulence losses.

7. The root sections of the impeller blades should have fillets of large radii. These fillet radii are limited by the number and thickness of the blades and the diameter of the root section. They should generally be of the order of 3/16".

8. The temperature ratio of an impeller, which is a measure of its performance, is influenced by its relative radial discharge velocity, which should be between 200 and 300 feet per second at the design condition.

9. On engines using a fuel spinner, the outside diameter of the spinner should not be larger in diameter than the root diameter of the impeller

blades. If the outside diameter of the spinner is too large, the impeller entrance will be in the contracted jet of the air stream. The spinner outside diameter should blend into and form a continuous surface between inlet casing boss and impeller blade root diameter.

Diffuser

1. Diffuser surfaces should be absolutely smooth, free from sharp changes in section, and each passage should be a geometrical duplicate of its neighbor. (It has been proven by test on standard diffusers of sand-cast construction that there was as much as 1.7 In.Hg. difference in total head between passages and a difference in the mass airflow from passage to passage of as much as 20% under extreme conditions. This was reduced to approximately .25"Hg. and 4% of mass airflow, respectively, by hand finishing and blending). These precautions are absolutely essential if good distribution is to be obtained in the engine installation.

2. The convex surface of the diffuser vane from the tip to the point where the throat is measured should follow the corrected logarithmic spiral path of the air stream from the impeller. If bolts go through the vanes, they must be thickened. This makes it necessary to lengthen the vane radius of curvature from the throat point downstream, in order to maintain the desired equivalent-cone-area change. The inlet and trailing edges of the vanes and side walls should have relatively sharp edges of approximately 1/32" radius or smaller.

   In view of the zone of "stagnation throttling" that exists at the diffuser throat, effectively reducing the throat area from 30 to 50%, it is necessary to increase the theoretical entrance area to compensate for this effect.

3. The area ratio through the diffuser should be at least two. The area change relative to passage length should conform to the equivalent cone as follows: For the first 1.5" of path length, diverge at an included angle of 3.5°; for the next 1.5" of path length, diverge at an included angle of 4.5°; and for the remainder of the passage length diverge at an included cone angle of 7°.

4. The radius of curvature of the center line of the diffuser passage from the throat out should normally be made as large as possible, consistent with other design and space limitations.

5. The temperature ratio of the diffuser is a measure of its performance, and it is influenced, among other things, by its discharge velocity. This discharge velocity should be between 200 and 300 feet per second.

6. The axial position of the center line of a diffuser passage should coincide with a continuation of the center line of the impeller passage at its discharge. For example, the center line of the diffuser channel should be made to follow the impeller discharge stream path when the impeller discharges with a backward axial component, and vice versa. Under no conditions should the air be required to make an abrupt turn.

7. Diffuser passages can be made to expand in both the radial and axial directions, about the path center line, for large area ratios.

Impeller-Diffuser Clearance

1. The clearance space between the impeller discharge and the diffuser inlet vane tip should be sufficiently large to allow the air to slow down to below the velocity of sound by the time it reaches the diffuser inlet vane tips. A diametrical clearance equal to approximately 10% of the impeller diameter will usually suffice.

Collector Case and Manifold

1. The inner surface of the collector case and manifolds which come in contact with the air stream should be smooth as in the case of the inlet.

2. The diffuser should not discharge against a flat wall. A collector design as sketched in Figure A would help to recover some of the vortex energy of the diffuser discharge. The collector cross-section should be approximately circular, its diameter D should be about 1/2 impeller diameter for radial engines. The inlet ports which lead off tangentially from this collector case should have large inlet radii.

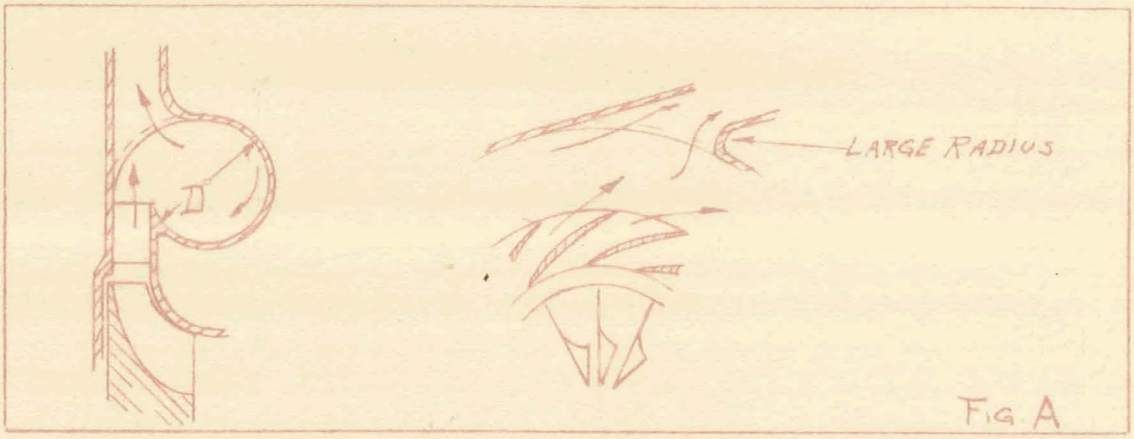

Fig. A

3. The axes of these ports should be continuations of the center lines of the diffuser channels. Offsetting these inlet ports axially with respect to the plane of discharge of the diffuser reduces the overall peak performance of the system and gives rise to more critical performance characteristics.

4. There should be no bosses, ribs or other unnecessary obstructions to interrupt the smooth flow surface.

5. To reduce heat transfer, the collector case should be separated as completely as practicable from any engine case which is in direct contact with hot engine oil.

6. Tangential inlet ports with large radii should materially decrease the inlet port losses due to throttling. (See Figure A)

METHOD OF ANALYSIS

PART I (No losses considered)

General Relations

On the assumption that the mass airflow rate through a system is steady, that is

$$\rho_1 A_1 C_{a_1} = \rho A C$$

the General Steady Flow Energy Equation for a compressible fluid can be written ①

$$\frac{C_{a_1}^2}{2g_s} + \frac{p_1}{\rho_1} + 778 c_v T_1 + \Delta E = \frac{C^2}{2g_s} + \frac{p}{\rho} + 778 c_v T \qquad (1)$$

provided differences in flow elevation and heat transfer to and from the working fluid are neglected. (See Figure 1)

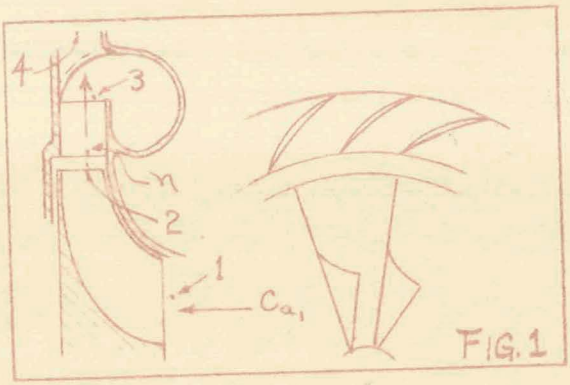

FIG. 1

This equation states that the mechanical work ΔE, which is done by the impeller on each pound of air changes the thermodynamic state of this air from the initial state indicated by subscript "1" to the arbitrary state which is indicated by unsubscripted symbols.

Let C_t and C_r represent the tangential and radial components, respectively, of the air leaving the impeller discharge with a velocity C with respect to the supercharger casing. (See Figure 2)

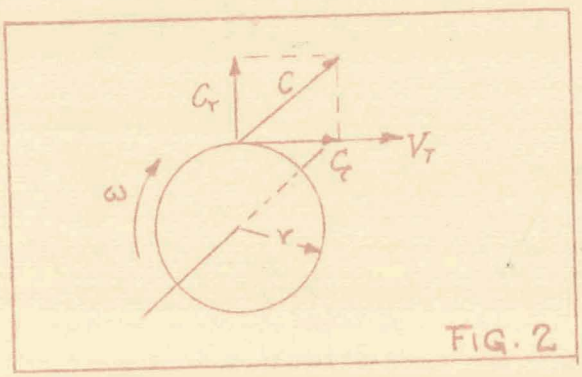

FIG. 2

If the air entering the impeller has no initial angular velocity, the work done per pound mass of the air (ΔE) by the impeller is

$$\Delta E = L\omega = \frac{C_t V_T}{g_s}$$

where L is the torque required to maintain the constant angular velocity of the impeller, ω, corresponding to the impeller tip-speed V_T.

Since the tangential component of the air velocity (C_t) can be greater than, less than or equal to the tip-speed of the impeller (V_T) corresponding to different discharge conditions, let $C_t = F_s V_T$ ② where F_s represents a dimensionless slip-factor. Then ΔE, can be expressed as

$$\Delta E = F_s V_T^2 / g_s$$

and the General Energy Equation (1) becomes

$$\frac{C_{a_1}^2}{2g_s} + \frac{p_1}{\rho_1} + k_v T_1 + \frac{F_s V_T^2}{g_s} = \frac{C^2}{2g_s} + \frac{p}{\rho} + k_v T \qquad (2)$$

or

① Assuming that the specific heats at constant pressure and volume are constant.

② For best efficiency, $F_s = 0.925$.

$$\frac{C_{a_1}^2}{2g_s} + k_p T_1 + \frac{F_s V_T^2}{g_s} = \frac{C^2}{2g_s} + k_p T \qquad (3)$$

where k_p = specific heat at constant pressure in mechanical units.

Combining the terms containing "T" and rearranging, the expression for the temperature rise through the supercharger in terms of the tip-speed, slip, initial and final velocities, etc. becomes

$$T - T_1 = \frac{1}{2g_s k_p}\left[(C_{a_1}^2 - C^2) + 2F_s V_T^2\right] \qquad (4)$$

or

$$\frac{T}{T_1} = \frac{1}{2g_s k_p T_1}\left[(C_{a_1}^2 - C^2) + 2F_s V_T^2\right] + 1$$

For an isentropic process

$$\frac{p}{p_1} = \left(\frac{T}{T_1}\right)^{\frac{\kappa}{\kappa-1}}$$

Thus, if the process occurring in the supercharger is assumed to be isentropic, the expression for the pressure ratio is

$$\frac{p}{p_1} = \left\{\frac{1}{2g_s k_p T_1}\left[(C_{a_1}^2 - C^2) + 2F_s V_T^2\right] + 1\right\}^{\frac{\kappa}{\kappa-1}} \qquad (5)$$

③

The two preceding equations (4) and (5) are expressions for the temperature and pressure ratio, respectively, from the entrance of the impeller to any point downstream, including the exit to the diffuser; that is, from point 1 to point 3 shown in Figure 1.

Impeller Performance

To determine the pressure and temperature relations at the impeller tip, we must know what portion of the input work has been absorbed by the air in the impeller to increase its pressure and temperature and what portion is discharged as kinetic energy. The input work is equal to the sum of the compression work done on the air in the impeller and the kinetic energy contained in the air stream leaving the impeller.

Referring to Figure 2, we see that the absolute velocity C is a measure of the kinetic energy in the discharged air stream. Thus,

$$K.E. = \frac{1}{2g_s} C_2^2 = \frac{1}{2g_s}\left(C_{r_2}^2 + C_{t_2}^2\right) = \frac{1}{2g_s}\left(C_{r_2}^2 + F_s^2 V_T^2\right)$$

---

③ Rigorously speaking, it is not correct to apply the steady flow General Energy Equation between any two arbitrary points on the impeller-diffuser combination, since the flow through both of these elements cannot be simultaneously steady. That is, if the frame of reference is fixed with respect to the impeller, then airflow with respect to the impeller is steady and that with respect to the diffuser is unsteady and vice versa. In the case at hand, however, the application is made from the inlet to a point in the clearance space between which two positions there is no relative motion.

If the kinetic energy term $C^2/2g_s$ in equation (3) is now expressed in terms of its components, according to the expression immediately preceding, the General Energy Equation becomes

$$\frac{C_{a_1}^2}{2g_s} + k_p T_1 + \frac{F_s V_T^2}{g_s} = \frac{1}{2g_s}\left(C_{r_2}^2 + F_s^2 V_T^2\right) + k_p T_2$$

and the corresponding new expressions for the temperature and pressure ratios through the impellers are

$$\frac{T_2}{T_1} = \frac{1}{2g_s k_p T_1}\left[\left(C_{a_1}^2 - C_{r_2}^2\right) + F_s V_T^2 (2 - F_s)\right] + 1 \qquad (6)$$

$$\frac{p_2}{p_1} = \left\{\frac{1}{2g_s k_p T_1}\left[\left(C_{a_1}^2 - C_{r_2}^2\right) + F_s V_T^2 (2 - F_s)\right] + 1\right\}^{\frac{K}{K-1}} \qquad (7)$$

respectively.

From equation (6), the trend of the effect of slip and radial velocity at the impeller discharge on the temperature ratio can be seen. For example, suppose that the area ratio through the impeller was such that this radial velocity could be controlled in accordance with the expression $C_{r_2} = N V_T$, where N is a dimensionless coefficient. Further, suppose that the slip could be varied at our discretion. Equation (6) then becomes

$$\frac{T_2}{T_1} = \frac{1}{2g_s k_p T_1}\left[\left(C_{a_1}^2 - N^2 V_T^2\right) + F_s V_T^2 (2 - F_s)\right] + 1 \qquad (8)$$

To reduce the number of variables, let us assume reasonable values for the impeller entrance velocity, tip-speed and inlet temperature as follows:

C_{a_1} = 300 ft. per sec.
V_T = 1225 ft. per sec.
T_1 = 450° F. Abs. (altitude air)
k_p = 189 ft. lbs. per lb. per deg. F.

The substitution of these values in equation (8) reduces it to

$$\frac{T_2}{T_1} = \frac{1}{2 \times 32.2 \times 189 \times 450}\left[\left(\overline{300}^2 - \overline{1225}^2 N^2\right) + \overline{1225}^2 F_s (2 - F_s)\right] + 1 \qquad (8a)$$

Here $T_2/T_1 = \Phi(F_s, N)$, where N will be considered as a parameter.

By assuming various values of N in the range 0 to 1.0, T_2/T_1 can be plotted as a function of F_s, covering the entire field of operation of a given impeller. These curves are shown in Figure 3.

The curves on Figure 3 are very interesting in that several far-reaching conclusions can be drawn from them. For example, for the impeller only, it is apparent that temperature rise is a maximum in the neighborhood of a slip of 1.0, which agrees fairly well with the correlation of experimental results on most impellers which fixes $F_s = 0.925$ (4). Also, the impeller temperature rise is reduced as the radial velocity increases. These conclusions are not obvious from the General Energy Equation, upon which equation (8) is based.

Combination Impeller-Diffuser Performance

In the case of an impeller-diffuser combination, equation (4) becomes

$$\frac{T_3}{T_1} = \frac{1}{2g_s k_p T_1}\left[\left(C_{a_1}^2 - C_3^2\right) + 2F_s V_T^2\right] + 1 \qquad (9)$$

Now, if C_3 is written $C_3 = N_1 V_T$, where N_1 is a dimensionless coefficient which may vary from 0 to 1.0, the temperature ratio T_3/T_1 can be written

$$\frac{T_3}{T_1} = \frac{1}{2g_s k_p T_1}\left[\left(C_{a_1}^2 - N_1^2 V_T^2\right) + 2F_s V_T^2\right] + 1 \qquad (10)$$

Provided the same reasonable values of impeller entrance velocity, tip-speed and inlet temperatures are assumed as in the case of the impeller (only) which led to equation (8a), equation (10) becomes

$$\frac{T_3}{T_1} = 1.016 - 0.28 N_1^2 + 0.55 F_s \qquad (11)$$

Now, again, by assuming various values for the parameter N_1 from 0.0 to 1.0, a family of straight lines can be drawn correlating the temperature ratios of impeller-diffuser combinations, T_3/T_1, as functions of the slip-factor, F_s, and bracketing the practical operating range. These straight lines are shown in Figure 3.

From the curves on Figure 3, the following facts regarding the performance of the impeller-diffuser combination are apparent.

1. The impeller should be operated at a slip factor in the neighborhood of 1.0 in order to obtain the highest impeller temperature ratio.

2. To maintain the highest impeller temperature ratio, the radial discharge velocity should be low, corresponding to a value of $N \approx 0.25$.

3. For a high overall supercharger temperature ratio, the diffuser exit velocity should be small, of the order of $N_1 \approx 0.25$.

4. It is also apparent that, when operating in the neighborhood of $F_s = 1.0$, the division of work is approximately equal between the impeller and diffuser

(4) This value of the slip agrees within about 5% of the theoretically calculated slip for the same impeller as calculated by the Stodola correction, which assumes an irrotational flow condition. (Ref. Steam and Gas Turbines - Stodola - sixth edition - p. 1259)

The part that the slip plays in controlling the amount of compression work done on the air in the impeller is also very effectively brought out by the curves of Figure 3. For example, if the slip is sufficiently increased above $F_s = 1$, a condition is reached at which the temperature rise through the impeller is zero. Under these conditions, the compression work which is done on the air by the impeller is also zero; that is, the entire energy output to the air is in the form of kinetic energy.

A reduction in the slip below $F_s = 1$ has the opposite effect. As the slip is reduced, the temperature rise through the impeller is also reduced. However, of the total energy input to the air by the impeller, a greater proportion is converted into compression energy in the impeller. This means that for a given tip-speed, the diffuser inlet velocities will be reduced and should result in higher overall efficiency, provided the impeller losses can be kept down to a reasonable value.

For a given impeller clearance and diffuser design, one practical way of reducing the impeller slip is to construct impellers with backward-curving blades similar to those which are used in centrifugal pump practice. Conversely, the slip can be increased by using forward-curving blades.

At this time, it should be pointed out that, while increasing the slip would seem to be an ideal way of increasing the overall temperature ratio, this condition would put such high service requirements on the diffuser that it might be impractical, even if the air supplied to the diffuser were of fairly uniform velocity.

For example, in the case of an impeller having backward-curving blades corresponding to an effective slip of 0.5, approximately 75% of the total compression occurs in the impeller and 25% in the remainder of the system. Due to the comparatively low diffuser inlet velocities, high overall efficiencies would be expected but at comparatively low pressure ratios.

On the other hand, if the impeller has forward-curving blades corresponding to a slip-factor of 1.5, about 75% of the total compression takes place in the diffuser and the balance in the impeller. A design of this type should produce high pressure ratios, but rather low efficiencies due to the necessarily high diffuser velocities.

In the case of radial-bladed impellers where usually the compression work is equally distributed between the impeller and diffuser, one has a compromise design. Structurally, this type of impeller is more suited to the high rotative speeds than either of the other two previously mentioned types. But, it is probable that impeller losses due to flow separation cannot be reduced to small enough values without excessive throttling to make it an optimum design.

These observations seem to indicate that more complete investigations should be made of both axial-flow and radial-flow turbine type compressors.

Clearance Space Calculations

Expressions have been established for both the temperature and pressure ratios between the impeller inlet and the diffuser exit, and between the impeller inlet and a point just beyond the impeller exit. Now similar relations must be derived to bridge the clearance space between the impeller and the diffuser.

If the temperature and pressure at the impeller exit and the mass airflow rate through the impeller are known, it is possible to calculate the mean radial discharge velocity from the impeller on the assumption that the passages actually run full. However, there is substantial experimental evidence resulting from static and rotating impeller tests, together with the correlation results which show conclusively that the passages of radial-bladed impellers now in current use rarely, if ever, run full.

This information coupled with the uncertain nature of the uncontrolled flow conditions which exist in the clearance space between the impeller and the diffuser make it desirable to develop a method which can be applied with some degree of certainty in this region.

From the altitude rating of the engine, the temperature, pressure and radial velocity at point (2) in the clearance space, just beyond the impeller, can be calculated by methods which have already been presented. On the basis of the assumed slip-factor, F_s, which has been verified by indirect methods, the tangential component of the air velocity with respect to the casing at this point can be calculated.

Now, if it is assumed that there is no sudden change in the thermodynamic state as the air moves from a point immediately inside of the impeller discharge to point (2), immediately outside of the impeller, the radial discharge velocity from the impeller can be computed. ⑤

Combining these radial and tangential velocities, the air velocity relative to the casing at a point in the clearance space, just beyond the impeller discharge, is determined both in direction and magnitude.

In the clearance space between the impeller and the diffuser of a supercharger which is rotating at constant speed, the Principle of the Conservation of Angular Momentum can be applied provided frictional losses are neglected. This statement is equivalent to the equation

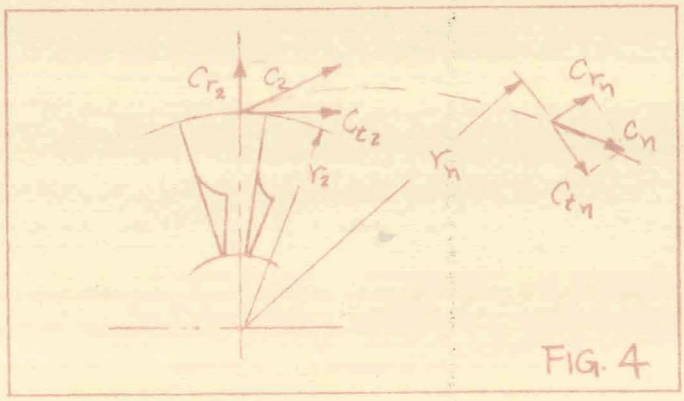

FIG. 4

$$C_{t_2} r_2 = C_{t_n} r_n \qquad (12)$$

which means that the tangential component of the air velocity with respect to the casing varies inversely as the radius (see Figure 4). Further, if in addition to being frictionless, the air is assumed to be incompressible, it can be shown that the path of an air particle will be a logarithmic spiral. Consequently,

⑤ This assumption is justifiable, provided the discharge ends of the impeller blades are sharpened by removing metal from their high pressure faces. The eddy-zones of the blade-tips probably make the flow-areas continuous even if they were not sharpened.

the radial component of the air velocity with respect to the casing also varies inversely as its radial distance from the impeller axis to the point at issue. This follows from the fact that a logarithmic spiral which is generated with respect to a given axis (the axis of the impeller) always makes a constant angle with any radius emanating from that axis. Under these conditions, the angle θ_2 shown in Figure (5) would remain constant.

However, the medium with which we are concerned cannot be assumed to be incompressible. Therefore, the radial component of the air velocity with respect to the casing will not vary inversely as the radius. It must be corrected for the temperature and pressure variations encountered by the air as it moves outwards radially.

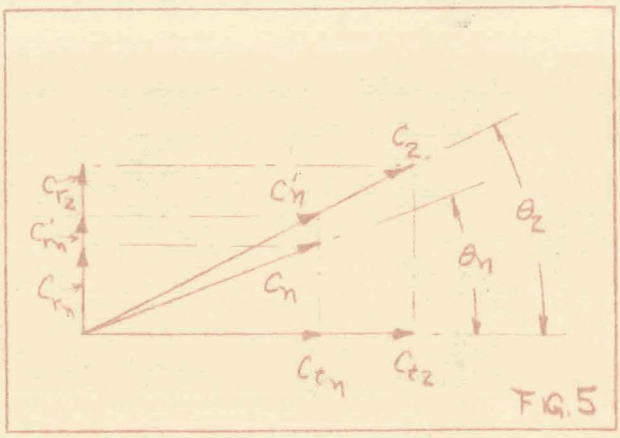

FIG. 5

In general, this correction produces a change in the angle made by the leading edges of the diffuser inlet vanes with the tangent of the order of 1° in the typical radial-blade superchargers which are now in use, when the diametral clearances are approximately 10% of the impeller diameter.

If the fluid is considered to be frictionless and incompressible, it can be assumed to a first approximation that the velocity C varies inversely as the radius.

That is
$$T_n - T_2 = \frac{1}{2g_s k_p}\left(C_2^2 - C_n^2\right) \tag{13}$$

or
$$\frac{T_n}{T_2} = \frac{1}{2g_s k_p T_2}\left(C_2^2 - C_n^2\right) + 1 \tag{14}$$

However, since
$$C_n = C_2 \frac{r_2}{r_n}$$

than it follows directly that
$$\frac{T_n}{T_2} = \frac{1}{2g_s k_p T_2}\left[1 - \left(\frac{r_2}{r_n}\right)^2\right] + 1 \tag{15}$$

where the subscript (2) refers to a position in the clearance space just outside of the impeller, and subscript (n) refers to the diffuser throat. (See Figure 6.)

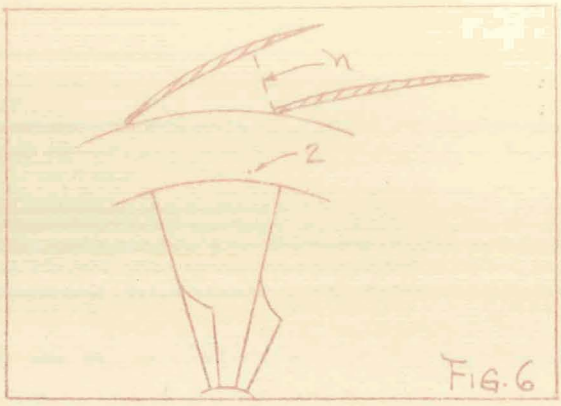

FIG. 6

Now, if the process (2-n) is considered to be isentropic

$$\frac{p_n}{p_2} = \left\{ \frac{C_2^2}{2 g_c R_p T_2} \left[1 - \left(\frac{r_2}{r_n} \right)^2 \right] + 1 \right\}^{\frac{K}{K-1}} \qquad (16)$$

These temperature and pressure ratios for a frictionless, incompressible fluid are used to correct the radial components of the air velocity and subsequently the resultant air velocities with respect to the casing at positions (2) and (n) according to the following formulae, viz:

Corrected radial velocity, $C_{r_n} = C_{r_2} \times \frac{r_2}{r_n} \times \frac{T_n}{T_2} \times \frac{p_2}{p_n}$ (17)

Corrected resultant velocity, $C_n = \sqrt{C_{t_n}^2 + C_{r_n}^2}$ (18)

C_n, makes an angle equal to the arc tangent $\frac{C_{r_n}}{C_{t_n}}$, with the tangent at the point at issue.

Vaned Type Diffusers

As has been previously pointed out, this refinement in the determination of the state point at (n) is frequently not justifiable, particularly in preliminary studies.

Knowing the temperature, pressure and the resultant velocity relative to the casing at the position (n), it is possible to calculate the diffuser throat area required to handle this quantity of air. Thus

$$A_n = \frac{W v_n}{M C_n} \qquad (19)$$

where

W =	mass airflow rate	lbs. per sec.
A_n =	cross-sectional area of the diffuser passage normal to flow	$ft.^2$
M =	number of diffuser passages	
v_n =	specific volume of the air at position (n)	$ft.^3$ per lb.
C_n =	air speed normal to cross-section of passage	ft. per sec.

The specific volume of the air at position (n) is calculated from the General Gas Law, namely $v = RT/p$
where R is the gas-constant, which for air is 53.3 ft. lbs. per pound per deg. F.

Having established the throat area of the diffuser passages, the remainder of the passage is designed so that it falls within the confines of the following

empirically determined equivalent cone. (See Figure 7.) These axial distances, 1.5" etc., are equal to the corresponding ℄ distances measured in the diffuser passages.

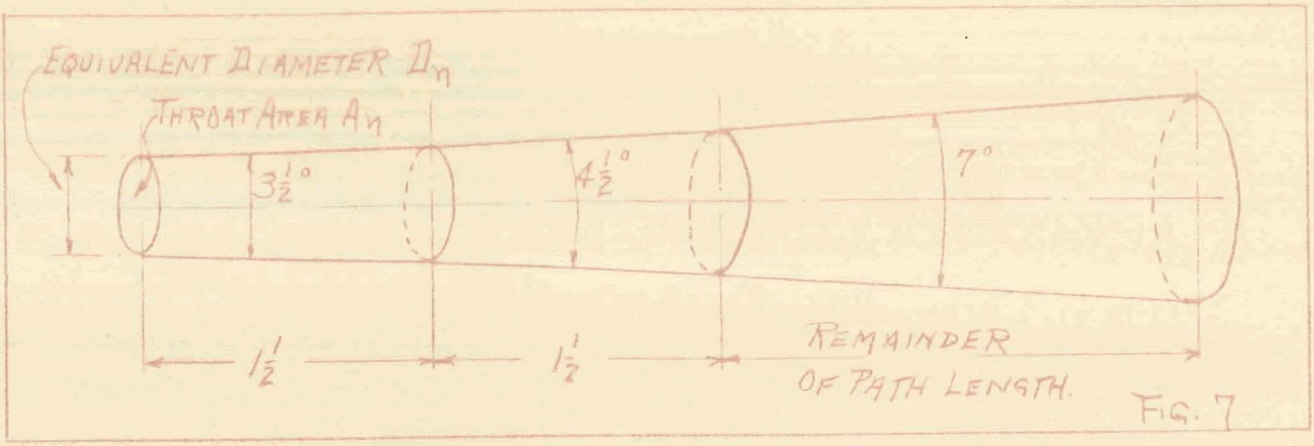

FIG. 7

These design details can be executed by either of the two following methods:

#1. Since the initial throat area A_n, has now been determined, the next throat area, A_x, is arbitrarily selected so that it falls within the limits of the equivalent cone, Figure (7).

If it is assumed that the flow through the diffuser passages is steady and isentropic, the following four simultaneous conditions can be written down.

$$\left.\begin{aligned} &A_n \rho_n C_n = A_x \rho_x C_x \\ &\frac{C_n^2}{2g_s} + \frac{p_n}{\rho_n} + JC_v T_n = \frac{C_x^2}{2g_s} + \frac{p_x}{\rho_x} + JC_v T_x \\ &\frac{p_n}{\rho_n^k} = \frac{p_x}{\rho_x^k} \\ &\frac{p_n v_n}{T_n} = \frac{p_x v_x}{T_x} \end{aligned}\right\} \qquad (20)$$

Equations (20) contain only four unknowns; but due to the nature of these equations, they cannot be explicitly solved. They can, however, be conveniently transformed and solved by cut-and-try methods.

#2. This alternative method (#2), which is more rapid than method #1, is also a cut-and-try method.

The diffuser throat area, A_n, having been established, the velocity (C_x) at the next downstream position (x) in question is assumed and the corresponding change in enthalpy is equated to the change in kinetic energy. This assumes that an isentropic process takes place between the two positions in question (6) and leads to the following expressions for the temperature and pressure ratios, respectively.

(6) It is unnecessary to assume that the process is isentropic until the expression for the pressure ratio (Eq. 22) is written.

$$\frac{T_x}{T_n} = \frac{C_n^2 - C_x^2}{2 g_s k_p T_n} + 1 \qquad (21)$$

and

$$\frac{P_x}{P_n} = \left[\frac{(C_n^2 - C_x^2)}{2 g_s k_p T_n} + 1 \right]^{\frac{k}{k-1}} \qquad (22)$$

where the subscript (n) refers to the diffuser throat, and (x) refers to the downstream position where the velocity (C_x) with respect to the channel has been assumed.

The specific volume (v_x) at position (x) can now be calculated from the formula

$$v_x = \frac{R T_x}{P_x} \qquad (23)$$

and the desired area (A_x) is given

$$A_x = \frac{W v_x}{M C_x} \qquad (24)$$

This channel area, A_x when reduced to an equivalent circle, must fall within the confines of the equivalent diffuser cone, Figure (7), at the position at issue.

Our usual procedure is to assume the velocity to decrease in increments of 100 ft. per sec. and proceed as indicated above. Of course, a certain amount of juggling is required at the transition points in the passage; but with some experience, the passages and vanes can be quickly laid out by straight-forward methods. That is, the ℄ of a passage is calculated by the Principle of the Conservation of Angular Momentum with suitable corrections for compressibility effects as included in equations (17) and (18). From this ℄ of the passage, various passage widths are laid off at right angles to the ℄ corresponding to the equivalent cone areas, and the outline of the vanes are drawn in with faired-in circular arcs.

These vane shapes, the edges of which should be fairly sharp at both leading and trailing edges, are usually somewhat complicated by the interference of various fastening arrangements. The resulting design is generally a compromise between flow and fastening complications.

Since the function of a diffuser is to convert the kinetic energy of the high speed air stream entering it into pressure energy with maximum availability, the final diffuser exit velocity should correspond to a maximum air density consistent with space limitations and discharge collector flow conditions.

A diffuser discharge speed of approximately 300' per second seems to be consistent with our best present design information.

PART II (Losses considered)

In PART I of the METHOD OF ANALYSIS no losses were considered. In Part II, however, an effort will be made to evaluate and allocate these various losses.

Both the (T-S) and the (h-S) diagrams are useful for visualizing the compression process which takes place in a centrifugal compressor. In the work which follows, the (T-S) diagram has been arbitrarily used, so that Part I and II will be more coherent. A typical (T-S) diagram is shown in Figure (8). However, the Mollier Chart (h-S) diagram should not be overlooked, as it has many advantages for this sort of work and is frequently used.

If the supercharger at issue operates along an isentropic path at an adiabatic efficiency of 100%, the corresponding process path in Figure (8) would be the vertical line $(1-\beta)$ connecting the initial and final thermodynamic state points. The length (height) of the line $(1-\beta)$, that is the temperature difference, being only a function of the initial state (1) and the specific energy input to the air by the impeller,

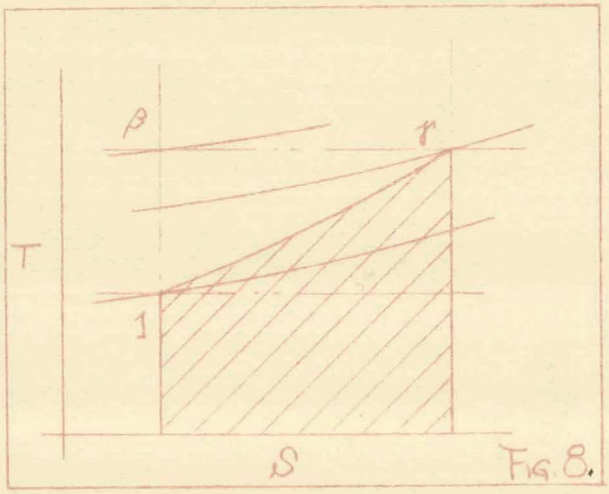

Fig. 8.

$$\Delta E = \frac{F_s V_T^2}{g_s}$$

However, the compression process which takes place in a supercharger does not occur at 100% adiabatic efficiency. Only a portion of the work which is done on the air by the impeller is available to compress the air; the remainder is transformed into heat which is not only unavailable but also reduces the final air density. Actually, the area under the process path $(1-\delta)$ represents the decrease in available energy which occurs when the compressor operates along the typically practical process path $(1-\gamma)$.

Equation 4, Part I, actually is the temperature-ratio for both the isentropic and the practical processes $(1-\beta)$ and $(1-\gamma)$, respectively, illustrated in Figure 8, since the temperature ratio is independent of the process path. However, the expression for the pressure ratio must be corrected as follows:

$$\frac{p_\gamma}{p_1} = \left\{ \frac{\eta_{AD}}{2 g_s k_p T_1} \left[\left(C_{a_1}^2 - C_\gamma^2 \right) + 2 F_s V_T^2 \right] + 1 \right\}^{\frac{K}{K-1}}$$

where (γ) refers to an arbitrary static state at which the velocity of the air with respect to the supercharger casing is (C_γ).

In equation (25), the adiabatic efficiency, $\eta_{AD} = \frac{T_3^1 - T_1}{T_3 - T_1}$, is shown in the diagram Figure (9), which is the (T-S) diagram for a typical impeller-diffuser combination.

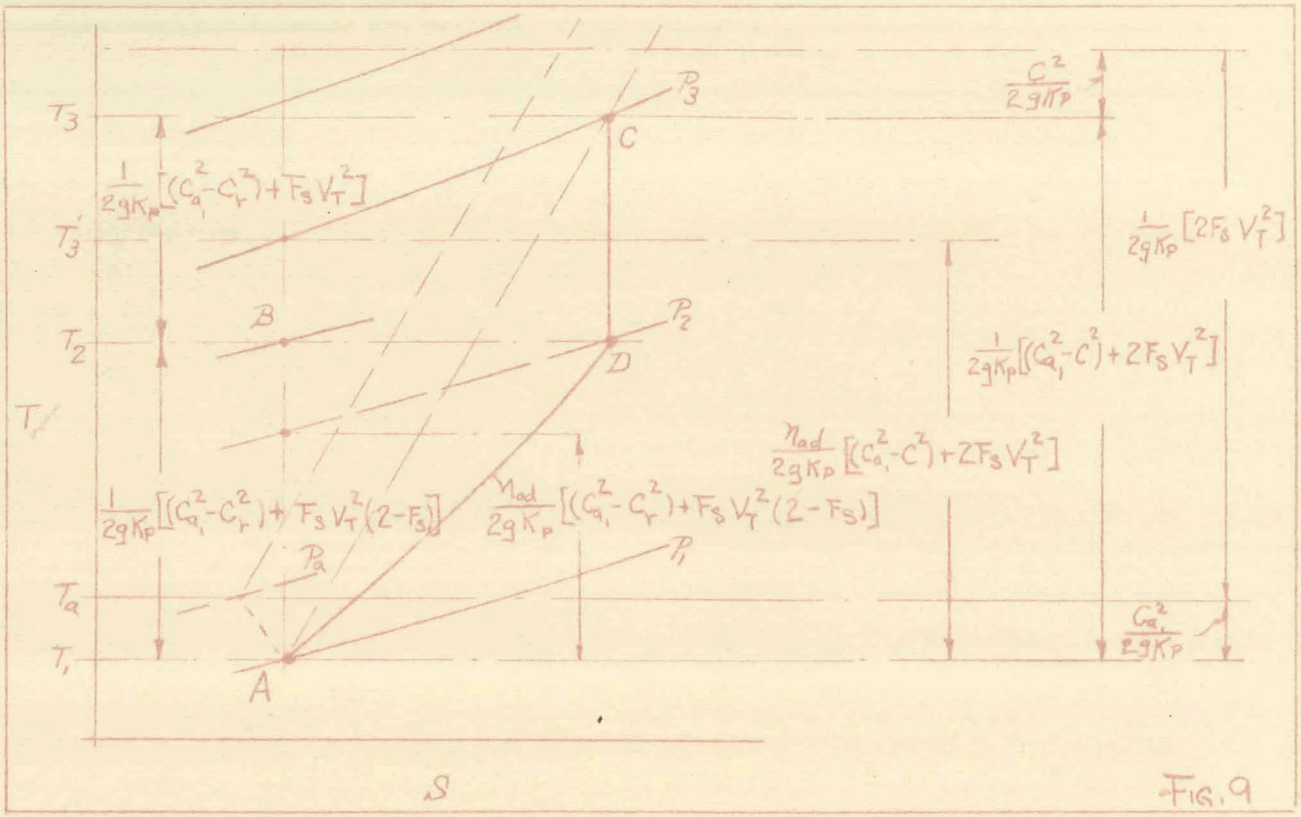

FIG. 9

That portion of the energy corresponding to $(T_3 - T_3^1)$ is transformed into undesirable heat which increases the specific volume of the air, thereby reducing the air density.

Two other important facts are also evident from a study of Figure (9). First, the kinetic energy of the air stream leaving the diffuser represents an incomplete conversion of the input work; and, second, the temperature drop $(T_a - T_1)$ which is necessary to produce the required approach velocity to the impeller inlet is chargeable against the impeller input work. Therefore, it would be desirable to reduce both of these velocities to a minimum, which design requirements dictate to be about 300 feet per second or less.

The initial and final thermodynamic state points for the overall impeller-diffuser combination are rather definitely established by engine ratings, and test-stand and field observations. Fairly accurate overall calculations can be made by previously described methods. However, the state point of the working fluid at the impeller tip is still partially indeterminate, and this information is necessary for the design of the diffuser throat and vane angle.

Experimental data on the state point at the impeller discharge are now within reach with the perfection of our new probes, visual flow, static tests, etc. However, to date this information has not been sufficiently well correlated for use.

The next step, therefore, is to establish a reasonable process path for the entire compression process, which, for the time being, will be used as the basis of actual design calculations. This will be accomplished, first, by blocking out a region within which the process path is known to lie, and then by actually establishing a reasonable process path within this region.

This region referred to will be blocked off as follows: If it is assumed that the impeller process has an adiabatic efficiency of 100% corresponding to 50% temperature rise in the impeller, the process path for the impeller would be the vertical line (A-B) shown in Figure (10). The remainder of the process through the diffuser could then be indicated by the line (B-C). Conversely, if an adiabatic efficiency of 100% was assumed for the process of the system exclusive of the impeller, the lines (A-D) and (D-C) would represent the process paths of impeller and the remainder of the system, respectively.

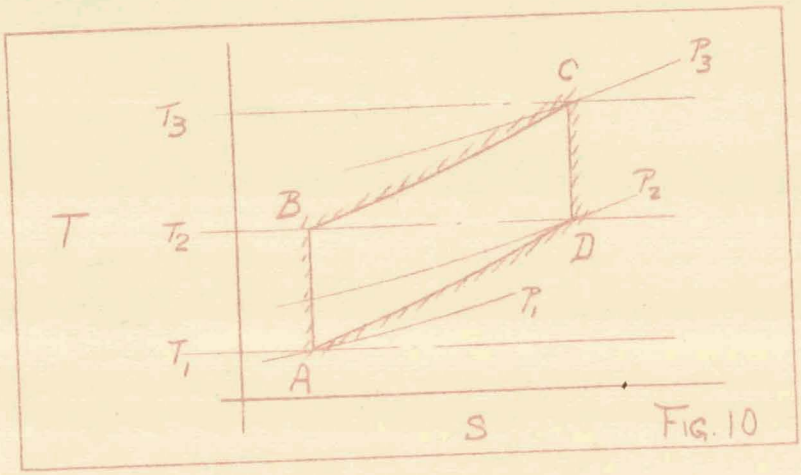

FIG. 10

These lines bound a region within which, it is reasonable to expect, the actual process path of the system (impeller-diffuser combination) lies.

The dimensions of existing designs and experimental tests indicate that the actual process path for the system corresponds more nearly to (A-D-C).

The question will immediately arise in the mind of the reader as to why such an apparently simple problem should have been made so complicated.

The bases of the uncertainty of the actual process path are largely experimental. Static impeller flow tests, which have been partially substantiated by visual flow tests and measurements on the corresponding actual rotating impellers, indicate that the average impeller channel runs, approximately, half full. Further, the radial discharge velocity distribution from the impeller is very irregular, having in some cases both positive and negative flow in the same passage.

Substantial improvement in impeller flow condition has been effected by reducing the impeller area-ratio, but the flow problem is obviously too complicated for a simple radial flow constriction to successfully eliminate.

The effects of partially full impeller passages are reflected throughout the entire system. For example, diffusers of normally high steady flow efficiency are known to operate in a correspondingly poor fashion when fed by such impellers. This fact has been proven by pressure, temperature and velocity traverses at the diffuser exit. Consequently, higher velocities actually exist in both the impeller and diffuser passages than were indicated by the preliminary theory. As has been previously pointed out, these excessive velocities are equivalent to incomplete energy conversions and lower efficiencies. In addition, the results of this type of flow are two-fold. First, the capacity of a machine which has been designed on the basis of simple theory (Part I) is invariably too low to meet its requirements. Second, the excessive amount of heat which is generated as a consequence of these higher velocities is largely unavailable for compression work.

One large energy loss which is difficult both to estimate and control is due to the impact of the impeller discharge stream on the diffuser inlet vanes at an angle other than the design angle. Stodola in Volume II, page 1261, of his treatise on "Steam and Gas Turbines" gives the curve Figure II showing the magnitude of impact loss in terms of the ratio

$$\frac{\text{Designed diffuser throat velocity}}{\text{Impeller discharge velocity relative to the casing}} = \frac{C_n}{C_2}$$

previously mentioned.

The impact loss, l_s, is given by the equation

$$l_s = \delta \times \frac{C_2^2}{2g_s}$$

See Figure 11. The values of δ taken from this curve indicate that the impact loss may constitute a large portion of the available energy in the impeller discharge stream. For best efficiency, this loss should be kept to a minimum by the choice of the correct vane angle.

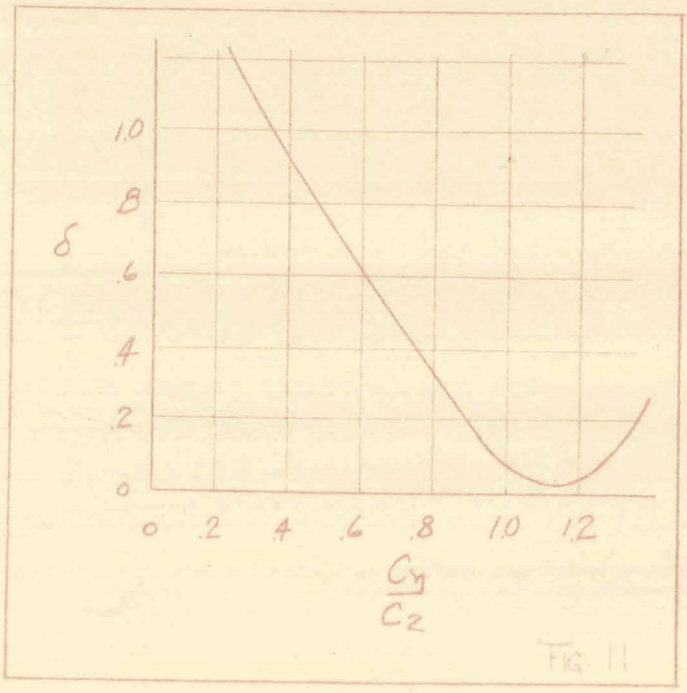

FIG. 11

Friction losses at normal subsonic flow velocities through various supercharger passages can be calculated by the usual conventional methods. However, some of the losses with which we are here concerned are due to the excessively high air velocities which are not usually encountered in ordinary practice. For example, the losses due to compression shock in the diffuser channels when the air velocities relative to these channels are supersonic.

As stated before, since the diffuser channels are fed by impeller channels which rarely run full, the inlet velocities in the diffuser at and near the throat can well be supersonic. Figure (12) at the end of this report, shows the flow temperature, pressure and velocity, changes in a straight venturi type of diffuser when the supersonic flow exists.

These curves Figure (12) bring out three important facts concerning passage shape for compression flow as follows:

1. For compression flow, when reducing the velocity from supersonic to subsonic, the flow area must first decrease to a throat section and then increase. The throat velocity will then be the velocity of sound at the prevailing thermodynamic condition.

2. For compression flow, when reducing the velocity from a high supersonic to a lower supersonic velocity, the flow area must decrease.

3. For compression flow from a high subsonic to a lower subsonic velocity the flow area must increase.

While the characteristics of this diffuser are for steady flow and consequently are not directly applicable to a supercharger diffuser; nevertheless, they do explain the approximate process in the diffuser channels.

Knowing that the flow through the supercharger diffuser is of a pulsating nature, due to successive impeller channels discharging into the diffuser, a second type of loss, namely "compression shock" undoubtedly exists to a marked degree. The loss in energy due to a compression shock in a diffuser channel where the flow is supersonic can be estimated in the following way. (7) The product of the supersonic velocity upstream of the shock and the subsonic velocity downstream of the shock equals the square of the velocity of sound. Mathematically,

$$a_1 a_2 = a^2$$

where a_1 - supersonic velocity upstream of the compression shock (ft. per sec.)
a_2 - subsonic velocity downstream of the compression shock (ft. per sec.)
a - velocity of sound - $49\sqrt{T}$ for air. (ft. per sec.)

The corresponding decrease in kinetic energy ΔK.E. is

$$\Delta \text{K.E.} \approx \frac{1}{2g_s}(a_1^2 - a^2)$$

From this equation, it is obvious that this type of loss can be comparatively large. (8)

One way of eliminating this type of loss is a diffuser would be to keep all velocities subsonic; however, this is impossible with present trends of design weight reduction, etc.

Therefore, if we agree that supersonic velocities must exist either locally or in the air-stream of diffusers, one way of reducing the possibility of compression shock actually developing in these passages is to make their surface very smooth and the changes in section very gradual.

---

(7) Flow of Gases at Rates Exceeding Accoustic Velocity (O. G. Tietjens - A.S.M.E. Trans. APM-53-4).

(8) This decrease in K.E. represents an upper limit of the compression-shock loss, since an increase in pressure accompanies it.

Other losses which can be reduced by proper design are the throttling and impact losses occurring at the ports of the inlet stacks of the collector case. The axes of these ports should be continuations of the ℄ of the diffuser channels.

Up to this time, the "heat transfer" problem has not been considered. While isothermal compression would be ideal, it is not possible to attain. While the heat transferred from the engine casings to the air does not appreciably affect the power required to drive the supercharger, it does have an effect upon the overall supercharger performance when it is installed on an engine. An estimate of the heat transfer from the engine casing to the supercharger air should be based on an overall heat transfer coefficient of from 15 to 25 BTU per sq. ft. per hour per degree F.

This effect can be overcome only at the expense of increased heat exchanger capacity for intercooling or aftercooling.

APPENDIX I (Illustrative example)

Assumed Specification Requirements

Mass Airflow	= 11400 lbs. per hour (3.17 lbs. per sec.)
C_{a_1}	= 250 ft. per sec.
T_1	= 470 deg. F. Abs.
P_1	= 18 In. Hg.
V_T	= 1225 ft. per sec.
F_s	= .925 (Best Efficiency)
Impeller Area Ratio Inducer on Impeller	= .8
Impeller Blades	= 22
Impeller Diameter	= 11"
Diffuser Vanes	= 9
Diffuser Exit Velocity	= 300 ft. per sec.

Inducer Design

For the inducer throat diameter find the specific volume of the air and, knowing the velocity at entrance C_{a_1}, calculate its diameter.

Specific Vol. $$v = \frac{RT}{P} = \frac{53.3 \times T}{144 \times .492 \text{ P In. Hg}} = .753 \frac{T}{P}$$

$$= .753 \times \frac{470}{18} = 19.65 \text{ ft. } 3/\#.$$

Throat Area $$A_1 = \frac{Q}{C_{a_1}} = \frac{3.17 \text{ \#/sec.} \times 19.65 \text{ ft.}^3/\# \times 144}{250 \text{ ft./sec.}} = 35.8 \text{ sq. in.}$$

And Throat Dia. $$\sqrt{\frac{4A}{\pi}} = \sqrt{\frac{4 \times 35.8}{\pi}} = 6.75" \text{ (Hub neglected.)}$$

Now that the throat size is established and the specifications call for an inducer, we shall assume that the inducer blade sections are to be similar to the N.A.C.A. #2412 thin-wing section. The reason for this choice is that this thin-wing section will give a larger net area within the inducer and still give the effect of stable entering edge with a 6^0 angle of attack.

As a further specification on the design of the inducer, the area expansion through it should be limited to a maximum of 8^0. The method of layout is illustrated on the following page.
Figure (13)

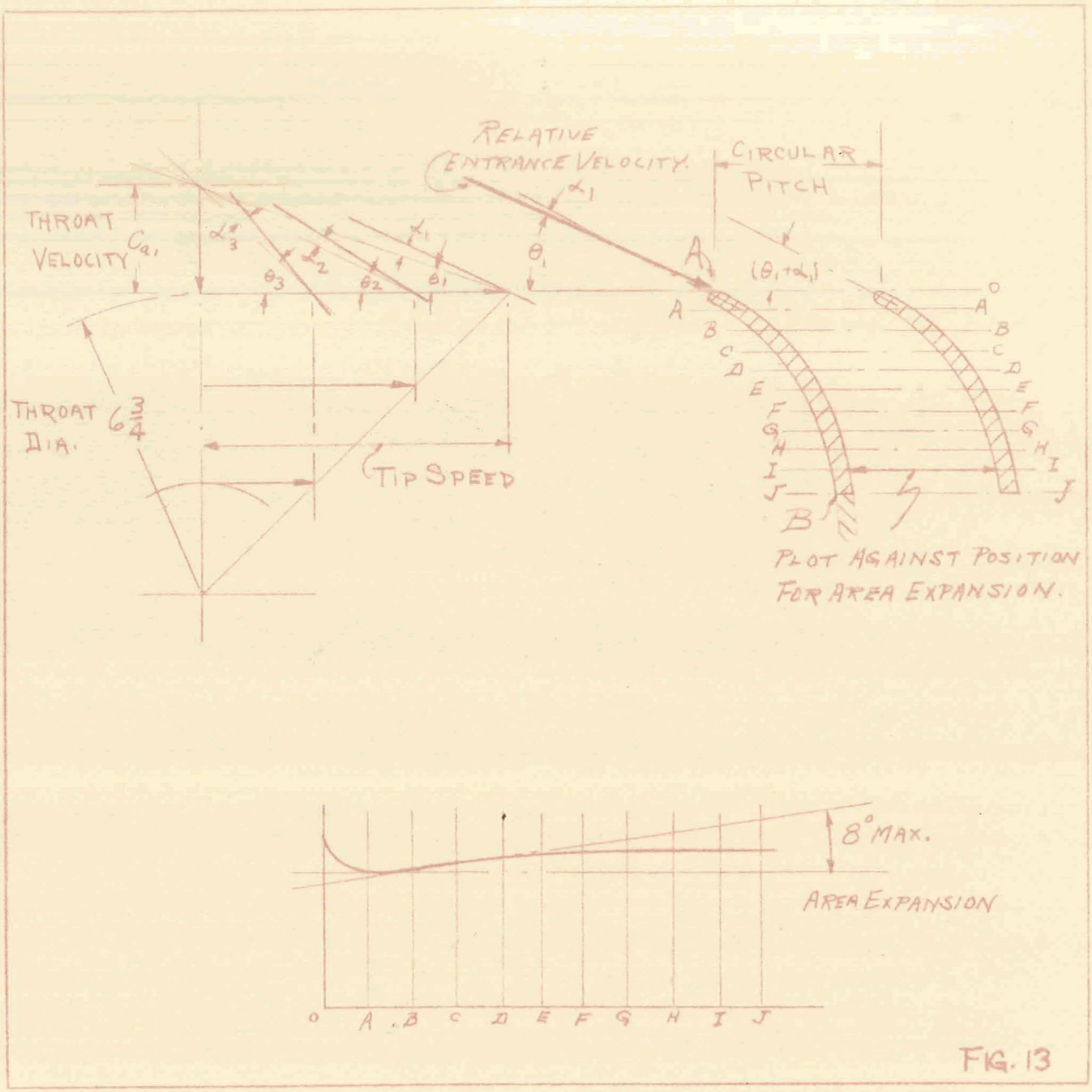

FIG. 13

While the above sketch is for the outer section of the inducer, the inner sections can be analyzed in the same manner. However, it will be found that the area expansion will always be greater at the outer sections than the inner ones, due to the decreasing circular pitch.

A point to bring out in the design of the entrance edge of the inducer is that the backside of the vane should be tangent to the relative entrance velocity as shown at "A".

Also the trailing edge should match the impeller blade as shown at "B". When mating the inducer to the impeller, particular care should be taken to make the transition radius "R" as large as possible, even to carrying it over into the inducer, as shown. The mating surface shown at "S", Figure (14), must also be well "faired-in".

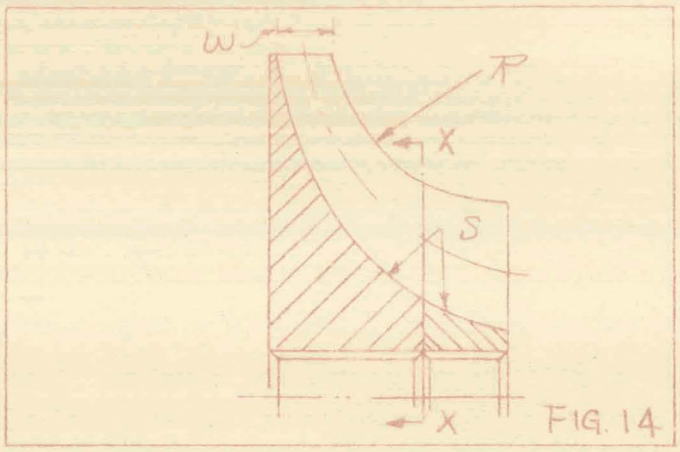

FIG. 14

Impeller Design

When an impeller has an inducer, find the net area at section X-X Figure 14 above, corrected for the blade thickness. Assume that this area is 30 sq.in., then the exit area is 30 x .8 = 24 sq.in. Assume that the mean blade thickness on the O.D. is 3/32", then the impeller channel width is

$$w = \frac{24}{(11\pi - 22 \times 3/32)} = .74" \text{ say } 3/4"$$

With the area ratio of 0.8, it can be said that the channel will run approximately full. Assume that the radial discharge velocity with respect to the impeller is 300 ft./sec. Using this value, calculate the state point immediately beyond the impeller tip, and then check back to see if the flow through the impeller equals 3.17 lbs. per sec. as specified. If not, change the velocity and recalculate until the correct results are obtained.

From equation (6), it follows that

$$\frac{T_2}{T_1} = \frac{1}{2g_s k_p T_1}\left[(C_{a_1}^2 - C_{r_2}^2) + F_s V_T^2 (2 - F_s)\right] + 1$$

$$= \frac{1}{64.4 \times 189 \times 470}\left[(\overline{250}^2 - \overline{300}^2) + .925 \times \overline{1225}^2 (2 - .925)\right] + 1$$

$$= \frac{1464500}{5.72 \times 10^6} + 1 = 1.256$$

or $T_2 = 1.256 \times 470 = 590^\circ$ F. Abs.

Likewise from equation (7) we have

$$\frac{P_2}{P_1} = \left\{ \frac{\eta_{AD}}{2g_s k_p T_1}\left[(C_{a_1}^2 - C_{r_2}^2) + F_s V_T^2 (2 - F_s)\right] + 1 \right\}^{\frac{K}{K-1}}$$

The value of "K" used in all of these calculations is = 1.395; then $\frac{K}{K-1} = 3.53$. As stated above for the impeller process shown from A to D Figure 10, the η_{AD} will be 0.5

So $\frac{P_2}{P_1} = \left[.5 \times .256 + 1\right]^{3.53} = 1.53$

$P_2 = 18 \times 1.53 = 27.5$ In. Hg

and the Specific Volume, $\mathcal{V} = .753 \times \frac{590}{27.5} = 16.15$ Ft.^{3} per lb.

Flow check for radial velocity:

$W = \frac{24}{144}" \times \frac{300}{1615} = 3.1$ lb. per sec. This is 2.5% low.

Recalculate assuming $C_{r_2} = 310$ ft. per sec.

Then $T_2 = 470 \left[1 + \frac{1458400}{5.72 \times 10^6} \right] = 590^\circ$ (no perceptible change)

and $P_2 = 18 \left[1 + 5 \times .255 \right]^{353} = 27.45$ In. Hg (slight change)

The Specific Volume, $\mathcal{V} = .753 \times \frac{590}{27.45} = 16.17$ ft.^{3} per lb.

Then the new flow rate is

$W = \frac{24}{144}" \times \frac{310}{16.17} = 3.19$ lbs. per sec. (check O.K.)

From these relations, the vector diagram for the air stream leaving the impeller tip is shown in Figure (15)

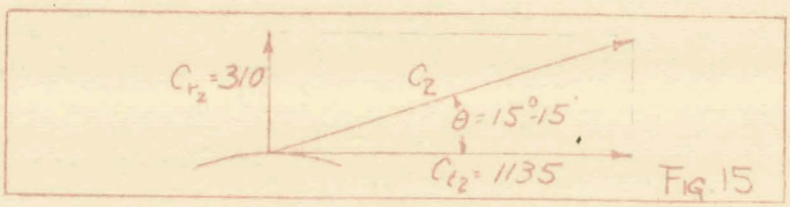

Fig 15

$\text{TAN}\,\theta = \frac{310}{1135} = 0.273$

$\theta = 15^\circ - 15'$

$C_{t_2} = F_3 V_T = 1135$

$C_2^2 = 1.384 \times 10^6$

The state point at the impeller tip is now established. The next step is to cross the clearance space between impeller tip and diffuser throat.

A point to bring out is the reason for and the amount of the clearance. The clearance should be designed so that the stream velocity is reduced to below the velocity of sound at the vane tips. A diametral clearance of 10% of the wheel diameter usually is sufficient. Therefore, on an 11" impeller the total clearance would be 11 x .1 = 1.1" or 0.55" radial clearance, say 9/16" in round figures.

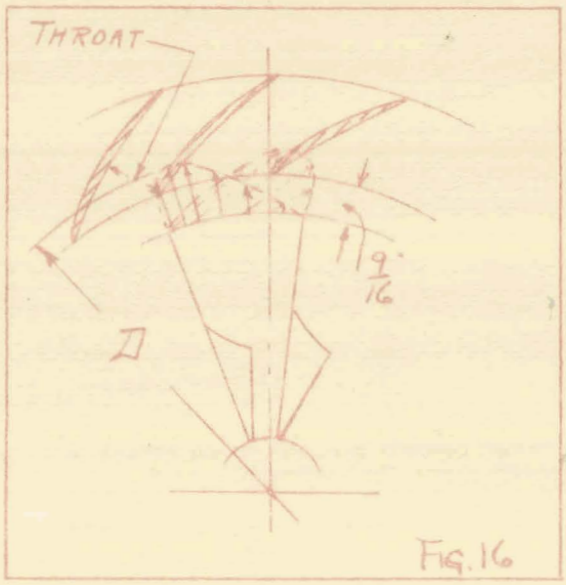

Fig. 16

One reason for this clearance space is that due to the finite thickness of both impeller blades and diffuser vanes there would be an abrupt change in flow area each time the blade passed a vane, with a consequent shock loss. This shock would produce a screech or noise which in itself is indicative of an energy loss. Also the frequency of these shocks may so excite the impeller blades as to produce an eventual fatigue failure. Another reason is that due to the irrotational component in the radial velocity all streamlines of flow from the impeller channel do not flow in a radial direction but slant backward (in some cases there is a forward slant due, among other causes, to turbulence set up from the impeller entrance vane) which when compounded with the tangential velocity produces an absolute velocity jet that has different direction and magnitudes for each point and spreads out like a fan. Therefore, in order to dampen out this condition, clearance must be provided which will allow all of the different components of velocity to stabilize to a common mean, which will strike the diffuser vane at the correct angle.

Theoretical Diffuser Design

Consider that the clearance space is a vaneless diffuser and, for this analysis, extends to the throat of the diffuser entrance as indicated by the dimension "D" Figure (16). Assume that from a preliminary layout of the supercharger D = 13". Then, using equation (15), we have

$$\frac{T_n}{T_2} = \frac{C_2^2}{2 g_s k_p T_2}\left[1 - \left(\frac{r_2}{r_n}\right)^2\right] + 1 = \frac{1{,}384{,}100\left[1 - \left(\frac{5.5}{6.5}\right)^2\right]}{64.4 \times 189 \times 590} + 1 = 1.0548$$

and $T_n = 590 \times 1.0548 = 623^\circ$ F. Abs.

Likewise from equation (16)

$$\frac{p_n}{p_2} = \left\{\frac{C_2^2}{2 g_s k_p T_2}\left[1 - \left(\frac{r_2}{r_n}\right)^2\right] + 1\right\}^{\frac{K}{K-1}} = (1.0548)^{3.53}$$

3.53

Then $p_n = 27.45\ (1.0548)^{3.53} = 33.2$ In. Hg

The Specific Volume $v_n = .753 \times \frac{623}{33.2} = 14.15$ ft.^{3}/#

The tangential velocity $C_{t_n} = 1135 \times \frac{5\ 1/2}{6\ 1/2} = 960$ ft./sec.

The radial velocity $C_{r_n} = 310 \times \frac{5\ 1/2}{6\ 1/2} \times \frac{1.0548}{1.207} = 229$ ft./sec.

Then the absolute velocity $C_n = \sqrt{\overline{229}^2 + \overline{960}^2} = \sqrt{974{,}500}$

$$C_n = 988 \text{ ft./sec.}$$

The theoretical throat area $A_n = \frac{3.17}{9} \times 144 \times \frac{14.15}{988} = .725$ sq.in.

and the Equivalent Dia. $D_n = .962"$

The corrected entrance angle $\theta_n =$ arc tangent $\frac{229}{960}$

$$\theta_n = 13^\circ - 25'$$

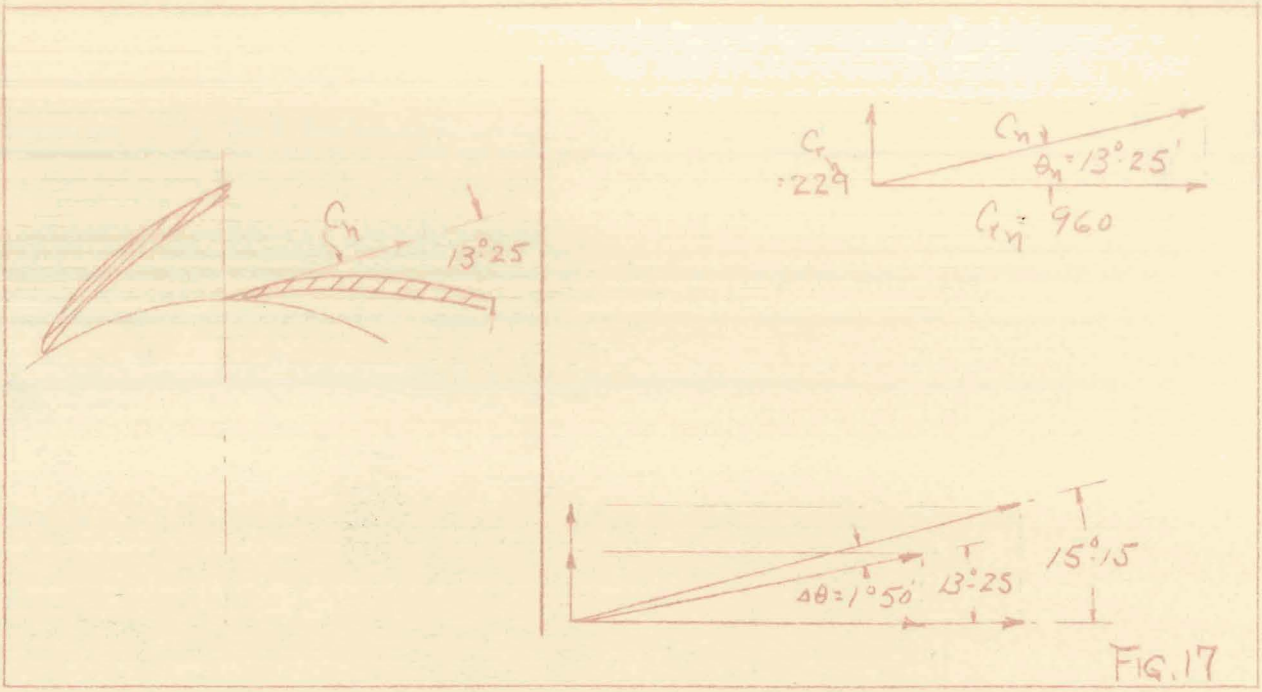

FIG. 17

The sketch at the right of Figure (17) shows the effect upon the airstream path of the change in the radial velocity due to compression of the air after it leaves the impeller. The diagram to the left points out that the diffuser vane should be shaped so that the convex side is tangent to the absolute airstream path as it enters the vane circle.

Using equations (21) and (22), establish the state point at the exit of the diffuser

$$\frac{T_3}{T_n} = \frac{C_n^2 - C_2^2}{2 g_s k_p T_n} + 1 = \frac{(974500 - \overline{300}^2)}{64.4 \times 189 \times 623} + 1 = 1.1166$$

Then $T_3 = 623 \times 1.1166 = 696°F$

And $$\frac{p_3}{p_n} = \left[\frac{\eta_{AD}(C_n^2 - C_2^2)}{2 g_s k_p T_n} + 1\right]^{3.53} = (1.1166)^{3.53} = 1.475$$

Then $p_3 = 33.2 \times 1.475 = 49$ In. Hg.

Begin at the theoretical diffuser throat and go through it in steps of velocity decrease, of say 100 ft./sec. approximately, for the first few sections.

Station I Assume $C_x = 900$ ft./sec.

$$\frac{T_I}{T_n} = \frac{(974500 - 810000)}{7.58 \times 10^6} + 1 = 1.0217$$

$T_I = 623 \times 1.0217 = 636°F$

$p_I = 33.2 (1.0217)^{3.53} = 33.2 \times 1.0765 = 35.7$ In. Hg.

$v_I = .753 \times \frac{636}{35.7} = 13.42$ ft.^{3}/lb.

Area $A_I = 50.7 \times \frac{13.42}{900} = .757$ sq. in. Equivalent Dia. = .977

Station II — Assume C_x = 800 ft./sec.

$$\frac{T_{II}}{T_0} = \frac{(974500 - 640{,}000)}{7.58 \times 10^3} + 1 = 1.0442$$

$$T_{II} = 623 \times 1.0442 = 652^\circ F \text{ Abs.}$$

$$p_{II} = 33.2\ (1.0442)^{3.53} = 33.2 \times 1.164 = 38.6 \text{ In.Hg.}$$

$$v_{II} = .753 \times \frac{652}{38.6} = 12.73 \text{ ft.}^3/\text{lb.}$$

Area $A_{II} = 50.7 \times \frac{12.73}{800} = .808$ sq.in. Equivalent Dia. = 1.012"

Station III — Assume C_x = 700 ft./sec.

$$\frac{T_{III}}{T_0} = \frac{(974500 - 490{,}000)}{7.58 \times 10^3} + 1 = 1.0638$$

$$T_{III} = 623 \times 1.0638 = 663^\circ F \text{ Abs.}$$

$$p_{III} = 33.2\ (1.0638)^{3.53} = 33.2 \times 1.244 = 41.3 \text{ In.Hg.}$$

$$v_{III} = .753 \times \frac{663}{41.3} = 12.1 \text{ ft.}^3/\text{lb.}$$

Area $A_{III} = 50.7 \times \frac{12.1}{700} = .876$ sq.in. Equivalent Dia. = 1.055"

Section IV — Assume C_x = 600 ft./sec.

$$\frac{T_{IV}}{T_0} = \frac{(974500 - 360{,}000)}{7.58 \times 10^3} + 1 = 1.081$$

$$T_{IV} = 623 \times 1.081 = 673^\circ F \text{ Abs.}$$

$$p_{IV} = 33.2\ (1.081)^{3.53} = 33.2 \times 1.316 = 43.6 \text{ In.Hg.}$$

$$v_{IV} = .753 \times \frac{673}{43.6} = 11.62 \text{ ft.}^3/\text{lb.}$$

Area $A_{IV} = 50.7 \times \frac{11.62}{600} = .983$ sq.in. Equivalent Dia. = 1.12"

Station V — Assume C_x = 450

$$\frac{T_V}{T_0} = \frac{(974500 - 202000)}{7.58 \times 10^3} + 1 = 1.1018$$

$$T_V = 623 \times 1.1018 = 686^\circ F \text{ Abs.}$$

$$p_V = 33.2\ (1.1018)^{3.53} = 33.2 \times 1.4 = 46.5 \text{ In.Hg.}$$

$$v_V = .753 \times \frac{686}{465} = 11.1 \text{ ft.}^3/\text{lb.}$$

Area $A_V = 50.7 \times \frac{11.1}{450} = 1.252$ sq.in. Equivalent Dia. = 1.262"

Station VI Assume $C_x = 300$

$$\frac{T_{VI}}{T_{II}} = \frac{(974500 - 90000)}{7.58 \times 10^3} + 1 = 1.1166$$

$$T_{VI} = 1.1166 \times 623 = 696°F \text{ Abs.}$$

$$P_{VI} = 33.2\ (1.1166)^{3.53} = 33.2 \times 1.475 = 49 \text{ In. Hg.}$$

$$v_{VI} = .753 \times \frac{696}{49} = 10.7 \text{ ft.}^3/\text{lb.}$$

Area $A_{VI} = 50.7 \times \frac{10.7}{300} = 1.8$ sq. in. Equivalent Dia. = 1.52"

From this data sketch the (T-S) diagram and show the process path. Figure (18).

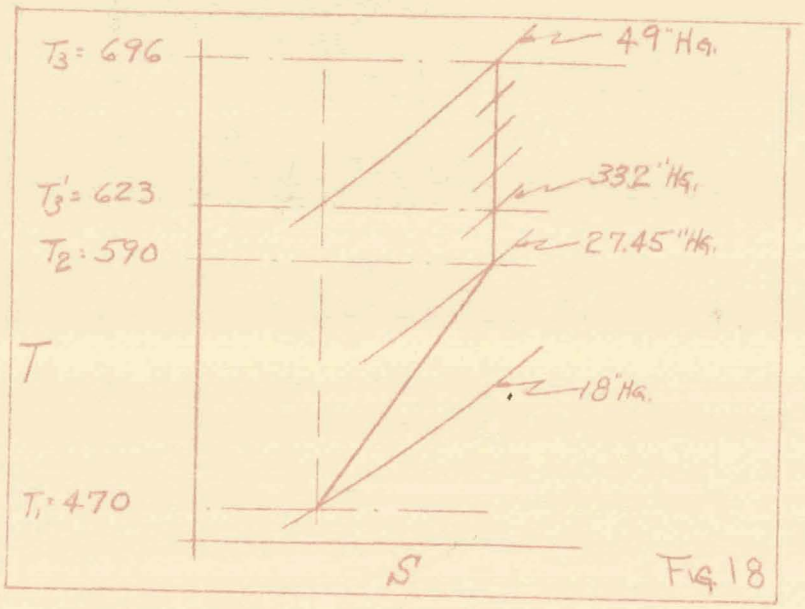

If the supercharger had an adiabatic efficiency, $\eta_{AD} = 100\%$, the temperature ratio would be

$$\frac{T_3'}{T_1} = \left(\frac{P_3}{P_1}\right)^{\frac{1}{3.53}} = \left(\frac{49}{18}\right)^{0.283}$$

and

$T_3^1 = 470 \times 1.326 = 623$; therefore, the total overall, η_{AD}, of the impeller-diffuser combination will be

$$\frac{T_3' - T_1}{T_3 - T_1} = \frac{623 - 470}{696 - 470} = 67.7\%$$

This is about 3% higher than what we actually find by test, and indicated that our impeller η_{AD} should have been approximately 49%. However, with the improvements enumerated elsewhere in this report, we hope to approach or exceed the above efficiency at the tip-speed specified.

Using this efficiency, calculate the state point of the impeller-diffuser combination using equations

$$\frac{T_3}{T_1} = \frac{1}{2 g_s k_p T_1}\left[\left(C_{a_1}^2 - C_3^2\right) + 2 F_s V_T^2\right] + 1$$

$$= \frac{1}{64.4 \times 189 \times 470}\left[\left(\overline{250}^2 - \overline{300}^2\right) + 2 \times 0.925 \times \overline{1275}^2\right] + 1 = 1.48$$

And $T_3 = 1.48 \times 470 = 696^\circ$ F. Abs.

Also $\frac{p_2}{p_1} = \left\{ \frac{\eta_{AD}}{2 g_s k_p T_1} \left(C_{a_1}^2 - C_3^2 \right) + 1 \right\}^{3.53}$ Let $\eta_{AD} = 67.7\%$

$= \left\{ 1 + .677 \times .48 \right\}^{3.53} = (1.325) = 2.73$

And $= 18 \times 2.71 = 48.8$ In. Hg

Theoretical Diffuser Passage Layout

Using the calculated values for the different diffuser stations together with the equivalent cone data previously given on page 17 (Figure 7), lay out the passage as shown on Figure (19)

$$\text{Tan } \frac{3.5^\circ}{2} = .0306$$

$$\text{Tan } \frac{4.5^\circ}{2} = .0393$$

$$\text{Tan } \frac{7^\circ}{2} = .0612$$

FIG. 19

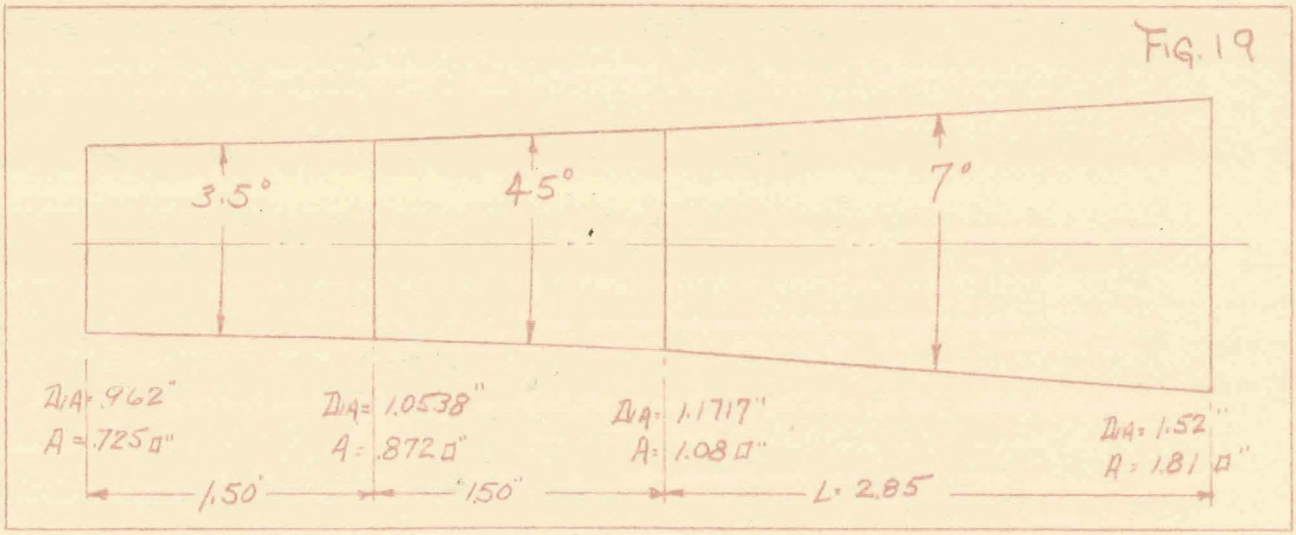

Area and Dia. at first transition point

$$\text{Tan } \frac{3.5^\circ}{2} = \frac{D_1 - D_o}{2L}$$

$$D_1 = 2L \text{ Tan } \frac{3.5}{2} + D_o = .0306 \times 2 \times 1.5 + .962 = 1.0538"$$

$A_1 = .872$ sq. in.

Area and Dia. of second transition point

$$D_2 = 3 \times .0393 + 1.0538 = 1.1717"$$

$A_2 = 1.08$ sq. in.

Length of 7 Divergence Cone - $L = \frac{1.52 - 1.1717}{2 \times .0612} = \frac{.3483}{.1224} = 2.85"$

Passage Length to Station I from throat

$$L_1 = \frac{D_1 - D_o}{2 \text{ Tan } \frac{3.5}{2}} = \frac{.977 - .962}{2 \times .0306} = .245"$$

Passage Length to Station II from throat

$$L_{II} = \frac{1.012 - .962}{2 \times .0306} = .817"$$

Station III falls approximately on the first transition point.

Passage Length from first transition point to Station IV

$$L_{IV} = \frac{1.12 - 1.0538}{2 \times .0393} = .842"$$

Passage Length from section transition point to Station V

$$L_V = \frac{1.262 - 1.1717}{2 \times .0612} = .737"$$

Actual Diffuser Design

From numerous airflow patterns which have been made on diffusers of various designs and sizes, it has been rather definitely established that the theoretical throat area of the diffuser has been reduced approximately 35% by the "Stagnation Zone", which apparently exists at the tip of the diffuser vane. A possible explanation of this phenomena is the lift effect of the diffuser vane tip as an airfoil section. See Figure (20).

The effect of this so-called stagnation zone is to effectively throttle the diffuser passage, so that if this effect is not corrected for in a diffuser, the resulting design will inevitably have a capacity which is too low.

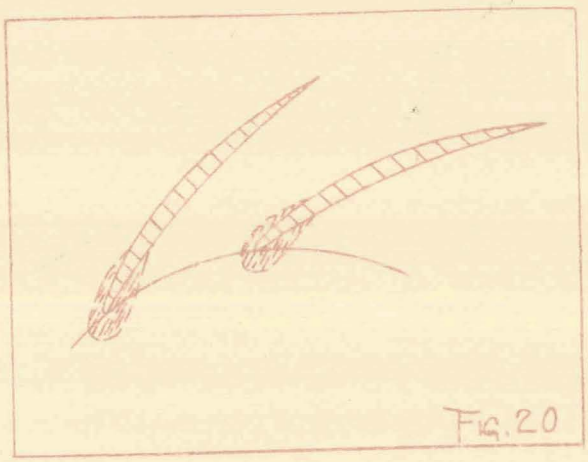

Fig. 20

It is necessary, therefore, to correct the theoretical diffuser throat area for this stagnation throttling. This is done by multiplying the theoretical diffuser throat area by a factor 1.35. So that in the case of the particular diffuser design at issue in this illustrative example, the throat actually used is

$$0.725 \times 1.35 = 0.978 \text{ sq. in.}$$

From this point on, the diffuser design follows the method previously outlined, but based on an initial throat area of 0.978 sq. in.

The calculation of the actual flow passage follows immediately, and the corresponding equivalent cone is shown in Figure (21).

Area and diameter at first transition point

D = 2 x 1.5 x .0306 + 1.115 1.207"

A = 1.140 sq.in.

Area and diameter at second transition point

D = 2 x 1.5 x .0393 + 1.207 1.674"

A = 2.18 sq.in.

Figure 21 shows the theoretical and actual diffuser passage contours together with the expected temperature and pressure variations. It is important to note that the velocity gradient is greatest in the throat section. Consequently, this throat (as well as the whole passage) should be very smooth and free from sudden changes in section.

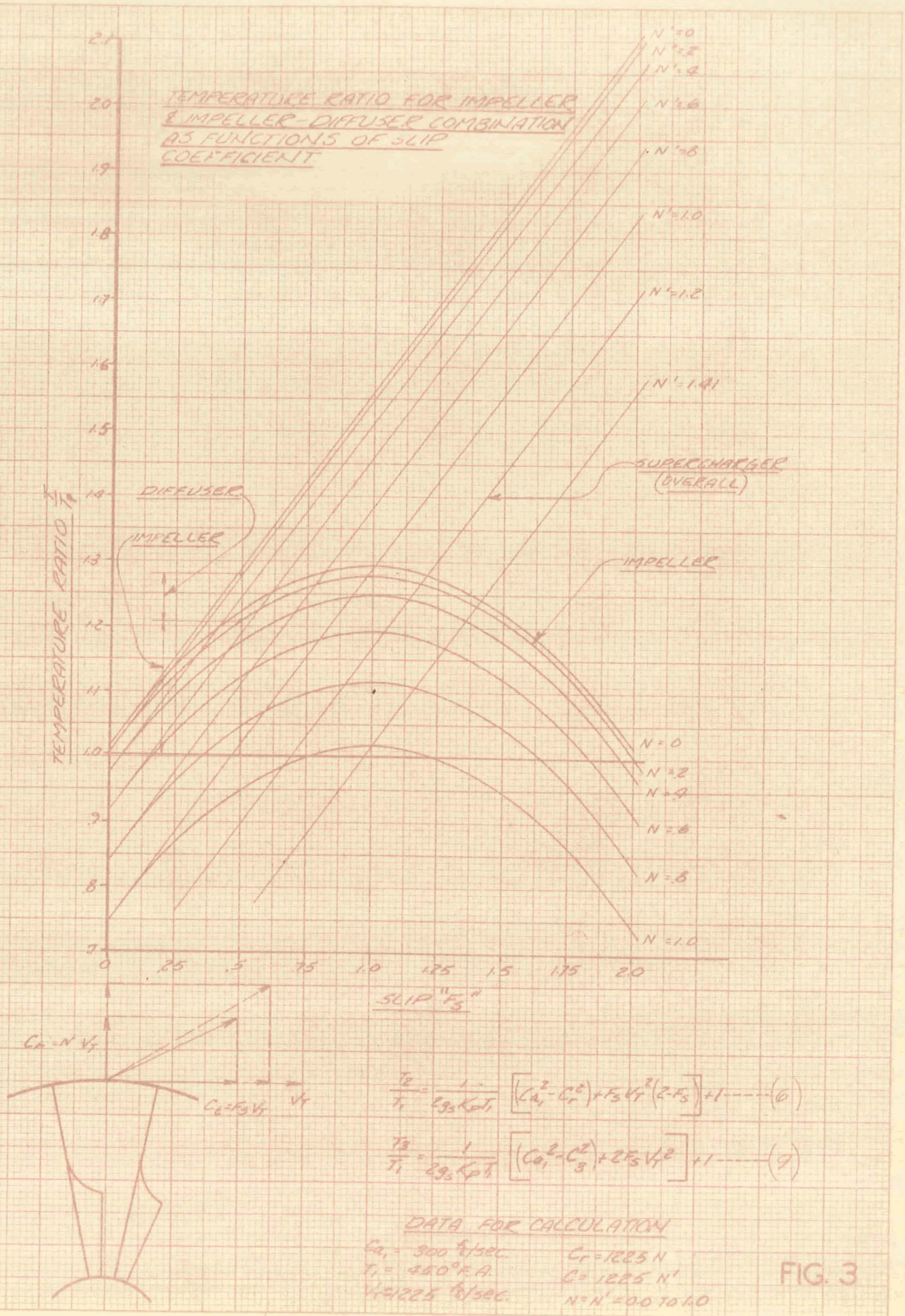

$$\frac{T_2}{T_1} = \frac{1}{2g_3 K_p T_1}\left[\left(C_{a_1}^2 - C_r^2\right) + F_3 V_f^2\left(2 - F_3\right)\right] + 1 \quad \text{---(6)}$$

$$\frac{T_3}{T_1} = \frac{1}{2g_3 K_p T_1}\left[\left(C_{a_1}^2 - C_3^2\right) + 2F_3 V_f^2\right] + 1 \quad \text{---(7)}$$

DATA FOR CALCULATION

C_{a_1} = 300 ft/sec.
T_1 = 440° F.A.
V_f = 1225 ft/sec.
C_r = 1225 N
C_3 = 1225 N'
N = N' = 0.0 TO 1.0

FIG. 3

KEUFFEL & ESSER CO., N. Y. No. 359-11
359 x 28 to the Inch, 10th Ruling.
MADE IN U.S.A.

FIG. 12

DIFFUSER CHARACTERISTICS

FOR COMPRESSION FLOW FROM SUPER-SONIC TO SUB-SONIC VELOCITIES

DATA FOR CALCULATION:

T = 1700 FAHRENHEIT ABSOLUTE

P = 29.9 "Hg.

V = 367 ft/sec.

ρ = 58.8 #/ft.³ of

n = 1.395

g = 2500 ft./sec.

A = AREA

VELOCITY OF SOUND $a = \sqrt{gnRT}$

CONTINUITY EQUATION = $\frac{A_1 \times \rho_1 \times V_1}{g} = \frac{A_2 \times \rho_2 \times V_2}{g}$

E = ENERGY $= \frac{n}{n-1} \frac{P}{\rho} \left[\left(\frac{P_2}{P_1} \right)^{\frac{n-1}{n}} + 1 \right] \frac{V_2^2 - V_1^2}{2g}$

THEN $\frac{A_2}{A_1} = \left[\left(\frac{V_2^2 - V_1^2}{2g} \right) \cdot \left(\frac{n-1}{n} \right) \cdot \left(\frac{P_1}{P_2} \right)^{\frac{n-1}{n}} + 1 \right] \frac{\rho_1}{\rho_2} \frac{V_1}{V_2}$

$= \left[1 - \frac{(V_2^2 - V_1^2)}{2gn} \left(\frac{n-1}{n} \right) \left(\frac{P_1}{P_2} \right)^{\frac{n-1}{n}} \right] \frac{\rho_1}{\rho_2} \frac{V_1}{V_2}$

$\frac{A_2}{A_1} = \frac{(1367.2)}{(1700)} = .804$

VELOCITY

TEMPERATURE

ENERGY

VELOCITY

AREA

VOLUME

INCORT SECTION

ENERGY ft. lbs x 10^3

PRESSURE "Hg

37

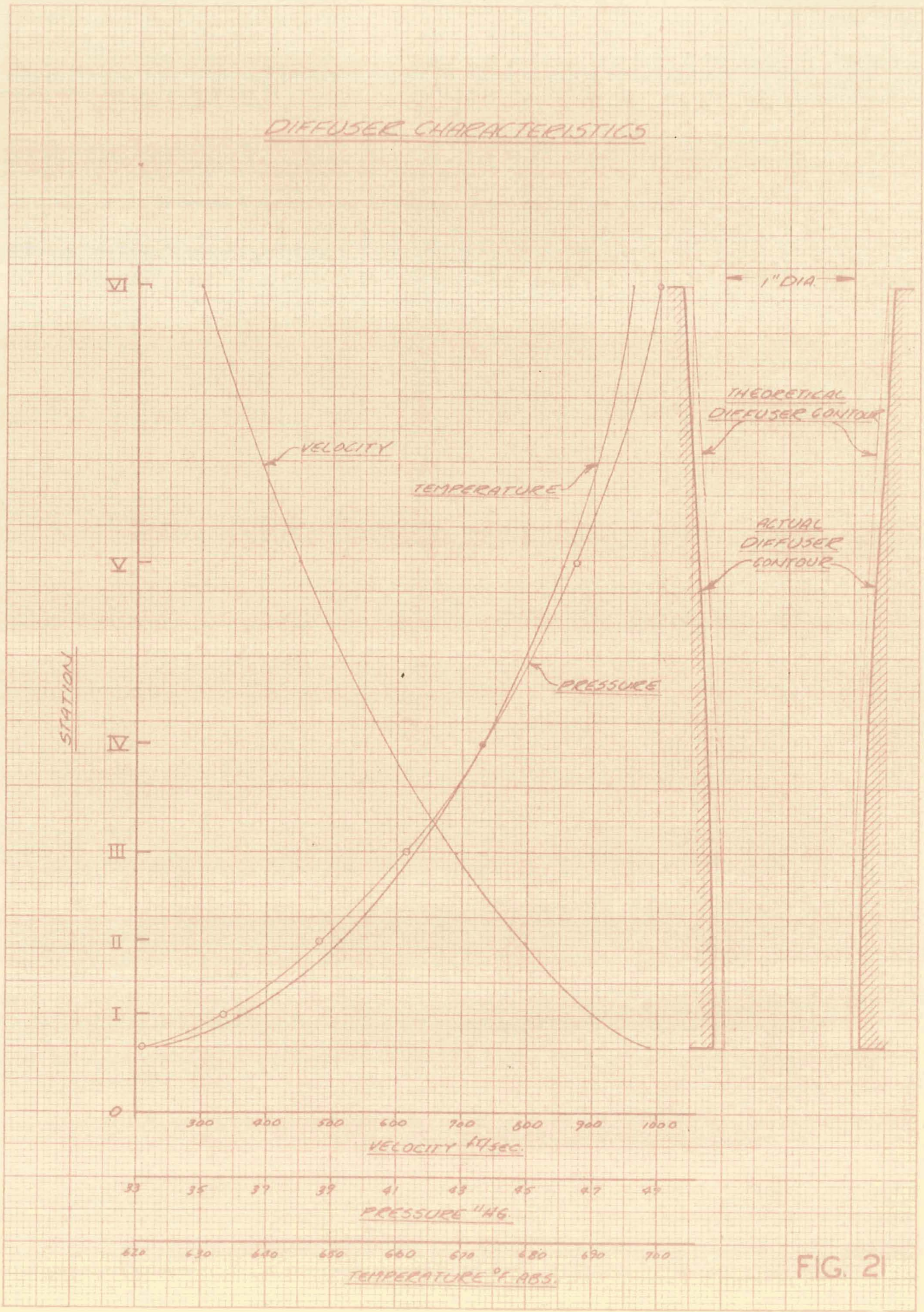
DIFFUSER CHARACTERISTICS
VI
V
IV
III
II
I
0
STATION
VELOCITY
TEMPERATURE
PRESSURE
1" DIA.
THEORETICAL DIFFUSER CONTOUR
ACTUAL DIFFUSER CONTOUR
300 400 500 600 700 800 900 1000
VELOCITY ft/sec.
33 35 37 39 41 43 45 47 49
PRESSURE "Hg.
620 630 640 650 660 670 680 690 700
TEMPERATURE °F ABS.

FIG. 21

List of Symbols

Definitions	Units
g_s = standard acceleration of gravity	32.174 (32.2) ft. per sec.^{2}
K = isentropic exponent = $\frac{c_p}{c_v}$	1.395
L = torque	lb. ft.
p = static pressure	lbs. per ft.^{2}
r = radius	ft.
T = absolute temperature	^{o}
V = air velocity relative to the impeller	ft. per sec.
V_a = axial component of air velocity relative to impeller	ft. per sec.
V_t = tangential component of air velocity relative to impeller	ft. per sec.
V_r = radial component of air velocity relative to impeller	ft. per sec.
V_T = impeller tip-speed	ft. per sec.
W = mass air flow rate	lbs. per sec.
Z = number of impeller blades	
c_p = specific heat at constant pressure	BTU per lb. per ^{o}F.
k_p = specific heat at constant pressure	Ft. lbs. per lb. per ^{o}F.
c_v = specific heat at constant volume	BTU per lb. per ^{o}F.
k_v = specific heat at constant volume	Ft. lbs. per lb. per ^{o}F.
F_s = slip coefficient	
ρ = mass density	lbs. per ft.^{3}
E = mechanical work done per lb. of air by the supercharger impeller	ft. lbs. per lb.
C = Velocity of the air, with respect to the supercharger casing	ft. per sec.
C_a = axial component of the air velocity with respect to the supercharger casing	ft. per sec.
C_t = tangential component of the air velocity with respect to the supercharger casing	ft. per sec.
C_r = radial component of the air velocity with respect to the supercharger casing	ft. per sec.
ω = angular velocity of the impeller	Radians per sec.
v = specific volume	ft.^{3} per lb.
Q = volume air-flow rate	ft.^{3} per sec.
A = cross-sectional area $\perp$ to the direction of flow	ft.^{2}
w = impeller channel width (see Figure 14)	inches
h = specific enthalpy	B.T.U. per lb.
s = specific entropy	B.T.U. per lb. per deg. F.
N = dimensionless factor	
N^1 = dimensionless factor	
θ = angle	Degrees
η_{Ad} = adiabatic efficiency	
R_a = area ratio	

List of Subscripts

1 - supercharger impeller inlet
2 - just beyond the impeller exit
3 - just beyond the diffuser exit
n - diffuser throat
x - arbitrary position in diffuser passage

REPORT C

"Pages missing from available version"

1 through 5 missing

SUMMARY OF SUGGESTED DESIGN PROCEDURE

Detailed impeller and diffuser design procedure recommended at this writing is set forth in the following pages. The procedure described is based on tests, calculations, and study of the literature available, results of which are discussed in other chapters of this report.

Preliminary Data

Preliminary data necessary for supercharger design are the desired horsepower and speed of the engine, the critical altitude, and the outline of the space available for impeller and diffuser. Estimate manifold pressure requirements from available data on performance of other engines.

Impeller Design

The tip speed (feet per second) required is then obtained by solution of the following equation:

$$V^2 = \frac{6082\ T_1 \left[\left({}^{P_2}/_{P_1} \right)^{.283} - 1 \right]}{.650}$$

Where P_1 = supercharger entrance pressure ("Hg. absolute)

P_2 = manifold pressure ("Hg. absolute)

.650 = a conservative value of pressure coefficient

T_1 = supercharger entrance temperature ($^{\circ}$F absolute)

The gear ratio and impeller outside diameter are selected to give the required tip speed as determined above. The impeller tip speed should not exceed values somewhat less than the speed of sound at the temperature existing at the impeller periphery. The compressibility effects near the speed of sound probably decrease the efficiency substantially. The speed of sound may be assumed as 1050 feet per second at 0°F and may be assumed to vary directly as the square root of the absolute temperature in degrees Fahrenheit. It is independent of the pressure. Good efficiencies are obtainable at 1250 ft/sec tip speed.

The next step is to determine the value of Q/n (cubic feet of air per impeller revolution at entrance conditions) at which the engine operates. From engine calibrations it has been found that the weight of air into an engine in #/min is approximately .110 times the HP. in low or 7.1:1 ratio and .117 times the HP. in high or 10:1 ratio. From the following formula one can find the value of Q/n:

$$Q/n = \frac{.754\ W\ T_1}{P_1\ N\ G}$$

Where W = lbs. of air flow per minute

T_1 = is the absolute temperature at the impeller entrance in $^{\circ}$F.

P_1 = is the pressure at the impeller entrance in "Hg.

N = engine revolutions per minute

G = gear ratio

.754 = cubic feet of air per pound x $^{P_o}/_{T_o} = 13.1 \times \frac{29.92}{520}$

Q/n may be calculated at sea level or the critical altitude. The Q/n at which the engine runs does not vary with altitude or throttle opening. However, it does increase slightly with increasing speed. To avoid any surging trouble from this fact, the supercharger or more particularly the diffuser should be designed to have a pressure performance peak approximately .02 Q/n to the left of the operating point of the engines. That is, the impeller should be designed to peak at the operating point of the engine, but the leading vane tip angle of the diffuser is reduced so as to reduce the Q/n at which the curve peaks and thus prevent surging. The impeller entrance diameter is selected so that the annular face area, A, is such that, at the operating value of Q/n, the axial velocity or Q/A is approximately equal to 18,000 ft/min. Because of the limitations of current machining methods, it seems preferable not to decrease the above velocity by increasing the entering area because the design of a smooth impeller passage then becomes more difficult. The theoretical angle of the impeller blade bucket tip at any radius is given by the following formula:

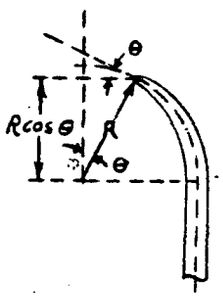

$$\tan\theta - \frac{Q_1/A}{U} = \frac{\left(Q_1/A\right) \times 12}{\pi D_1 N G}$$

Where U = peripheral velocity in ft/min
Q_1/A = axial velocity in ft/min
D_1 = diameter in inches at entrance
θ = blade bucket angle with the tangent

Experience dictates that it is best to calculate the theoretical angle of the tip at the extreme entrance diameter and add an arbitrary 10° to give the bucket angle at this diameter. This angle should not be below 20°. The tip angle at the inner diameter of the entrance should be made approximately 80° which is as much of an angle as it is practicable to bend. These angles are the angles of the center line of the blade to the front face of the impeller. The bend should have a radius greater than 3/4" and become tangent to the blade at least 1" in an axial direction from the front face of the impeller. This distance is equal to the product of the radius of the bend and the cosine of the bucket angle at the tip. The angle at any distance back is the angle whose cosine is the quotient of the distance from the point of tangency to the point in question divided by the radius.

The impeller is designed so that the change in cross section area with flow path length is uniform. This design is made by first laying out a profile view of the proposed impeller (see sheet 1B of drawing SS-7062). Cross sections are drawn between points of contact of a circle with each side of the passage as shown in the side elevation view. The length of this cross section is the distance between points of contact of the circle with each side of the passage as shown as "L" in sheet 1B. The width of the cross section is determined at several points along the length of the cross section as in the example shown in sheet 2B and 2C, which has the following headings for each of the columns:

No. of Blades = 22
Section
Radius at Point on Section = R
Circumference = $2\pi R$

Center line to Center line Width of One Passage = $\frac{2\pi R}{\text{No. of Blades}}$

Vane Thickness = t

Width of One Passage = $\frac{2\pi R}{\text{No. of Blades}} - t$

True Distance from Center of Bucket Radius to Point on Section = d

Cosine of Bucket Angle at Point on True Section = $\cos \theta_1$ = $\frac{d}{\text{True Bucket Radius}}$

Bucket Angle at Point on True Section = θ_1

Tangent of Bucket Angle at Point on True Section = $\tan \theta_1$

Cosine of Angle between True Section Plane and Plane of Flow Path = $\cos \alpha$

Tangent of Bucket Angle at Point on Flow Path Section =

$$\tan \theta = \frac{\tan \theta_1}{\cos \alpha}$$

Bucket Angle at Point on Flow Path Section = θ_1

Sine of Bucket Angle at Point on Flow Path Section = $\sin \theta$

Effective Width of Passage at Point on Flow Path Section =

$$W = \left(\frac{2\pi R}{\text{No. of Blades}} - t\right) \sin \theta$$

Total Effective Width = W_T = sum of W

Average Effective Width = $W_A = \frac{W_T}{\text{No. of Points on Section}}$

Length of Section = L

Area of Section = A = L W_A

Effective Mean Path Length = P

Total Path Length = P_T

Radius of Equivalent Circle = $r = \sqrt{\frac{A}{\pi}}$

The path length referred to above is measured as the chord length between sections as shown as P on sheet 1B. The areas are then plotted as the radius of an equivalent cone against the length of the air flow path as shown in sheets 3B and 3C. This cone should always be kept below a 3° maximum and should preferably be close to 0°. However, the smaller this cone angle, the smaller the area serving the impeller and, thus, the larger the angle of air flow off the impeller tip. A greater impeller flow angle means a greater diffuser vane-tip angle, which for a given-size supercharger means less expansion area.

In the sample calculation shown, you will note that the impeller dimensions were changed slightly as shown on sheet 1C in order to obtain a smoother area change and cone divergence. This is why the calculation sheet shows the first calculations crossed out and other calculations made at the same cross sections.

Diffuser Design

It is first necessary to estimate the pressure and temperature conditions at the impeller outlet. The pressure at the impeller outlet is found by assuming that ½ the actual pressure rise in the supercharger or 33 percent of the theoretical rise takes place in the impeller. The actual pressure rise in the supercharger is known if the manifold pressure desired at a certain altitude is given. The theoretical pressure rise in the supercharger is the pressure rise possible if all the kinetic energy at the wheel tip were converted into pressure, and this pressure is given by the following formula:

$$\frac{P_2}{P_1} = \left(\frac{V^2}{6082T_1} + 1\right)^{3.53}$$

Where V = peripheral velocity in ft/sec.
T_1 = temperature at entrance to impeller in °F absolute.
P_1 = pressure at entrance to impeller in "Hg.
P_2 = pressure at exit of diffuser in "Hg.

Given the pressure before and after the impeller and temperature before the impeller, the adiabatic temperature after the impeller may be calculated by the following formula:

$$\frac{T_3}{T_1} = \left(\frac{P_3}{P_1}\right)^{.283}$$

Where P_3 and T_3 are the pressure and temperature after the impeller.

It is assumed that the actual temperature rise in the impeller is twice as great as the adiabatic temperature rise in the impeller. We thus obtain estimated values of both pressure and temperature at the impeller exit. The volume of flow Q_3, leaving the impeller is then:

$$Q_3 = \frac{.754\ W\ T_3}{P_3}$$

From the known width of impeller tip (blade width only not including shroud or scallops or clearance between impeller and diffuser) and the number and thickness of the blades, a circumferential area of impeller passage at the tip circle is obtained. The volume of flow Q_3, divided by this area gives the radial component of velocity (assuming radial blades) at the impeller tip circle. The radial velocity coupled with the peripheral velocity defines the absolute velocity and the angle of flow off the impeller. If this angle is greater than 25°, the dimensions of the impeller should be changed to reduce the angle but still maintain the smooth low area expansion ratio.

It has been found from experience that there should be approximately $\frac{1}{2}$" of radial clearance between the impeller tip circle and the inner vane tip circle of the diffuser. Avoid abrupt change in direction from impeller to diffuser passage.

The outer surface of the inner vane tip of the diffuser is set at an angle with the tangent 2° greater than the computed angle of flow off the impeller. Experience has shown that there is approximately a 2° greater angle of air flow with the tangent at the leading vane tips than the angle off the impeller as computed with no allowance for slip. This probably applies only to present 22 vane impellers.

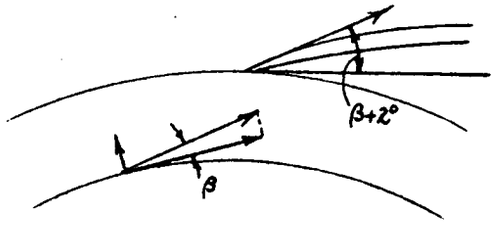

The two diffuser walls may be designed to diverge, if convenient, thus providing expansion of the diffuser passage cross section in an axial direction as well as in the plane of the impeller. The angle of axial divergence of the diffuser walls depends on the nature of the diffuser passage under consideration. For passages made with spiral thin vanes of constant thickness, a divergence between the walls of 10° measured along a radius is not too great. For straight passages, divergence of about 5° is usually more suitable.

The diffuser vane shape should now be laid out so as to give the desired rate of expansion of passage area. This rate of expansion is best expressed as the shape of a round cone of path length equal to the length of path through the diffuser, whose cross sectional areas equal the areas of the diffuser passage at the corresponding path lengths.

Two requirements should be met in the design of the passage:

(a) The included angle of divergence of the equivalent cone should start at about 4° and gradually increase to about 8°.

Path Length	Typical Cone Angle
0-1"	$3\frac{1}{2}^{\circ}$
1"-2"	$4\frac{1}{2}^{\circ}$
2"-3"	$5\frac{1}{2}^{\circ}$
3"-4"	$6\frac{1}{2}^{\circ}$
4"-	$7\frac{1}{2}^{\circ}$

(b) The final area should be at least 3 times the initial area.

Detailed procedure for passage layout is described below, first for the general case of any passage shape, and then for the simpler case of spiral vanes of constant thickness.

General Case - Passages of Any Shape

This method of passage construction is best discussed by reference to the example of Fig. 1. In this example a passage of straight form has been chosen.

Determine the inner and outer vane tip circles and the angle which the vanes shall make with the tangent to the inner vane tip circle. (In this case the vane tip angle is 14°.) Lay out (lower left hand sketch of Figure 1) a half section of the equivalent round cone desired. In this case the cone included angle increases from 4° to 8°. The construction of the cone requires an assumption of the path length which is first approximated. Check the ratio of areas of the two ends of the desired cone as plotted to determine whether this ratio is large enough. (Over 3:1 ratio desired.) If ratio is not great enough, increase the number of vanes. This makes the absolute areas smaller throughout the cone and, with cone included angles maintained the same, the area ratios become greater. (See Appendix X) (In this case 18 vanes have been chosen as the number.)

Draw a line representing the assumed shape of the inner side of the passage. (In this case a straight line.) This line must make the required vane tip angle with a tangent to the inner vane tip circle. (In this case 14°.)

Draw in the 1/32" radius vane tip between the line just drawn and the inner vane tip circle.

Using any reasonable trial radius draw in a first portion of the other side of the passage beginning at the inner vane tip circle. This arc must be so drawn as to make the required angle (14°) with the inner vane tip circle. Beginning at the intersections of the sides of the passage with the vane tip circle, lay off equal distances to a point on each side of the passage.

In the example these are 0-1, 0'-1', 1-2, 1'-2', etc. Determine the distance of each pair of points from the center of the diffuser, Y. These distances will not be the same for the two points of each pair. The average of these two values is the radius R shown in the example. Draw a short arc of radius R across the center of the diffuser passage. Determine the point D of this arc which is equally distant from the two corresponding station points (3-3' in example.) This point D lies on the mean path of the passage.

Construct an arc of a circle through the two corresponding station points and the mean path point. (3-D-3') This arc represents the front of equal velocity, pressure, and temperature, in the diffuser passage.

Determine the angles θ_1 and θ_2 which this arc makes with the two sides of the passage. Take the mean of these two angles and determine the sine of this mean angle. Determine the length of the arc W. (3-D-3') From cross section of the diffuser, determine the thickness of the passage, T, at the mean path point, D. Obtain the effective area of the passage between the station points (3-3') by obtaining the product of the values W, T, and sine $\theta_{average}$. Convert this area to an equivalent circle. Determine the radius of the equivalent circle. Check this radius against the radius of the desired round equivalent cone at the corresponding path length as laid out at the beginning of the study.

If the radius of equivalent round cone at the first two station points of the trial passage does not check the radius of the desired cone, start a new vane tip arc with another trial radius. Lay off a few station points and repeat the above procedure. When a vane curvature of the proper shape for the first 3 or 4 stations has been found, the curve may be continued according to the same procedure for 3 or 4 more stations. In this way the entire vane passage is finally completed.

It will be observed that, in this general case applicable to vane passage of any shape, the cross sections drawn between corresponding stations on opposite sides of the passage are not necessarily concentric about the center of the diffuser. In Figure 1, for example, it will be observed that the cross sections found in the outer portion of the passage are circular arcs which are distinctly not concentric with the diffuser inner and outer circles.

The calculation tables shown in Figure 1 represent the final results of the design procedure.

In the particular case shown, a straight passage was intended. It will be observed that while one side of the passage was assumed straight, the other side of the passage had a slight diverging curvature and, consequently, the center line of the passage also is curved. A small adjustment to the center line is shown to make its outer portion straight. By shifting the two sides of the passage at corresponding stations an amount equal to the change made to the center line at their mean passage point, the effective area enlargement through the diffuser is maintained the same as worked out in the design while the original intention of making a straight path is fulfilled.

Special Case

Curved vanes of constant thickness.

Estimate the approximate length of path. Lay out the desired equivalent round cone (or half cone showing cone on one side of center line only). Draw concentric circles of uniformly increasing radius, R, about the center of the diffuser. (See Figure 2) Using any reasonable radius, draw the outer edge of a trial vane making it intersect the vane tip circle at the desired angle with the tangent. Draw vane inner edge for a constant thickness vane of approximately .10". Draw the center line of the vane. The angle of the center line of the vane with a circle of any radius represents the mean angle of the air path. This angle is obtained by measuring the angle, θ between the radius of the vane curvature at the point under consideration and the radius from that point to the center of the diffuser. The effective area of the passage at each radius is then equal to:

$$\text{Area} = W\left(\frac{2\pi R}{N} - t\right) \text{sine } \theta$$

Where N = number of vanes
t = thickness of the vane measured along a circle whose center is the diffuser center
R = radius of the circle
W = axial width at the radius considered

The mean length of path of the cross section considered is measured along the center line of the vane. Convert the effective passage area for the first two or three concentric cross sections to the equivalent circular areas. Compare the diameters or radii of these circles with those of the desired equivalent cone already laid out, at the corresponding path length. Note the discrepancy. Redraw

vanes. Repeat procedure. When first few equivalent circles check with desired round cone, extend vane further and repeat until entire vane has been completed. Figure 2 shows final results of analysis for diffuser 0, and Figure 3 shows half of the equivalent round cone for this diffuser.

THEORY AND CRITERIA FOR COMPARISON OF PERFORMANCE

Theory

A Massachusetts Institute of Technology thesis by C. W. Smith, now with the General Electric Company, (Reference 4) contains an extended derivation and discussion of the general equation of performance of a supercharger.

It justifies the use of the parameter Q/nD^3 (Cubic feet of flow per revolution per cube of some diameter or other dimension) as the measure of operating conditions against which to plot supercharger characteristics for comparison purposes. Theoretically, this applies to superchargers which are geometrically similar. For a given design, D will be constant and the performance may be plotted against Q/n. For a change in design, the performance should really be plotted against Q/nD^3. But a change in design usually involves so many changes in dimensions that it is of doubtful value to do this. Also the effect of plotting the performance against Q/n instead of Q/nD^3 has only a very slight effect on the ability to predict the comparative performance of different designs. However, the choice of abscissa may have a measurable effect on the relative position of the surge point for the various designs. We have decided to use the parameter, Q/n, in comparing supercharger performances partly because of the foregoing and partly because all previous literature on the subject has done so.

The following is a condensation of important parts of Reference 4, and also of a paper by Sanford A. Moss (Reference 3) presented in order to explain the choice of the important supercharger characteristics, "pressure coefficient" and "Temperature rise ratio," and to clarify other points not usually understood.

One pound of fluid is assumed throughout this discussion. Reference 4 first establishes by dimensional analysis the formula for one pound of fluid:

$$P_m = D^2n^2d\ \varphi\left(Q/nD^3,\ \mu/nD^2d,\ V_s/nD\right)$$

where P_m = the mean effective pressure of the work or energy area required for the compression and expansion process.

n = revolutions per unit time
D = any dimension
d = density
φ = "function of"
Q = Volume of flow
μ = absolute viscosity
V_s = velocity of sound

The second parameter, μ/nD^2d, is dependent on the variation of the viscosity. It is stated in the report that variations in viscosity have little effect when the flow is turbulent, which is certainly true in an impeller. Therefore, this parameter may be neglected.

The third parameter V_s/nD or V_s/V_w is dependent on the compressibility of the air or on the closeness of approach of the air velocity to the velocity of sound. In superchargers the velocity at some points does approach the velocity of sound, but

Theory (Continued)

is probably not close enough to allow the compressibility of the air to effect the result judging from information in the literature. Besides, performance comparison of full scale and rig supercharger tests are made at identical speeds. Thus this parameter may be neglected.

This leaves only the parameter Q/nD^3 which we have reduced to Q/n for the reasons given several paragraphs previously.

Thus the formula may be written:-

$$\frac{P_m}{D^2n^2d} = \varphi\left(Q/n\right)$$

But Dn = impeller tip speed = V_w
and $d = \frac{1}{\mathbf{v}g}$ where $\mathbf{v}$ = specific volume and g = acceleration of gravity

$$\frac{P_m}{D^2n^2d} = \frac{P_m}{V_w^2/\mathbf{v}g} = \frac{P_m\mathbf{v}}{V_w^2/g} = \varphi\left(Q/n\right)$$

But V_w^2/g = the energy input from the impeller
and $P_m\mathbf{v}$ = work area or energy area theoretically required for compression.

Therefore, a measure of supercharger performance is the efficiency $P_m\mathbf{v}/V_w^2/g$, which is the ratio of the energy theoretically required for compression, to the wheel input energy. But there could be calculated any number of efficiencies of a supercharger depending on the exponent of compression chosen to compress the air from the given specific volume and pressure at entrance, to the final given pressure (See figure below).

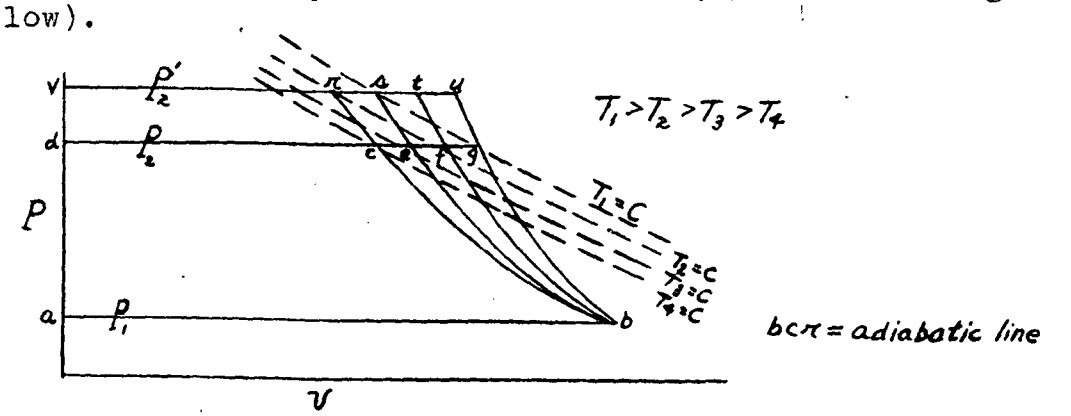

The exponent of compression depends on the final volume which depends directly on the final temperature selected since we are dealing with a given pressure rise. The energy theoretically required for compression and, therefore, the calculated efficiency becomes greater as the final temperature selected is increased from T_4 to T_3 to T_2 to T_1. Therefore, if the efficiency of the supercharger is based

Theory (Continued)

on the existing inlet and outlet temperatures, the performance is improved by having hotter outlet air temperature and such higher temperatures are, of course, not desirable. Such an efficiency is known as the actual hydraulic efficiency.

We use a pressure coefficient which is the efficiency obtained if the compression curve is assumed to be adiabatic and thus independent of the actual outlet temperature. Such an efficiency penalizes the performance somewhat because it does not take account of the fact that losses increase the final temperature which increases both the actual exponent of compression and the specific volume at the outlet thus increasing the work area or energy theoretically required to attain the observed condition.

The actual hydraulic efficiency is misleading in comparing supercharger designs because it adds to its output energy the extra energy due to the temperature rise above adiabatic. But this temperature rise is contributed by undesirable eddy and friction losses and thus the machine should be penalized for the extra temperature rise.

Therefore, it seems better to have one factor of performance, pressure coefficient, which is independent of the existing temperatures, and then have another factor of performance, temperature rise ratio, which will give the effect or amount of losses. This temperature rise ratio is the ratio of the adiabatic temperature rise, for the existing pressures, to the actual temperature rise. That is, it is the ratio of the temperature rise if compression were adiabatic to the temperature rise for the actual exponent of compression. These efficiencies may be explained perhaps more clearly by reference to the previous diagram.

W_k = area a b e d = energy for adiabatic compression.
W_n = area a b e d = energy for hyperadiabatic compression or compression with the existing temperatures.
W_s = energy at shaft = W_n plus eddy and friction losses in the impeller, that is, it is the energy required to compress the gas to the given pressure with the actual temperature rise plus the energy losses which caused that temperature rise to be greater than adiabatic. The eddy and friction energy losses in the impeller are dissipated as heat and give the temperature rise $T_e - T_c$ or $T_3 - T_4$.

W_o = W_k + eddy and friction losses in the impeller.
The actual hydraulic efficiency = $e_n = W_n / V_w^2/g = W_n/W_s$

The pressure coefficient = $e_k = W_k / V_w^2/g = \frac{W_k}{W_s}$

Temperature rise ratio = W_k/W_n

Adiabatic shaft efficiency = W_k/W_s + (disk and bearing friction)

"Pages missing from available version"

16 & 17 missing

Relation of Test Data to Theory (Continued)

Where V_w = periphial velocity in feet per second.
g = acceleration of gravity in feet per second squared.

But pressure coefficient = $\eta = \frac{P_m v}{V_w^2/g}$

$$\eta = \frac{C_p J T_1 Y}{V_w^2/g} = \frac{C_p J T_1 Y g}{V_w^2}$$

But C_p = .243 B.T.U. per degree Fahrenheit for air.
J = 778 foot pounds per B.T.U.
g = 32.174 feet per second squared.

$\therefore gC_pJ = 6082$

Therefore $= \frac{6082\ T_1 Y}{V^2}$

Inspection of the two formulas:-

$$= \frac{6082\ T_1 Y}{V^2} = \frac{6082 T_1 \left[\left(\frac{P_1}{P_2}\right)^{\frac{n-1}{n}} - 1\right]}{V^2}$$ (Pressure coefficient)

and $$\frac{\Delta T_a}{\Delta T_o} = \frac{T_2' - T_1}{T_2 - T_1} = \frac{T_1 Y}{T_2 - T_1}$$ (Temperature rise ratio)

shows that a variation in $T_1 Y$ changes both pressure coefficient and temperature rise ratio. Therefore, it can be seen that at constant speed a variation in pressure coefficient means a variation also in temperature rise ratio by the same percentage. But the temperature rise ratio may also vary independently of the pressure coefficient if the actual temperature rise varies. The expansion in the diffuser part of the supercharger is usually considered to be adiabatic. That is, the losses are throttling losses and thus are evidenced as pressure losses and not as a change in temperature. Throttling causes a decrease in pressure and temperature and therefore increases in turbulent velocity so that the eddy losses increase and are converted into heat which raises the temperature to its original value. Therefore, the actual temperature rise in the diffuser is usually considered to be equal to the adiabatic temperature rise in the diffuser based on the theoretical pressure rise in the diffuser. Thus, any change in temperature rise ratio which is due to the change in actual temperature rise comes about because of change in efficiency in the impeller alone. Therefore, a factor which varies the temperature rise ratio and not the pressure coefficient is a factor effecting the impeller efficiency alone.

At the beginning of this chapter, it was demonstrated that supercharger performance is a function of volume of air flow per impeller revolution, Q/n. "Q" is cubic feet of air flow per minute at impeller entrance conditions.

Relation of Test Data to Theory (Continued)

$$Q = \frac{kw}{\rho} = \frac{k^1 w T_1}{P_1}$$

w = pounds of air flow into the cylinder per minute.

$$w = \rho_i \; V_i \; N \; e_v$$

V_i = volume of intake into cylinder or displaced volume per engine revolution.

ρ_i = density at cylinder intake = $k'' \frac{P_2}{T_2}$

N = engine revolutions per minute.

e_v = volumetric efficiency

V_i = does not vary.

$$w = k''' \rho_o \frac{P_2}{T_2} N V_i e_v$$

At a given supercharger gear ratio, and entrance pressure and temperature, or altitude, the manifold pressure (P_2) and temperature (T_2) increase and the volumetric efficiency decreases with increasing engine RPM. But the effect of the manifold pressure on the weight flow of air is the greatest so that the weight of air flow per engine revolution increases with engine speed. And since

$$\frac{Q}{n} = \frac{k^1 w T_1}{NGP_1}$$

Where G = supercharger gear ratio and N = Engine revolutions per minute and G, $T_1 P_1$ and k^1 are assumed constant.

Then $\frac{Q}{n}$ increases slightly with increasing speed. This increase is shown by the calculations of figure 7 taken from full scale engine tests at N.A.F.

If the supercharger gear ratio is changed, then the manifold pressure and temperature are different at the same engine speed. Therefore, W/N is different and Q/N is different. Q/N increases slightly with an increase in gear ratio.

As shown in figure 7, at a given supercharger gear ratio and engine speed, the pressure coefficient and Q/n do not change appreciably with change in altitude.

Superchargers are sometimes unstable in operation at certain values of flow. Such unstable operation is known as "surging" or "pumping". According to Kearton, Reference No. 1, surging may be explained in the following manner:-

"Consider the characteristic curve in figure 6. Q_A is the normal capacity of the machine and P_A the normal delivery pressure. Suppose that the compressor delivery pipe is coupled to a large network of pipes having a considerable capacity. If the demand for air decreases, then the delivery will naturally decrease and the point A moves along the characteristic curve towards the peak C. Meanwhile, the air pressure in the system of delivery pipes gradually increases.

Similarly, if the consumption of air by the driven machine increases beyond the normal value Q_A to some value Q_D, then as this increase is taking place the pressure in the pipe system steadily falls until the value P_D is reached, at which pressure the compressor will deliver the quantity Q_D steadily for an unlimited time.

Suppose now that the air consumption gradually falls and reaches the value Q_C. As already explained, the pressure in the system approaches and reaches the value P_C. If now, the consumption is further diminished, the pressure in the pipe system exceeds that in the compressor outlet pipe and the air commences to flow backwards into the machine. The delivery ceases and the operating point suddenly moves from C to F. If the consumption of air is still going on, then the pressure in the distributing mains gradually falls and eventually reaches a value lower than P_B, at which moment the compressor immediately recommences to deliver, and the operating point jumps from B to F.

As the volume being delivered is now in excess of the requirements, the pressure rapidly rises and reaches the maximum value Pc, and delivery again ceases abruptly. Such unstable operation is known as "surging" or "pumping"."

Since at constant engine speed and impeller gear ratio, an engine operates at approximately the same volume of flow, Q, and, therefore, at the same value of pressure coefficient, the ratio of manifold pressure to entrance pressure is constant with changing entrance pressure and constant entrance temperature. Therefore if a supercharger is operating at a volume of flow close to its surge point, surging trouble may be encountered if the variation of throttle pressure drop or variation of pressure drop before the supercharger entrance is changed. This may be explained by reference to the curves of figure 6. If the entrance pressure did not vary with the volume of flow, then the manifold or outlet pressure, P_2, would vary in the same way and peak at the same position as the pressure ratio, P_2/P_1, or pressure coefficient curve of figure 6. Now, if the pressure drop at the entrance varied in a normal way with the volume of flow (as the square of the volume), as shown by the curve of inlet pressure at n_2 revolutions per minute in figure 6. Since, as shown above, surging occurs at the volume of flow corresponding to the peak value of manifold or outlet pressure, the surging point occurs at a lower and lower volume of flow as the entrance pressure or throttle pressure drop curve falls off more and more from a straight line of constant pressure. Therefore, at one volume of flow, the tendency to surge is decreased by increasing the drop through the scoop and carburetor.

"Page missing from available version"

21 through 23 missing

IMPELLER DESIGN

Design Factors Studied:

Attention has been given in varying degree to the following principal factors influencing the efficiency of impellers:

1. Rate of impeller passage expansion.
2. Provision for low impeller entrance velocity.
3. Impeller bucket synchronism.
4. Number of impeller blades.
5. Other factors effecting flow at impeller entrance.
6. Reduction of impeller re-circulation.

1. Rate of Impeller Passage Expansion

Reference is first made to "Test Results" under the heading "Comparison of wide and narrow type standard G.E. designs". These superchargers consisted of the currently used standard narrow entrance impeller H and corresponding diffuser I and a wide entrance wide tip impeller J with two diffusers K and L. It will be observed that at high impeller speeds, the efficiency of the wider impeller J fell off badly with its first diffuser K. (See figure 8). It was thought possible that this could be explained by the fact that the G.E. gave the diffuser vane for this wide impeller the same tip angle as in the case of the narrow diffuser. Under this condition a larger flow would be required to obtain peak diffuser performance which might not coincide with the peak impeller performance. Calculation of the proper tip angle for the vanes of a new diffuser to peak at the same volume of flow as in the case of the narrow supercharger checks the angle on such a diffuser (L) subsequently provided by the G.E.Company for this purpose. However, test results of this diffuser, shown in test results figure 28 indicate that the efficiency of the combination still fell off at higher impeller speeds. This condition is not true of the current standard narrow impeller H and diffuser I whose performance is illustrated in figure 8, and hence some other reason must be sought for it.

The rates of expansion of area of passages for the above two impellers and also for the rework of the wide type impeller as described below are plotted in Appendix V figure A. Note that the ratio of exit to entrance area of a passage for the wide impeller J is 2.0, while that for the narrow type, H, is 1.3. Reference is now made to "Test Results" under the heading "Impeller Outlet Widths", and corresponding exhibits, figures 51 to 53. By reducing the tip width of the wide type impeller J while keeping the inlet diameter constant, the efficiency at high impeller speed was made comparable with that obtained at low speed. This rework reduced the passage exit to entrance ratio to approximately 1.3. A first rework, which gave an area ratio of only 1.6, failed to show any improvement in efficiency at high speed. It will also be observed from the area plots Appendix V that for these reworks the smoothness of passage area expansion had to be sacrificed as the nature of the rework of the impeller was dictated by the requirement that the impeller fit the curvature of the same diffuser plate so as to avoid making up a new diffuser. This resulted in a very irregular series of expansions and contractions through the impeller passage and it is believed that further improved efficiency will result in so designing the impeller as to obtain a smooth expansion.

1. Rate of Impeller Passage Expansion (Continued)

Referring to similar tests under "Impeller outlet width" conducted on an 11" diameter wide impeller M reworks of this impeller were made to reduce the tip width in successive stages so as to reduce the volume of flow for peak pressure coefficient performance. Plots of the passage area, Appendix V figure B, show that the area ratio was reduced from 2.2 to less than 1.37. The plot for the final rework giving the best high speed efficiency is not shown. The test results, figures 54 to 57, show that while the exceptionally high efficiency at low speed (.78) was reduced to .76 by these reworks, the efficiency in high ratio was apparently increased from about .66 to .70. As in the case of the previous rework, the smoothness of passage area change was sacrificed.

In all new impellers now in process of manufacture pains have been taken to design these impellers for smooth enlargement of passage area. Further comments on factors effecting the attainment of this type of design are made in the next section of this Chapter entitled "Provision for Low Impeller Entrance Velocity". Appendix V shows in detail the method of analysis of any given impeller passage. Actual design procedure to get a smooth passage area change is very tedious, as many as 20 trials and analyses following the methods of appendix V sometimes being required before attainment of a satisfactory result. Figure D of appendix V shows the final design for a new impeller, N, and Figure E is a plot of the passage area change resulting. Tests of this and another new impeller will give the first information on a rational treatment of the above mentioned relations not obtainable by simple reworking alone.

2. Provision for Low Impeller Entrance Velocity

It is well known that one of the principal losses occurring in centrifugal fans and pumps occurs at the entrance to the impeller. Generally speaking, if the entrances to such impellers can be made large so that entrance velocity is low, this loss is greatly reduced.

With impellers of conventional GE construction having straight blades with bent buckets, it appears that adequate control of the rate and smoothness of expansion of the impeller passages requires some limitation to entrance diameter, which, if reasonable bucket synchronism is to be obtained, limits the extent to which the low entrance velocity requirements may be met. That is, to obtain a low entrance velocity, a relatively large entrance area is required. This, in turn, requires that the buckets be bent to a relatively small angle with the face of the impeller both because of lower axial velocity of the air and of higher peripheral velocity at the bucket tip. Due to this extreme bending of the buckets and to the large radial dimensions of the impeller passage resulting from a larger entrance diameter, the cross sectional area of an impeller passage undergoes a very sudden enlargement on rounding the bend of the buckets. Thus a smooth enlargement of impeller passage is sacrificed with a large entrance using this type of impeller construction. The method of compensation for this is, of course, to alter the shape of the two sides of the passage not bounded by the blades. However, three considerations limit the effectiveness of this remedy: (a) machinability of the inner curve; (b) proper shape of the inner curve for withstanding stress; (c) avoidance of too abrupt a change of direction of the outer curve.

2. Provision for Low Impeller Entrance Velocity (Continued)

It is possible that with some other type of impeller construction which avoids such changes in impeller passage area by elimination of sharp bends near the entrance, a large entrance area and lower velocity may not be inconsistent with a smooth path and limited area expansion. This remains to be seen from coming tests of such an impeller.

Methods of calculation of absolute entrance velocity are discussed in Appendix VI. Analysis of impeller passage area has already been referred to in Appendix V. In applying these methods to design of several superchargers, it was found that when impeller entrances were enlarged to give a maximum absolute entering velocity lower than 15000 feet per min., the above described limitations were encountered.

3. Impeller Bucket Synchronism

Several bucket and blade reworks of GE impellers were tested on the rig to obtain some experience in this feature of design. For detailed results of these tests refer to "Test Results" under the heading "Impeller Blades and Buckets", with corresponding exhibits figures 58 to 66.

Comparison A involves reworks of wide entrance impeller J which increased the bucket angle of the standard GE design at the entrance outside diameter. This decreased performance in varying amounts at low impeller speeds but had little effect at high speeds. See figure 61A, B, and C.

Comparison D involves reducing the GE bucket angle for the wide entrance impeller J to the theoretical value, a reduction of 10° at the entrance outside diameter. No change in performance resulted. See Figure 66.

From the above it appears that, using the present method of calculation of the theoretical bucket angle per appendix VI, about 10° should be added at the impeller entrance diameter to the result as a factor of experience. This should approach bucket synchronism and at the same time maintain passage entrances as large as possible, facilitating design of smooth impeller passage area expansion.

Only one variation of bucket angle of the narrow entrance impeller was investigated. Comparisnn C involves reducing the bucket angle of this impeller to the theoretical value, a reduction of 17½° at the impeller entrance outside diameter. The results show that performance is slightly better with the higher bucket angle. As no other angles were tested for this impeller, the optimum angle is not known, and hence no checks on the results obtained with the wide entrance impeller are available.

4. Number of Blades

Tests to investigate this factor in design were necessarily limited since efforts were confined to reworks of existing impellers. Referring again to "Test Results" under "Impeller Blades and Buckets", it will be observed that elimination of the bucket and lower portion of every other blade had substantially no effect on pressure coefficient but reduced the efficiency in low speed to the high speed values. See figures 61 A, B, and C. On the other hand, elimination of all of every other blade caused a reduction of pressure coefficient, but increased the high speed efficiency to a value approaching that for low speed. The low speed efficiency was not improved.

4. Number of Blades (Continued)

The following reasoning is suggested in explanation of the above results:

The reason for the reduction in pressure coefficient with half the number of blades is "slip" or increased angle leaving the impeller, resulting in a reduced value of absolute velocity at that point, similar to the effect of backward sloping blades (Quinones, Reference No. 5.)

A change in temperature rise ratio in these comparisons depends on three factors (a) change in pressure coefficient, (b) change in friction losses, (c) change in entrance losses.

With the lower portion of every other blade and bucket removed, we have no change in pressure coefficient. The removal of part of every other blade reduces friction somewhat, which tends to increase temperature rise ratio, especially at high speed. Nevertheless, no improvement in temperature rise ratio is observed at high speed indicating that the effect of the changed entrance loss on temperature rise ratio must be adverse. At low speed, where friction is of less importance, a distinct loss in temperature rise ratio takes place with the reworked impeller.

With every other blade entirely removed, pressure coefficient is decreased as explained above. This in turn tends to lower the temperature rise ratio. The reduced friction tends to increase it. The change in entrance conditions tends also to decrease the temperature rise ratio, as indicated above. At high speed, where friction losses are relatively high, their reduction is the important factor, resulting in increased temperature rise ratio. At low speed, the effect of reduced friction is counterbalanced by the other factors, resulting in no change in temperature rise ratio.

Considering these test results as a whole, it appears that there is little to be gained by changing the present number of impeller blades.

5. Other Factors Affecting Flow at Impeller Entrance.

Reference is made to "Test Results" under the heading "Improvement of Flow Entering Impellers", and corresponding figures 67 to 71. It will be seen from these that substantial improvement may be expected by increasing the axial clearance at the entrance to impellers. It has been recommended that this be done the next time a supercharger section is re-designed for production.

Figures 69 and 70 A, B, and C, for the wide entrance type impeller J show the improvement in pressure coefficient and temperature rise ratio resulting from a 1" increase in the axial clearance at entrance. Figure 71 shows similar results for the standard narrow entrance type impeller H with axial entrance increased 1.2". In the case of the wide type supercharger, Figures 70 A, B, and C, also show that no gain resulted from increasing the axial clearance from 1" to 1.2".

In all cases, increasing the axial clearance at the supercharger entrance shifted the peak performance to a higher value of flow, this shift being slight for the

5. Other Factors Affecting Flow at Impeller Entrance (Continued)

narrow entrance impeller, and substantial for the wide entrance impeller. It appears that the proximity of the wall of the rear section to the entrance not only constitutes a restriction to flow with consequent decrease in performance, but also impairs the opportunity of the approaching air to assume synchronism with the buckets.

Experiments were conducted to determine the effect of enlarging the rounded lip on the diffuser plate at the entrance to the impeller. Refer again to "Test Results" under "Improvement of Flow Entering Impellers", and Figure 68. It will be observed from Figure 68 that a slight improvement in pressure coefficient and temperature rise ratio resulted at the high impeller speed, and the peak performance occurred at a slightly higher value of Q/n. It is possible that reduction of turbulence at the entrance lip is another factor in attaining synchronism of the entering stream with the buckets in this region. The G.E.Company have advised us that they are submitting a diffuser in which this rounding of the lip is carried to an extreme. That is, the lip of the diffuser plate will be converted into a large flat flange extending the entire diameter of the entrance chamber. Tests on this have not yet been conducted.

6. Reduction of Impeller Recirculation

It is well known that a principle loss in impeller efficiency is that useless work is done on a certain percentage of the air which, after being compressed and heated, flows back outside of the impeller passages to the low pressure region and then again undergoes the compression and heating process. During the return flow, the air does not lose its temperature, and, in fact, additional work is done on it by friction, which heats the stream still further.

In GE impellers, two principle opportunities for this recirculation are evident. (a) No shroud on one side of the impeller, (b) Thrust relieving holes in the impeller. Steps have been taken to purchase a completely shrouded impeller closely simulating the standard narrow type H impeller in all respects except that it incorporates shrouding on both sides. This has not yet been received for test.

It has long been maintained by the G.E. Co. that elimination of the thrust relieving holes in their impellers would increase impeller thrust about 100 percent. These holes pass through the shrouded side of the impeller so as to connect the clearance space between the shroud and housing, where pressures are assumed to be high, with the entering portion of the impeller passages, where the pressure is low. The holes are intended to reduce the pressure in the clearance space, thereby reducing the differential pressure across the impeller and keeping down the net thrust. By functioning in this manner these holes necessarily also constitute an opportunity for recirculation. Tests were made to determine, experimentally, the effects of elimination of these holes both on impeller thrust and on supercharger performance. Reference is made to "Test Results" under the heading "Elimination of Pressure Relieving Holes" and to Figures 72, 73, and Appendix VII.

From figure VIIA, it is seen that elimination of the holes changed the pressures in the clearance space materially only over the smaller area near the axis. Integrated over the entire area of the impeller circle the change in net thrust was relatively small.

6. Reduction of Impeller Recirculation (Continued)

From Figures 72 and 73, it is seen that the elimination of the holes improved the pressure coefficient slightly and the temperature rise ratio substantially. It is estimated that for higher gear ratio performance, intake pipe temperatures may be reduced about 10°F by this change. While such a reduction may appear small, it may favorably effect present detonation limitations to high ratio performance for a given octane rating of fuel. Also, the reduced supercharger horsepower consumption due to the improved efficiency may improve fuel consumption under any condition of operation.

DIFFUSER DESIGN

General Comments on the Investigation of Diffuser Design Factors:

Rig tests to observe the effect of small changes in design of diffusers by reworking certain features of existing production parts were begun simultaneously with study of the available literature. As more knowledge was gained from the literature and analysis of test data, many of the earlier rig test results became confirmations of what was by then obviously to be expected. If the tests were to be started at the present state of theoretical information, several design reworks previously tested could be omitted. Nevertheless, valuable information was obtained from which present design procedure has been taken directly or deduced.

GENERAL THEORY OF Diffuser Action:

The purpose of a diffuser is, of course, to convert the high velocity energy of the air imparted to it by the impeller into pressure energy by slowing down the stream with as little loss as possible. In Appendix IV, explaining the determination of impeller and diffuser performance separately, it is shown that losses in the diffuser are manifested by reduced pressure conversion only. Figure A, B, and C, Appendix IV show that present diffusers have a pressure conversion of only .4 to .6 of theoretical. Three fundamental limitations make the securing of a high performance diffuser an interesting problem; (a) the law of conservation of angular momentum; (b) the limited radial distance in which to accomplish retarding of the air; (c) the high velocity of the entering stream.

The principal factors in diffuser design appear to be the following:

1. Rate of passage expansion.
2. Angle of vane at tip with respect to calculated angle of flow off the impeller.
3. Shape of diffuser leading vane tips.
4. Distance of tips from impeller.

1. Rate of Passage Expansion

At first thought it might appear (erroneously) that a particle on leaving the tip of the impeller should move in a straight path according to Newton's first law. If this were true, a parallel walled vaneless diffuser would

1. Rate of Passage Expansion (Continued)

provide a rapid expansion of area, since the effective area at any radius is the circumferential area at that radius times the sine of the angle, θ: which the flow direction makes with a tangent to the circle considered. Appendix VIII figure A shows that this angle would increase rapidly with distance along the straight path assumed. By varying the axial width of the vaneless diffuser passage by the method carried out in Appendix VIII, a condition of constant deceleration of the air could then be obtained. Unfortunately, tests on such a design of diffuser, as well as on other types of vaneless diffusers, demonstrated that the basic assumption was erroneous and that the path is not straight. Refer to "Test Results" under the heading "Experiments with Vaneless Diffusers" which show that a particle follows a spiral path in a vaneless diffuser.

The particles leaving the impeller are not independent of each other but constitute a vortex. In a vortex the law of conservation of moment of momentum holds, so that, for each small unit of mass, the product of the tangential component of velocity and the radius is a constant, or reduction of the tangential component of velocity depends only on the increase in radius and varies inversely with it. The radial component of velocity varies inversely with the circumferential area or, if the diffuser has parallel walls, inversely with the radius also. For a parallel walled diffuser, then, the radial and tangential components of velocity retain nearly the same relation, and thus the air path retains the constant angle, with the tangent at any radius. This is the definition of a logarithmic spiral, which the path approximates. Actually, the radial component of velocity also varies inversely with the density, so that the path lies slightly inside of a logarithmic spiral if the diffuser has parallel walls.

Thus, no matter in what manner the width of the vaneless diffuser be varied to vary the radial component of velocity, the tangential component cannot be greatly reduced except by a great increase in radius, with which it varies inversely. While the axial width of vaneless diffusers can be designed to give a straight path, or a path of any other shape, by varying the radial component of velocity, the purpose of the diffuser is still defeated if its outside diameter is limited. The tangential component decreases with increasing diameter only, and, therefore, the absolute velocity leaving the diffuser, which can never be less than any component, cannot be greatly reduced. In vaneless diffusers of our current inside and outside diameters, the absolute velocity decrease or effective area increase amounts to only about 33 percent.

Figure C Appendix VIII demonstrates the above comments showing the necessity for a large diameter of vaneless diffuser if reduction of absolute exit velocity is to be relatively effective.

In order to obtain an effective area increase of from 2:1 to 3.5:1, it is necessary to pass the air through expanding passages. By inserting vanes which constrain the air to flow in a path whose angle, θ, with the tangent is slightly increasing, the effective passage area (proportional to the sine of this angle and the radius) may be made to enlarge more rapidly. By controlling the rate of variation of θ and of the axial width of the diffuser

1. Rate of Passage Expansion (Continued)

with increasing radius, the rate of effective passage expansion may be varied in any manner desired by the designer.

It should be noted at this point that if, with the insertion of vanes in the diffuser, the vortex principle of constant angular momentum still applied, the performance results would be the same as in the case of the vaneless diffuser. That is, any particle would attempt to follow the constant angular momentum law and, therefore, tend to leave one of the vanes, defeating the purpose of an expanding passage. As shown in figure 13, in which performance with several vaneless designs is compared with a vaned diffuser, substantial improvement in performance is obtained with the latter. The path shape through the vaned diffuser of figure 13 differs only in small degree from the spiral paths of some of the vaneless diffusers tested. Therefore, reduction of the tangential component of velocity at the exit is accomplished not by any appreciable change in path direction, but by the effectiveness of the expanding passage, that is, by eliminating the effect of the vortex law. It would appear that with the vortex effect no longer present, the diffuser passages may be made any desirable shape, as long as rate of expansion is properly controlled.

One extreme type of expanding passage resulted from installation of straight vanes in the special converging vaneless diffuser plate of Appendix VIII, already discussed, which was intended to give constant deceleration of the air when flowing in a straight path. The test results under the heading "Straight Vane Diffusers" show peak performance comparable with more conventional designs, and a photograph of the flow path, also included with the test results, shows a smooth flow pattern.

This straight vaned diffuser was tested during the early part of the investigation, and it was thought that, while ultimately good results might be obtainable with a straight passage diffuser because of its short path length and reduced friction, more could be learned at that stage, of the principles of passage design and other design features by adhereing to reworks of the many conventional designs on hand. Therefore, the remainder of the test data reported herein is on spiral passage diffusers.

With design principles fairly well established, however, thought has recently been redirected toward the straight passage type. Two of these diffusers have been designed according to the general methods at the end of the chapter entitled "Summary of Suggested Design Procedure".

A good basis for analyzing the effective rate of expansion of a diffuser passage is to determine the shape of an equivalent round cone, having cross sectional areas equal to the passage areas at corresponding path lengths. Two methods have been used for determining the equivalent round cone. The later method, believed to be the correct one, is outlined in detail in the latter part of the chapter entitled "Summary of Suggested Design Procedure". It is based on the assumption that the particles of air leaving the impeller

1. Rate of Passage Expansion (Continued)

at the same time travel the same distance along the vane on both sides of the diffuser passage. Thus, by virtue of the extreme inclination of the passage, particles which have traveled the same distance and are at points of equal velocity and pressure lie in a curved plane which is very oblique with respect to the direction of flow (Figures No. 1 and No. 2). In the case of conventional spiral thin vanes of constant thickness these planes of equal velocity and pressure are closely approximated by concentric circles about the center of the diffuser. In the case of other types of diffuser passages, such as the straight type, these planes are not concentric but are determined by measuring off equal distances along the two vanes bounding a passage and constructing according to the chapter entitled "Summary of Suggested Design Procedure".

Figures A to D, Appendix IX, show plotted the equivalent round cones for all the principle G.E. diffusers, certain reworks of these, and certain WAC diffuser designs. These figures also show the divergence angles for those diffusers.

It is obvious that, when determination of the equivalent round cone is based on the above conception, the innermost portions of the diffuser vanes become very important in forming the first portion of the diffuser passage, which pressure gradient studies through the diffuser show to be especially effective in pressure conversion (See Figures 41, 42A and 42B).

An earlier method of measuring passage divergence was to consider only the portion of the passage in which minimum cross sections between two adjacent vanes could be drawn. This left out of consideration the most effective and most critical portion of the diffuser passage, just mentioned, resulting in a misleading picture both of effective divergence and of effective path length. Table I Appendix IX lists the divergence angles of round cones of the various diffusers previously determined in this manner.

At present tip speeds corresponding to high impeller gear ratios, the velocity entering the diffuser is about 3/4 of the speed of sound at the mixture temperatures prevailing. This high velocity must be given consideration in two respects of primary importance:

A. The rate of expansion of a frictionless passage should be less the higher the velocity.

B. The longer the path length through which the high velocity is maintained, the greater will be the friction loss.

These two considerations conflict and make necessary a proper compromise for optimum rate of diffuser passage expansion.

A third desirable factor in design is obvious, namely:

Provide sufficient expansion of cross sectional area of passage to reduce the final velocity to a negligible value.

1. Rate of Passage Expansion (Continued)

With the limitations of considerations "A" and "B" on cone divergence angle, and with the diametral space limitations imposed by the general engine design, a large expansion is difficult to obtain efficiently. Analysis of the equivalent cones of General Electric diffusers, (see Figures A and B, Appendix IX) shows that these have effective area expansion ratios of between 2.0 and 2.8:1. It appears entirely possible, however, with conventional spiral vanes, to obtain area expansion ratios of between 3.0 and 4.0:1 and recent designs have attained these values, using a normal number of vanes.

In the case of straight-passage diffusers, present limitations to diameter make the path length relatively short. With the restriction of maximum allowable cone divergence angle also imposed, a large area expansion ratio cannot be obtained with a small number of vanes (9). However, by increasing the number of vanes, giving smaller passages of substantially the same length, having the same cone divergence angle, the larger area expansion ratio can be attained. Further information is required before a limiting number of vanes can be set. However, a good rule for present general dimensions appears to be to provide sufficient vanes to obtain an area expansion ratio of not less than 3:1. Diffusers with 12 and 14 vanes, and with long paths, do not show excessive losses due to friction.

In this connection, it should be pointed out that the number of intake pipes should not determine the number of vanes, if they are of the thin spiral type. Fourteen cylinder engines have been operating with 9 vaned diffusers, for thousands of hours and do not show any symptoms of poor fuel distribution. The first tests to investigate the effect of varying the rate of passage expansion were conducted by the simple expedient of reworking G.E. diffusers so as to remove the axial divergence of the diffuser walls. The data from these tests are detailed and discussed under the heading "Effect of Removal of Axial Divergence of Diffuser Walls" in the Chapter "Test Results". The calculated equivalent area cones of the diffusers tested are indicated in the plots of Figures A to D appendix IX. It will be noted that the shapes of the equivalent cones calculated in this manner are very illogical, having the largest included angle at the high velocity end and the smallest angle at the low velocity end.

The effect of reduction of divergence angles by the reworks described above was small and difficult to interpret. It appears possible that the high velocity end may have been benefited at the expense of the low velocity end whose angle was already small.

In this connection, attention is directed to tests to observe the pressure gradient through the diffuser passage. (See figures 41 and 42 A & B). More than half of the pressure rise in the diffuser occurs in the relatively short portion of the path prior to the "throat". In view of the calculated equivalent cone divergence angles described above, this is to be expected, with the designs tested, since, the largest portion of area expansion occurred in this region.

1. Rate of Passage Expansion (Continued)

A further indication that the divergence angles of the low velocity ends of the equivalent cones for G.E. diffuser passages is ineffective is that reduction of the outside diameter of the diffuser by 1" had no noticeable effect on performance, and the effect of reduction of two inches in diameter was relatively small. Refer to "Test Results" under the heading "The Effect of Changes of the Outside Diameter of the Diffuser Plate."

Experiments to vary the equivalent cone divergence angles of diffusers were continued by installation of "fillers" of various shapes in the passages of existing diffusers. The principles on which these various passage shapes were designed, and the results of rig tests are discussed under the heading "Diffuser Vane Passage Fillers", in the chapter "Test Results". These changes did not show improvement due to the fact that the designs of the passages were based on the earlier conception of the effective passage as existing only in the portion between the "throat" and the outlet of the diffuser. It has been demonstrated above that this conception of effective passage area was erroneous, and subsequent analysis of these passages by the later method showed that the effective cone divergence angles created were quite different from those originally intended. This was particularly evident with respect to choice of the "throat" area as defined above. When this was made equal, by the older method, to the effective area at the inner vane tip circle, subsequent analysis by the later method showed that the equivalent round cone for this region was in reality converging, thus forming a severe restriction which was all too evident in the results (See figure 33 A, B and C and also plot of equivalent cone figure B appendix IX.

The two principle scurces from which information on the optimum equivalent cone angles was obtained were Eastman Jacobs (reference 6) and S. A. Moss (reference 2). For the velocities and temperatures in high supercharger gear ratio, and the path length available in the current size of diffuser, optimum cone divergence angles starting at 3-1/2 to 4° and increasing to from 5-1/2 to 7° were calculated from the above information. This rate of expansion has been applied to recent designs.

2. Angle of Diffuser Vane at Tip with Respect to Calculated Angle of Flow off Impeller

In the discussion on impellers, a method of calculating the angle of flow from the tip of the impeller is explained. A considerable number of tests were made to evaluate by experience the relation between the actual optimum diffuser vane tip angle and the calculated angle off the impeller. The results of these tests are given under the heading "Diffuser Vane Tips" in the chapter "Test Results". Comparison of these results with the calculated impeller exit angle indicate that approximately 2° should be added to the calculated impeller exit angle for optimum angle of the diffuser vane tip. This discrepancy is probably due to the fact that the mean direction of the relative velocity of flow leaving the radial impeller passages falls slightly behind a radial direction due to a whirling velocity component superimposed on the

2. Angle of Diffuser Vane at Tip with Respect to Calculated Angle of Flow off Impeller.(Continued)

radial velocity component in the impeller passage (Quinones, reference 5). This results in an increased angle which the absolute velocity makes with the impeller tip circle. This phenomenon is commonly known as "slip".

3. Shape of Diffuser Leading Vane Tips.

The velocities under consideration at the diffuser leading vane tip are, as previously stated, about 75 percent of the speed of sound. Local velocities, as in the case of airfoils, can easily exceed sonic values unless precautions are taken in design. Early tests with a bulbous, "non-critical", vane tip (see results under heading "Diffuser Vane Tips) made before this point was realized, show very inferior performance on this account. The ideal tip, from this point of view, would be a very sharp one. However, such a tip is critical, making sharper peaks of performance characteristics curves when plotted against Q/n (See comparison D in result under the heading "Diffuser Vane Tips"). At the present stage of design experience, it is considered more profitable to compromise on this feature, and the adoption of vane tips tapering to a 1/32" radius similar to G.E. practice involves little loss in performance with the better chance of a new design fitting a given capacity.

4. Distance of Tips From Impeller.

Tests varying this feature (See data under Heading "Clearance between Impeller Outlet Diameter and Diffuser Inner Vane Tip Diameter") indicate rather conclusively that the G.E. standard clearance of 1/2" is advisable rather than wide variations of this value in either direction. Apparently shock losses with close clearances are detrimental unless vane tips are very sharp, in which case the above mentioned critical performance condition is objectionable. Increase in clearance reduced the length of the inner expanding portion of the G.E. diffuser passage which probably had considerable adverse effect on pressure conversion. When clearance is increased by use of a smaller impeller without spoiling the diffuser passage, only slight reduction in performance results. Probably small variations in clearance are of negligible importance.

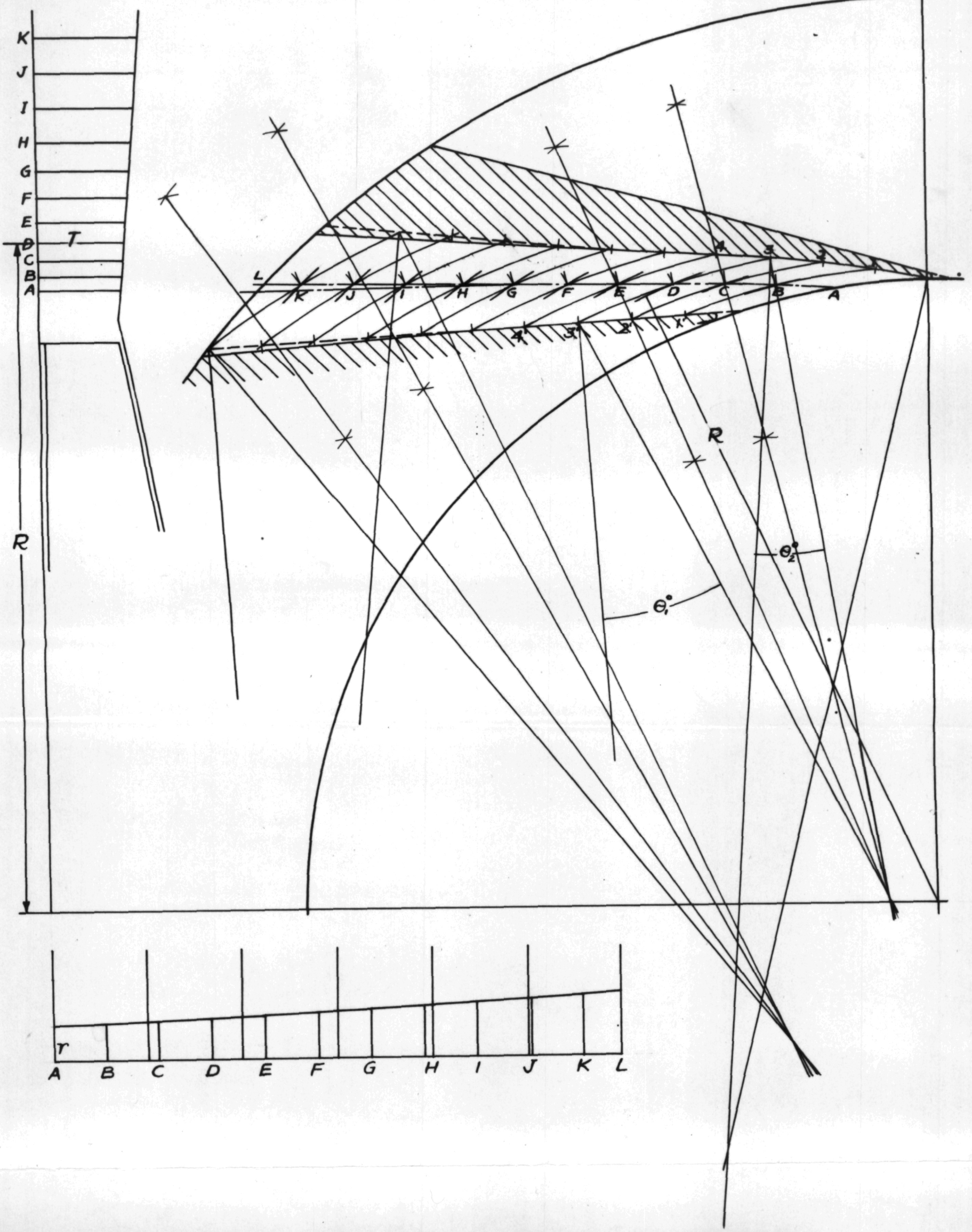

STATION	RADIUS R	THICK. T	WIDTH W	θ_1 °	θ_2 °	θ ° AVG.	SIN θ ° AVG.	AREA A	RADIUS EQUIV. CIRCLE F
A	6	.77	1.855	14	14	14	.242	.346	.332
B	6.13	.79	1.86	17.50	14.75	16.12	.278	.409	.36
C	6.30	.80	1.89	21	14.25	17.62	.303	.458	.382
D	6.47	.81	1.90	23.50	13	18.25	.313	.482	.391
E	6.67	.83	1.92	25	14.25	19.62	.336	.536	.412
F	6.90	.85	1.94	26.50	15.75	21.12	.361	.596	.435
G	7.16	.87	1.96	28	19	23.50	.399	.681	.465
H	7.44	.90	1.99	28.50	23.25	25.88	.436	.781	.497
I	7.76	.92	2.04	31.75	25	28.38	.475	.892	.532
J	8.09	.95	2.07	33.50	27.75	30.62	.510	1.003	.565
K	8.44	.98	2.12	35	30	32.50	.538	1.12	.596

Figure 1

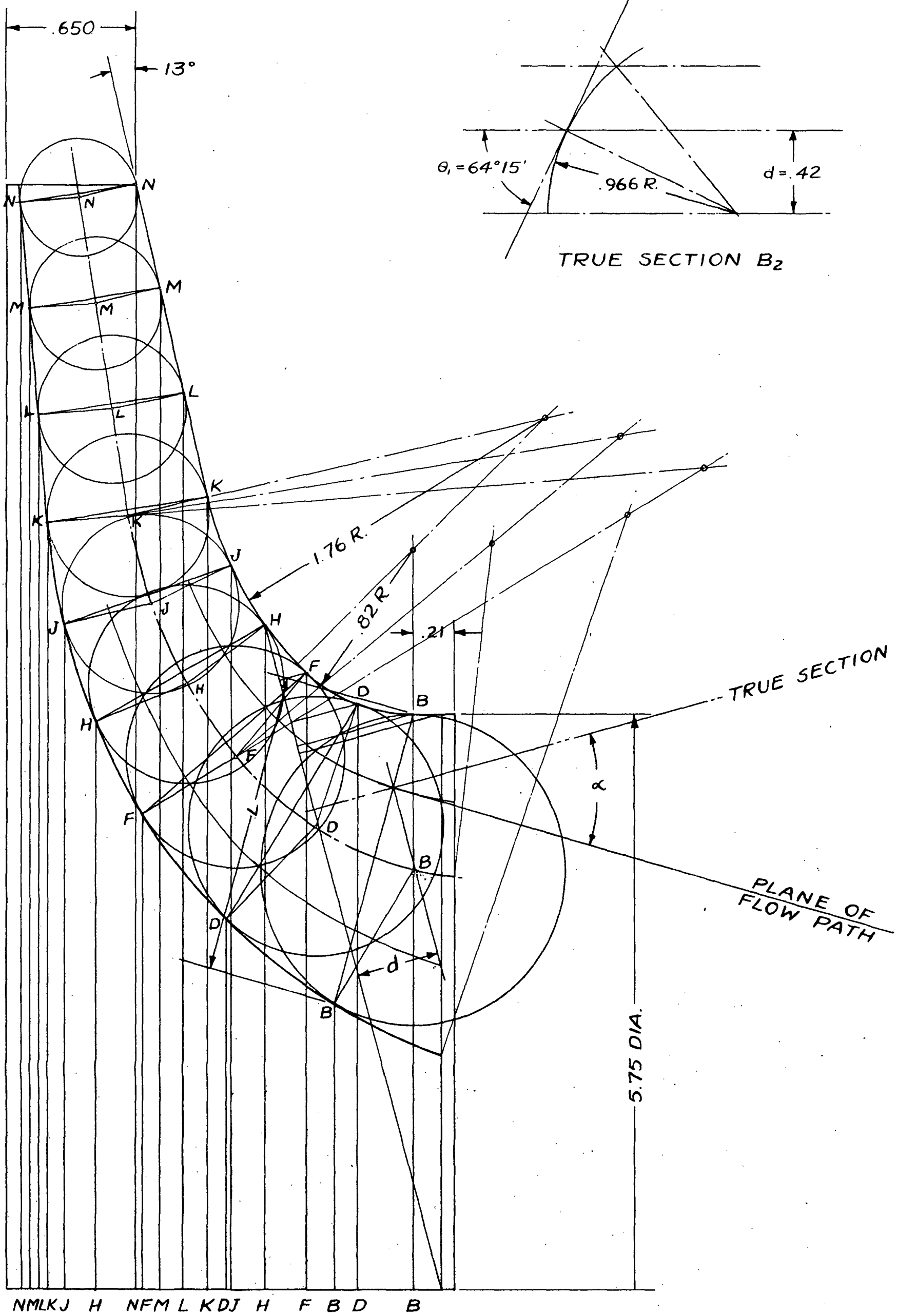

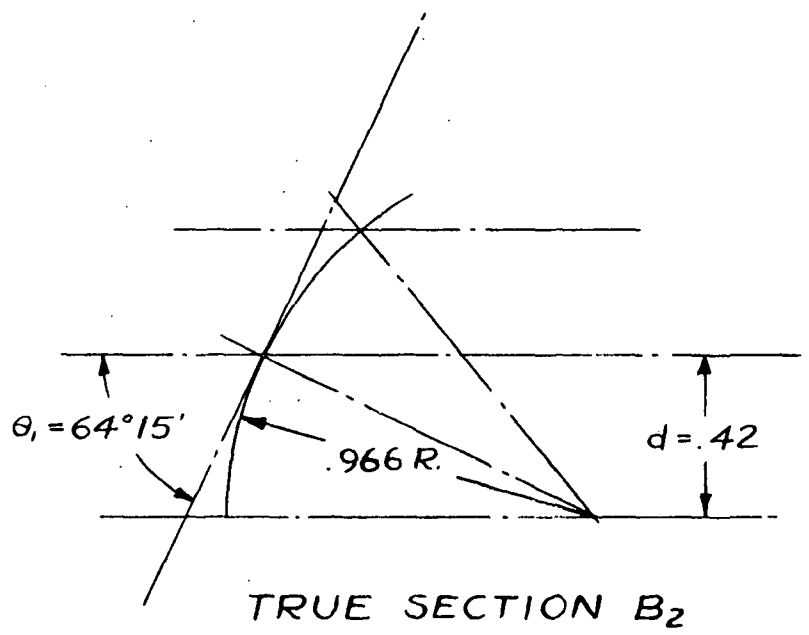

TRUE SECTION B_2

AREA EXPANSION RATIO 1.41 TO 1

SEE SHEETS # 2B & 3B

SS-7062

SHEET # 1B

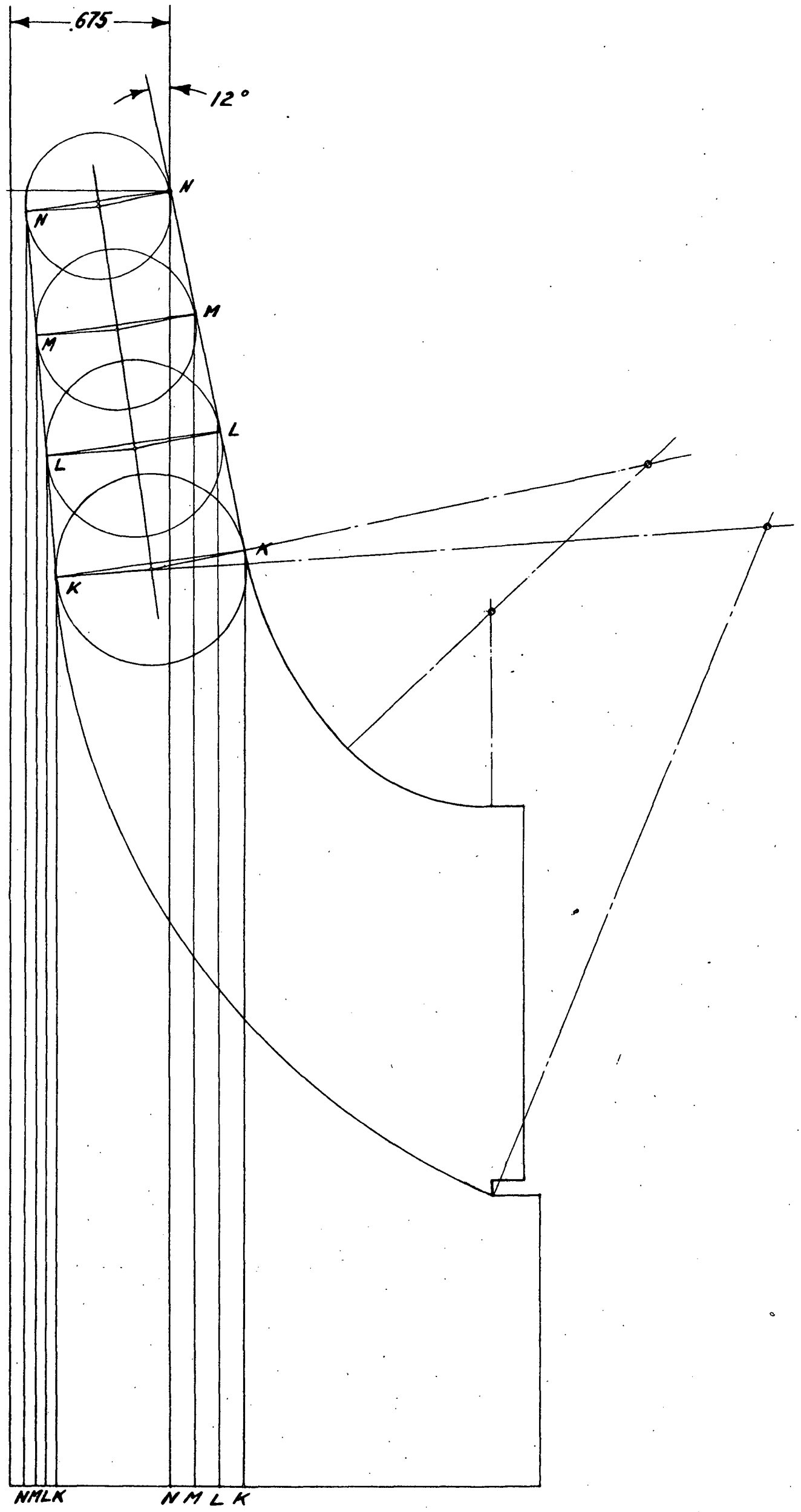

AREA EXPANSION RATIO 1.48 TO 1

FOR ALL OTHER INFORMATION SEE
SHEET #1B. REFER #2C & 3C

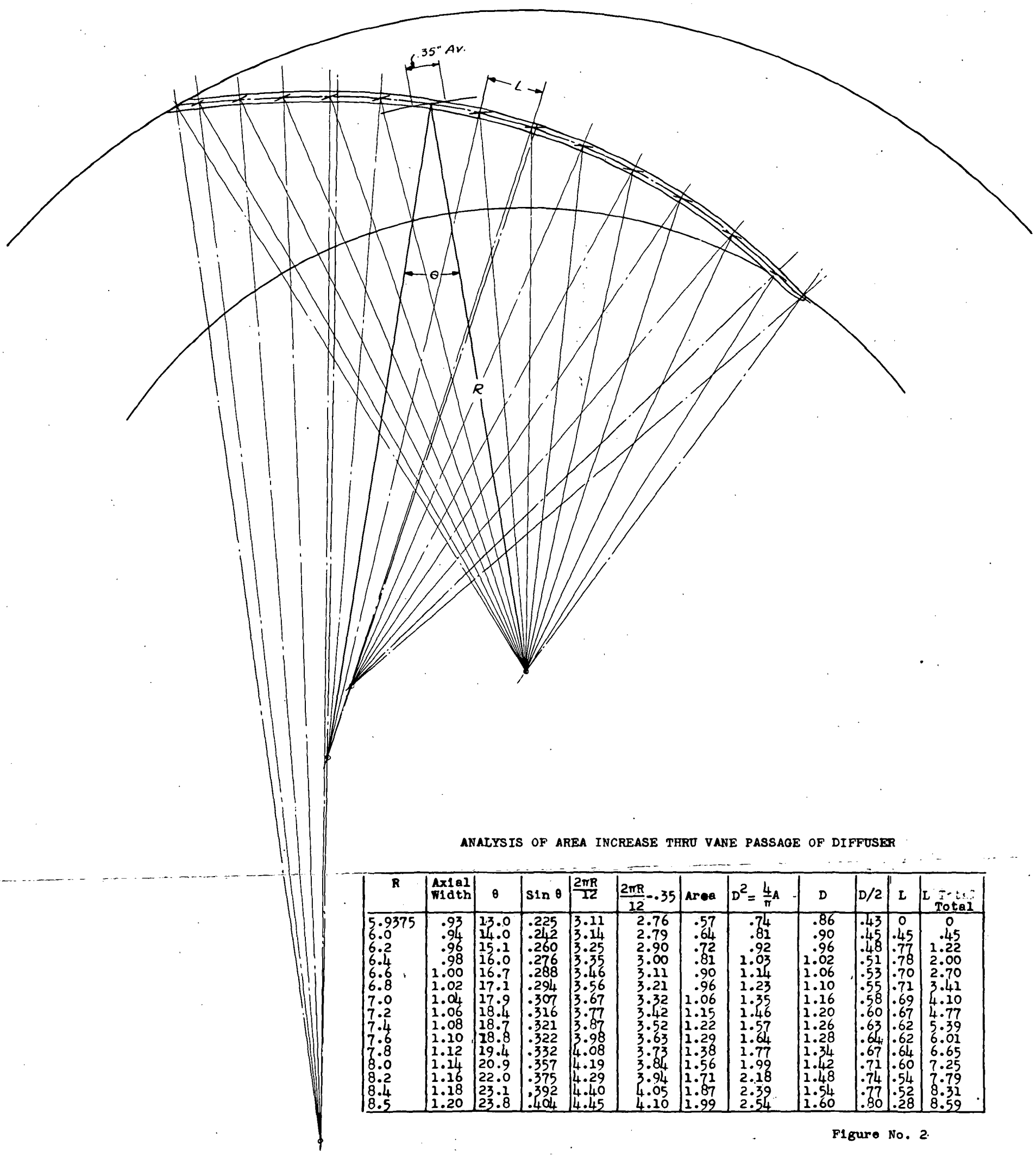

ANALYSIS OF AREA INCREASE THRU VANE PASSAGE OF DIFFUSER

R	Axial Width	θ	Sin θ	$\frac{2\pi R}{12}$	$\frac{2\pi R}{12}$ -.35	Area	$D^2 = \frac{4}{\pi}A$	D	D/2	L	L Total
5.9375	.93	13.0	.225	3.11	2.76	.57	.74	.86	.43	0	0
6.0	.94	14.0	.242	3.14	2.79	.64	.81	.90	.45	.45	.45
6.2	.96	15.1	.260	3.25	2.90	.72	.92	.96	.48	.77	1.22
6.4	.98	16.0	.276	3.35	3.00	.81	1.03	1.02	.51	.78	2.00
6.6	1.00	16.7	.288	3.46	3.11	.90	1.14	1.06	.53	.70	2.70
6.8	1.02	17.1	.294	3.56	3.21	.96	1.23	1.10	.55	.71	3.41
7.0	1.04	17.9	.307	3.67	3.32	1.06	1.35	1.16	.58	.69	4.10
7.2	1.06	18.4	.316	3.77	3.42	1.15	1.46	1.20	.60	.67	4.77
7.4	1.08	18.7	.321	3.87	3.52	1.22	1.57	1.26	.63	.62	5.39
7.6	1.10	18.8	.322	3.98	3.63	1.29	1.64	1.28	.64	.62	6.01
7.8	1.12	19.4	.332	4.08	3.73	1.38	1.77	1.34	.67	.64	6.65
8.0	1.14	20.9	.357	4.19	3.84	1.56	1.99	1.42	.71	.60	7.25
8.2	1.16	22.0	.375	4.29	3.94	1.71	2.18	1.48	.74	.54	7.79
8.4	1.18	23.1	.392	4.40	4.05	1.87	2.39	1.54	.77	.52	8.31
8.5	1.20	23.8	.404	4.45	4.10	1.99	2.54	1.60	.80	.28	8.59

Figure No. 2

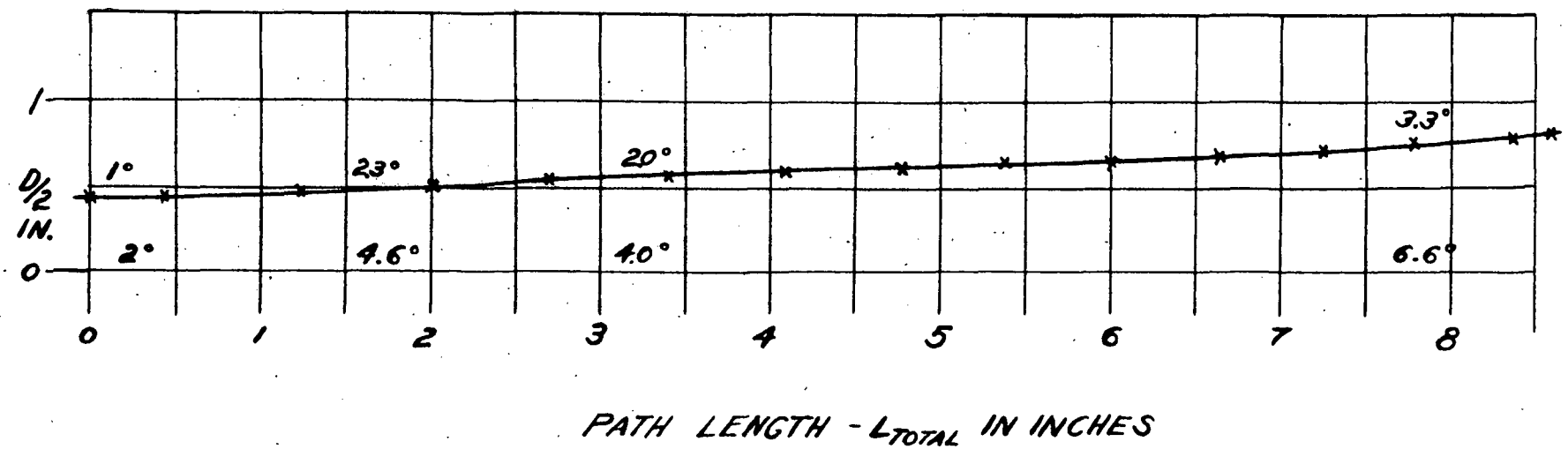

FIGURE 3. DIVERGENCE OF ROUND CONE EQUIVALENT TO AREAS OF VANE PASSAGE OF DIFFUSER.

"Pages missing from available version"

Figures 4 & 5 Missing

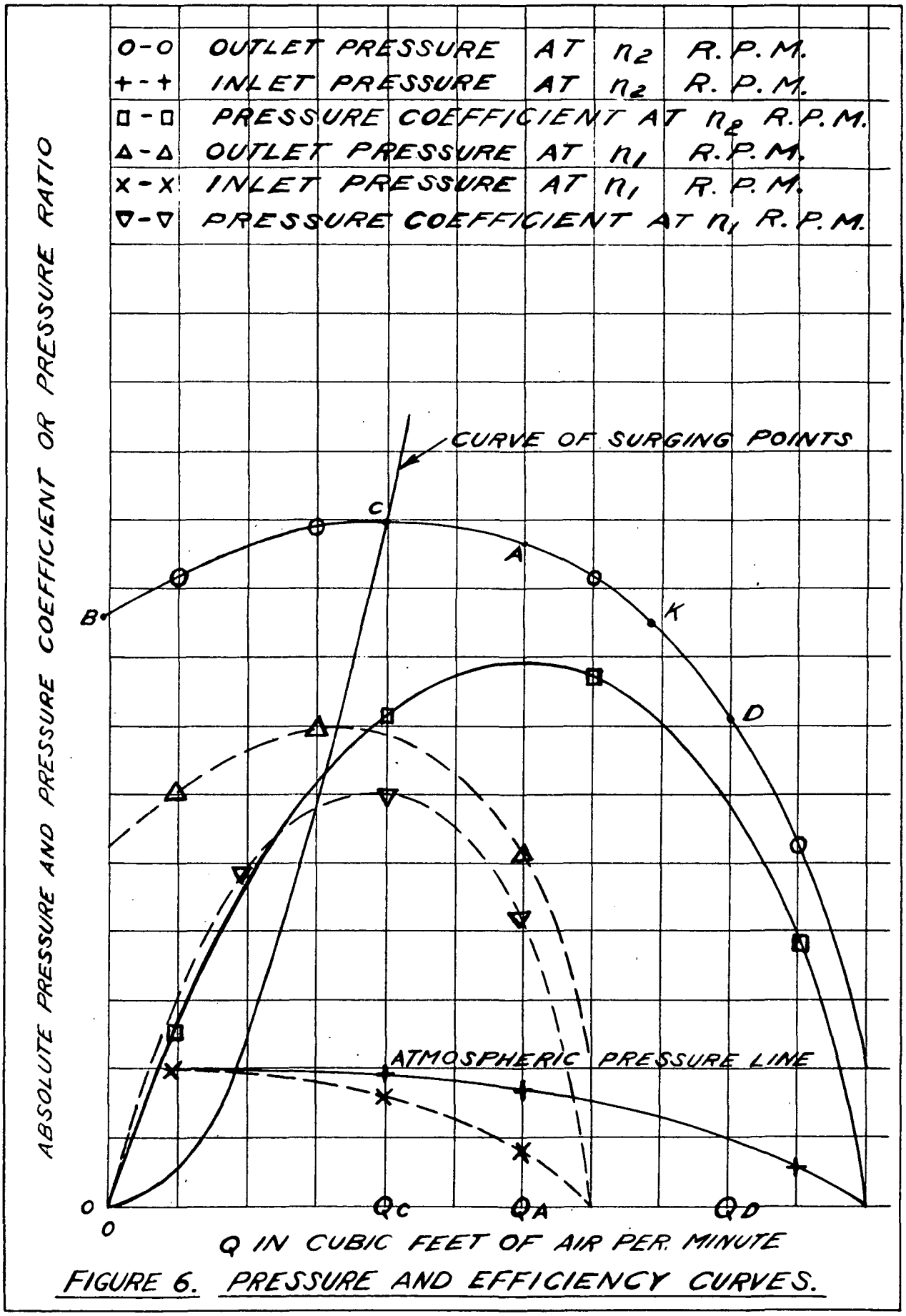

FIGURE 6. PRESSURE AND EFFICIENCY CURVES.

REPORT D

The following comments pertain to the design of single stage supercharger elements for in-line liquid-cooled engines wherein the carburetor is located ahead of the impeller inlet.

The design of supercharger inlet depends upon the shape and size of the carburetor flange. Ideally the inlet should be designed for minimum loss. Actually the inlet elbow is generally designed to prevent accumulation of liquid fuel during idling conditions while at the same time maintaining a gradual change of cross sectional area along the flow path.

The impeller generally comprises two elements; machined steel rotating inlet guide vanes ahead of dur-aluminum radial rotating vanes. The leading edge of the steel rotating inlet guide vanes lie in a plane which makes an angle of 45° with a plane normal to the impeller axis. This angle is gradually increased to 90° at the interface between steel and dur-aluminum elements. It is found advantageous to have the periphery of the steel rotating inlet guide vanes overhang the center by as much as 1/4 inch. Impeller thrust can be reduced by peripherial scallops between radial vanes of the dur-aluminum element; also by balancing holes drilled through the web of the dur-aluminum element. Provision of balancing means apparently does not appreciably detract from the impeller efficiency. The tapered vanes of the dur-aluminum element are designed to prevent resonance with the diffuser. Fifteen impeller guide vanes running with an even number of diffuser vanes ranging in number between six to ten has been found to be a satisfactory combination from the standpoint of both efficiency and vibration.

The leading edge of the diffuser vanes should be separated from the impeller vane tips by at least 3/8". The diffuser leading edge generally lies in the plane parallel to the average absolute velocity of air leaving the impeller. The rate of change of area in the diffuser passage expressed as the rate of change of the equivalent circular radius should be such as to provide an initial slope of 2° with a smooth transition to 4° slope at the diffuser exit. The actual sidewall divergence of the diffuser passage can be as much as 12° with satisfactory results. The scalloping of the diffuser rim is recommended as a means of reducing the overall diameter of the collector beyond the diffuser.

The collector area is increased uniformly around the periphery of the diffuser to maintain constant velocity therein. To avoid constriction the minimum area is arbitrarily made about 20 percent of the discharge area. Best results are obtained if the increase of collector area is accompanied by an increase displacement of the area center with respect to the impeller axis. A symmetrical disposition of the collector area relative to the diffuser outlet is desirable. An unsymmetrical disposition of the collector relative to the diffuser outlet will induce a spiral flow which tends to aggravate turning losses beyond the collector.

The engine manifolding system should ideally be designed to maintain uniform velocity from collector discharge to inlet valve ports. Actually compromises have to be made to accommodate backfire screens. Whatever the final design of manifolding system the discharge area of the diffuser collector should match the inlet area of the induction system. Velocities of 250 feet/second in the collector passage are not uncommon. Similar velocities are maintained at the impeller inlet. Adiabatic efficiencies ranging between 70 and 75 percent are attainable with impeller tip speeds as high as 1100 feet/second. Rotational speeds as high as 30,000 R.P.M. are in satisfactory use.

The general rule for supercharger design is to proportion areas to give a smooth rate of change of velocity relative to adjacent surfaces and to keep the extent of friction surfaces down to a minimum. All turns in direction should be as gradual as possible even to the extent of increasing the axial length of impeller beyond that now commonly employed. In the absence of exact quantitative correlations of pertinent parameters, reliance must be placed upon comparative tests expressing temperature rise ratio and pressure co-efficient as a function of Q/N(inlet volume flow divided by impeller R.P.M.)

In designing the impeller, account must be taken of fuel vaporization at the inlet. At take-off, with rich mixtures, the refrigeration due to fuel vaporization probably exceeds 40° F. A lower temperature depression is to be expected with increasing altitude.

The optimum impeller proportions can best be arrived at by experiment. It is important to realize that optimum impeller proportions for one set of flow conditions (as for example a low Q/N) do not necessarily correspond to the optimum impeller proportions for a different set of flow conditions (as for example a high Q/N.) A Q/N of .20 ± .05 is well suited to single stage superchargers for in-line liquid cooled engines with the carburetor ahead of the impeller.

Langley Memorial Aeronautical Laboratory,
National Advisory Committee for Aeronautics,
Langley Field, Va., September 26, 1941.

BS
VWD